UNIVERSITY OF SOUTHAMPTON

FACULTY OF NATURAL AND ENVIRONMENTAL SCIENCES

School of Ocean and Earth Science

Describing the Fate of Diazotroph-derived New Nitrogen

by

Elizabeth Colby Sargent

Thesis for the degree of Doctor of Philosophy

February 2014

UNIVERSITY OF SOUTHAMPTON

ABSTRACT

FACULTY OF NATURAL AND ENVIRONMENTAL SCIENCES

Ocean and Earth Sciences

Thesis for the degree of Doctor of Philosophy

DESCRIBING THE FATE OF DIAZOTROPH-DERIVED NEW NITROGEN

Elizabeth C. Sargent

Marine diazotrophs play an important role in marine biogeochemical cycles by fixing N_2 into bioavailable forms, thus sustaining oceanic productivity over broad timescales through maintenance of bioavailable nitrogen stores. However, as assessments of diazotrophic organisms are traditionally constrained to the upper ocean, the fate of diazotroph-derived new nitrogen is not clear. Many previous assessments of the fate of diazotrophs has assumed that the majority of new nitrogen produced in these organisms is recycled in the upper ocean through the microbial loop and that diazotroph contribution to export is minimal except following blooms of diazotrophic diatom associations (DDAs). In this study, a combination of light microscopy, transmission electron microscopy, and qPCR of sinking particulate material from the subtropical and tropical Atlantic Ocean and Gulf of Mexico has revealed that filamentous, heterocystous and unicellular cyanobacterial diazotrophs are present below 100 m, and provides some of the first evidence that this appears to be a widespread occurrence. Herein we identify the mechanisms by which diazotrophs are exiting the mixed layer via passive sedimentation, aggregation, and incorporation in faecal material. Diazotrophs also appear to be contributing to the export of particulate organic nitrogen with *Trichodesmium* composing up to 3% of PON standing stock and 1 – 17.5% of PON flux at 10 m below the mixed layer in the (sub-)tropical Atlantic Ocean. The likelihood that the subsequent remineralisation of diazotroph-derived material at depth is contributing to the N* anomaly observed in the thermocline in the North Atlantic sub-tropical gyre is also discussed. This work provides some of the first descriptions of mechanisms by which diazotrophs contribute to these anomalous nutrient distributions, such as through remineralisation of diazotroph biomass following cellular lysis. These results aid in the elucidation of the extent to which *Trichodesmium* and other

diazotrophs are contributing to the biogeochemistry of deeper waters and provides novel insight into the cycling of fixed nitrogen in the oligotrophic ocean.

Contents

List of tables

List of figures

DECLARATION OF AUTHORSHIP

I, Elizabeth C. Sargent, declare that the thesis entitled DESCRIBING THE FATE OF DIAZOTROPH-DERIVED NEW NITROGEN, and the work presented in the thesis are both my own, and have been generated by me as the result of my own original research. I confirm that:

- this work was done wholly or mainly while in candidature for a research degree at this University;
- where any part of this thesis has previously been submitted for a degree or any other qualification at this University or any other institution, this has been clearly stated;
- where I have consulted the published work of others, this is always clearly attributed;
- where I have quoted from the work of others, the source is always given. With the exception of such quotations, this thesis is entirely my own work;
- I have acknowledged all main sources of help;
- where the thesis is based on work done by myself jointly with others, I have made clear exactly what was done by others and what I have contributed myself;
- none of this work has been published before submission

Signed: 

Date: 20 Feb 2014

Acknowledgements

First and foremost, I would like to thank my supervisors, Alex Poulton, Mark Moore, and Tom Bibby. Your support and feedback has been invaluable in my growth as a scientist, and I truly appreciate the time and effort you have each contributed to my progress over the last 3 years. I must also express my gratitude to Mike Zubkov and Alan Kemp for their helpful participation in discussions about the scope of this work, and for their guidance as this project has developed.

I also wish to extend my appreciation to all those that have aided in the collection and processing of samples discussed herein, as well as to those who contributed their data for use in my analyses. Specifically, thank you Rebecca Langlois for the copious time contributed to training me and for subsequent data contributions. My sincerest thanks are also extended to the staff of the Biomedical Imaging Unit at Southampton General Hospital for the time they devoted to my training and for their continued interest in, and support of, my analyses. In addition, thank you to David Honey and Katsia Pabortsava for their help with deployments and for data contributions and to Andreas Johansson for taking time away from the lab to accompany me on a research expedition. Likewise, many thanks to Joe Snow for help with deployments and sample processing, and for countless discussions that have aided in data interpretation. I am also grateful to Eric Achterberg, Tracy Villareal, and Pia Moisander for providing me with space on their research cruises and to the crew and officers of the RRS Discovery, R/V Cape Hatteras, and R/V Atlantic Explorer for facilitating each of those expeditions. I am also indebted to GSNOCS for providing me with the funding to pursue a PhD at the University of Southampton.

Though many friends are deserving of mention, I will here limit acknowledgement Dave, Helen and Harriet. We have shared in an arduous journey, and I will always remember how much we laughed through the good and the bad. Dave, I will forever be appreciative of our echoed effort to keep one foot firmly grounded outside of academia, and for the entertainment provided by your policing of my vocabulary. Helen, thank you for continually offering a fresh perspective, for your support in and out of the lab, and for always knowing when it is time for wine. Harriet, you have been an amazing

friend and teacher, and I attribute my sustained sanity nearly completely to your never being too busy for a coffee break. We share an enthusiasm for communicating science that I find refreshing and fulfilling, and I look forward to our continued progress in science and our friendship throughout it.

I am also grateful to my parents for continued encouragement and support of my educational pursuits. Your advice and guidance has been integral to my successes, and I am continually appreciative of your tolerance to my geographic flexibility. I also extend my familial appreciation to Jana. You have made me better person both personally and professionally, and I credit you in all of my achievements.

Finally, I express my gratitude to Geordie, my partner, and my best friend. You have been remarkably patient and encouraging through the most difficult stages of this PhD, and your sustained belief in me has helped to ensure that I never doubted myself. I count myself lucky to have your support in all that I do. Thank you.

Definitions and Abbreviations

BCP	Biological Carbon Pump
DAPI	fluorescent stain which binds to A-T rich regions in DNA
DCM	deep chlorophyll maximum
DDAs	diazotrophic diatom assemblages/associations
diazotroph	a nitrogen-fixing organism
DOM	dissolved organic matter
DON	dissolved organic nitrogen
dsDNA	double stranded DNA
MLD	mixed layer depth
monoploid	the condition of having a single chromosome/genome
MSC	marine snow catcher
N	nitrogen
N*	defined by equation 1, page 2
PCD	programmed cell death
PCR	polymerase chain reaction
PHB	poly-β-hydroxybutyric
POC	particulate organic carbon
polyploid	condition of having more than genome per cell
POM	particulate organic matter
PON	particulate organic nitrogen
qPCR	quantitative PCR
SAPS	*in situ* stand alone pumping systems
SST	sea surface temperature
TEM	transmission electron microscopy
TEP	transparent exopolymer particle

1. Introduction

Phytoplankton and other microbes are ubiquitous throughout the global oceans and are fundamental contributors to the Earth system. Many of these organisms are photoautotrophic, and are thus capable of influencing atmospheric carbon dioxide (CO_2) concentrations through primary production, the photosynthetic conversion of aqueous CO_2 into particulate organic material (POC). This creates disequilibrium at the air-sea interface resulting in oceanic uptake of CO_2 (Sabine *et al*. 2004).

Primary production is also dependent on light and nutrient availability. In addition to CO_2, phytoplankton also assimilate nutrients, such as nitrate and phosphate, into their cells. The source of these nutrients, specifically nitrate, has implications for carbon cycling. New production, or production utilising allocthonous nitrate inputs to the surface ocean (Dugdale and Goering 1967) can be used to approximate export of organic matter to the deep ocean (Eppley and Peterson 1979) and is unique to regenerated production, which results from the uptake of nutrients that have been recycled and regenerated in the form of ammonia (Dugdale and Goering 1967). The resultant ecological interactions and biological transformations of the phytoplankton-produced particulate organic material (POM) is the foundation of almost all other life in the sea.

1.1 Marine Particulate Organic Matter

Particulate Organic Matter (POM) encompasses a variety of organic compounds. Autotrophic fixation of carbon and biological uptake and incorporation of nitrogen, and phosphorus into biomass typically occurs in a relatively conserved ratio known as the Redfield ratio. Redfield (1934) documented that on average, phytoplankton biomass in the euphotic zone has a carbon to nitrogen to phosphorus (C:N:P) ratio of 106:16:1, but this ratio can be quite plastic across ocean regions and in different depth ranges

(Arrigo 2005). Regardless, an excess or deficit in the availability of any of these elements can promote or limit the growth and productivity of different phytoplankton and thus the fate of their biomass, which has implications for biogeochemical cycles of carbon, nitrogen and phosphorus.

1.2 Biological Carbon Pump (BCP)

The biological carbon pump (BCP) is the downward export, or transfer of carbon from the surface to the ocean's interior, of biogenic material (Volk and Hoffert 1985; Falkowski *et al*. 1998; Boyd and Trull 2007). This POM includes phytoplankton biomass, zooplankton faecal material, and resultant detritus, which can be subsequently colonised by heterotrophic bacteria, often resulting in further breakdown, remineralisation and eventual mixing and recycling of the resultant nutrients and dissolved carbon into the upper ocean. However, some of that POM continues to settle through the water column with eventual sequestration of the material to the deep ocean where it remains isolated from the atmosphere. This loss of material from the surface layer results in a continual disequilibrium of ocean-atmosphere CO_2 concentrations driving continued uptake of CO_2 by the oceans (Volk and Hoffert, 1985). The ocean is a major global reservoirs of carbon, is crucial in the global carbon cycle and hence in the regulation of climate. In the ~12,000 years prior to the industrial era, and excluding the earth's crust and sediments, the deep ocean held an order of magnitude more carbon than all other carbon reservoirs combined (Sigman and Boyle 2000). Following industrial revolution, anthropogenic activities have resulted in an unprecedented increase in atmospheric CO_2 to 390.5 ppm as of 2011 compared to 278.9 ppm in 1750 (Hartmann *et al*. *In press*). The ocean has been integral in buffering this increase as without continued oceanic uptake, we would currently be facing atmospheric CO_2 concentrations in excess of 450 ppm (Doney *et al*. 2009).

1.2.1 Mechanisms of Export

There are a variety of mechanisms by which export of POM occurs in the oceans, such as aggregation and sinking of marine snow, grazing and faecal pellet production, passive sedimentation, and active transport of POM by eddies. Marine snow consists of large (>0.5 mm) aggregate particles that are typically composed of a mixture of phytodetritus, refractory material, biominerals, and mucoid matrices or other polymeric materials (Alldredge and Silver 1998). The size, sinking speed, and composition of marine snow varies widely (Alldredge and Gotschalk 1988), although ballasting of biominerals is thought to increase sinking rates and aid in direct transfer of POM to depth (Armstrong *et al*. 2002; Sanders *et al*. 2010; Riley *et al*. 2012). Faecal material is also a large contributor to POM export as faecal pellets are dense and often have enhanced sinking speeds (Alldredge and Silver 1988; Turner 2002; Wilson *et al*. 2008). Other particles such as dead zooplankton or large phytoplankton may sink passively through the water column. These, and breakdown products of marine snow aggregates and faecal material, compose the slow sinking pool of POM, and may be more susceptible to remineralisation (Riley *et al*. 2012), although the relationship between particle size, sinking speed, and susceptibility to remineralisation is still in debate (De La Rocha and Passow 2007). Further breakdown products of these particles can become part of the suspended pool of particulate material. Active transport of all of these pools of material by eddies has also been shown to occur with both enhanced POM production and export within eddies compared to the adjacent waters (Bidigare *et al*. 2003; Guidi *et al*. 2012).

1.2.2 Remineralisation

As this POM sinks through the mesopelagic layer (or twilight zone defined as the depths between the base of the euphotic zone ~200 m and 1000 m (Buesseler and Boyd 2009)) up to 90% of the POM can be remineralised back into inorganic constituents by heterotrophic bacteria

and/or zooplankton (Martin *et al*. 1987), resulting in a release of nutrients into the water column where it is then available for reincorporation into biomass either at depth or in the surface layer following vertical mixing (Robinson *et al*. 2010). Remineralisation of POM can also occur in the surface ocean and subsequent incorporation of the derived dissolved organic matter (DOM) into the biomass of the microbes, which is then available for grazing/breakdown and cycling of that material through various trophic levels and eventually back to the POM and dissolved organic matter DOM pools is known as the "microbial loop" (Azam *et al*. 1993). The attenuation of POM between the surface and depth, and thus the ability or inability of material to remain resilient to remineralisation as it sinks through the mesopelagic, can be assessed by calculating the attenuation coefficient of a power law function, *b* (Martin *et al*. 1987).

However, remineralisation of the multiple components of the POM pool does not occur at the same rate. Anderson and Sarmiento (1994) proposed an amendment to the Redfield ratio to 117:16:1 for sinking particles and regenerated nutrients between 400 and 4000 m, which was consistent with the C:N:P ratio of samples collected at all depths during cruises of the World Ocean Circulation Experiment (WOCE) in the Atlantic, Pacific, and Indian Oceans (Gruber 2008). This increase in carbon relative to nitrogen and phosphorus in this depth range may be due to the differences in the remineralisation rates of these elements, i.e. PON and phosphorus are preferentially remineralised relative to POC (Anderson and Sarmiento 1994; Christian *et al*. 1997; Shaffer *et al*. 1999; Schneider *et al*. 2003; Monteiro and Follows 2012).

1.3 The Marine Nitrogen Cycle

Nitrogen is a major component of both nucleotides (the components of DNA and RNA) and amino acids (the building blocks for proteins), and it is thus required by all living organisms. These essential requirements potentially make nitrogen a crucial limiting factor in biological processes,

such as throughout most of the (sub-)tropical surface ocean globally (Moore *et al.* 2013). In the marine environment, nitrogen exists in six stable forms: dinitrogen (N_2), nitrous oxide (N_2O), nitrite (NO_2^-), nitrate (NO_3^-), ammonium (NH_4^+), as well as dissolved organic nitrogen (DON). The nitrogen cycle is the complex series of reactions that control the abundance of each of these nitrogen species. Each reaction is biologically mediated, including the assimilation of NO_2^-, NO_3^-, and NH_4^+ by phytoplankton, the nitrification of NO_2^- and NH_4^+ by oxidizing organisms, ammonification by bacteria and zooplankton, anaerobic oxidation of ammonium (Anammox) and denitrification by bacteria, and nitrogen fixation by cyanobacteria (Table 1-1).

The microbes involved in the various transformations of N are also pivotal in the regulation and cycling of phosphorus in the oceans. In trying to determine the primary limiting nutrient in marine environments, Redfield (1934) theorized phosphorus must be limiting because any excess phosphorus that decreased the N:P ratio could be 'corrected' back to 16:1 by biological nitrogen fixation. Conversely, an increased N:P ratio due to excess nitrate could be corrected back to 16:1 through biological denitrification (and/or Anammox) (Gruber 2008). Thus the nitrogen cycle is closely linked to the phosphorus (and carbon) cycles, and perturbations in any of the three can have a result on, or result from changes in, the other two (Figure 1.1) (Gruber 2008).

Table 1-1. Summary of biologically mediated N transformation processes in the marine environment (Modified from Gruber 2008).

Process		Organism	Redox environment	Trophic Status	Biochemical Role
NO_3^- assimilation	$NO_3^- \rightarrow PON$	Phytoplankton	Aerobic	Photo-autotrophic	Source of N
NO_2^- assimilation	$NO_2^- \rightarrow PON$	Phytoplankton	Aerobic	Photo-autotrophic	Source of N
NH_4^+ assimilation	$NH_4^+ \rightarrow PON$	Phytoplankton Bacteria	Aerobic Aerobic/Anaerobic	Photo-autotrophic Heterotrophic	Source of N
Ammonification	$P/DON \rightarrow NH_4^+$	Bacteria/Zooplankton	Aerobic/Anaerobic	Heterotrophic	Release of N
NH_4^+ oxidation	$NH_4^+ \rightarrow NO_2^-$	NH_4^+ oxidizers	Aerobic	Chemo-autotrophic	Source of energy
NO_2^- oxidation	$NO_2^- \rightarrow NO_3^-$	NO_2^- oxidizers	Aerobic	Chemo-autotrophic	Source of energy
Denitrification	$NO_3^- \rightarrow NO_2^- \rightarrow NO + N_2O \rightarrow N_2$	Bacteria	Anaerobic	Heterotrophic	Nitrogen Sink
Anammox	$NH_4^+ + NO_2^- \rightarrow N_2 + 2H_2O$	Bacteria	Anaerobic	Chemo-autotrophic	Source of Energy
N_2-fixation	$N_2 + 8H^+ \rightarrow 2NH_3 + H_2$	Cyanobacteria Bacteria	Aerobic Aerobic/Anaerobic	Photo-autotrophic Heterotrophic	Source of N

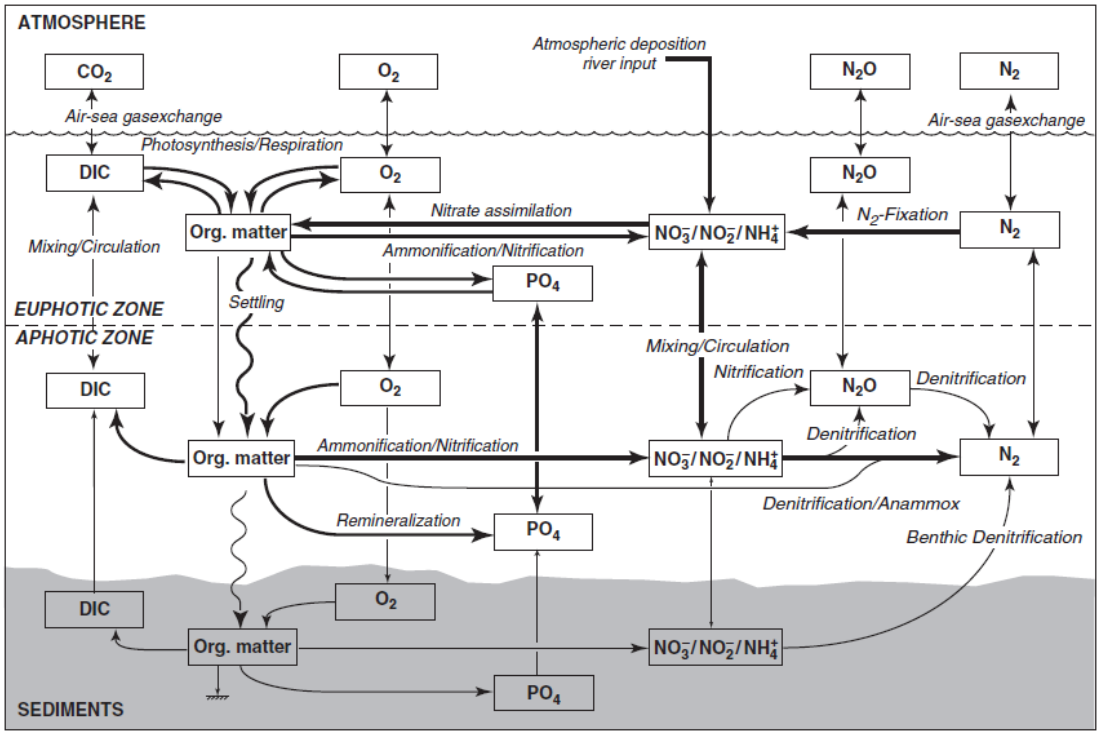

Figure 1-1. Simplified schematic representation of the marine nitrogen cycle and its coupling to the oxygen, phosphorus, and carbon cycling in the marine environment. (reproduced from Gruber 2008)

The relative abundances of nitrate and phosphate are typically described in terms of N*, which measures the departure from the Redfield ratio, herein, we define N* by defined by equation 1, which is similar to the base DIN_{xs} equation; Other groups have previously added a constants to the equation to force the global average of N* to zero (Gruber and Sarmiento 1997; Deutsch *et al*. 2001; Hansell *et al*. 2004, 2007; Moore *et al*. 2009):

$$N^* = NO_3^- - 16 \times PO_4^{3-} \qquad \text{(eq. 1)}$$

Throughout the majority of the global ocean N* is negative within the thermocline and in deeper waters (Gruber and Sarmiento 1997; Moore *et al*. 2009), but north of the equator in the Atlantic Ocean there is a positive N* anomaly in the subtropical thermocline to ~1100 m. In this region nitrate is

accumulating in excess at a rate of 7.8 ± 1.7x10^{11} mol N yr^{-1} (Hansell *et al.* 2007) along the σ_θ=26.8 density surface, which corresponds to the median of the range of densities composing the Subantarctic Mode Water (SAMW) (Sarmiento *et al.* 2004) (Figure 1-2).

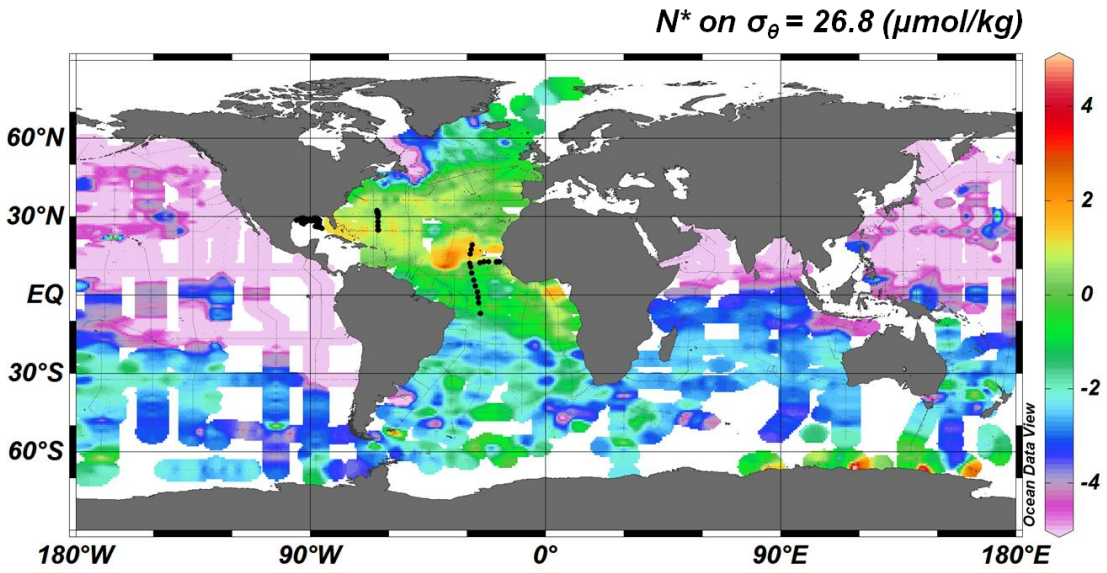

Figure 1-2. Global distribution of N* along the σ_θ=26.8 surface corresponding to the median of the range of densities composing the SAMW (Sarmiento *et al.* 2004) illustrating excess nitrate accumulation in the thermocline of the subtropical North Atlantic. Nutrient data from Key *et al.* (2004). Black dots represent areas sampled in this study.

Gradients of increasing N* can hence be used to infer a net gain of nitrogen, which is tantamount to the high dissolved N:P ratios, and in turn appears to result in phosphate becoming severely depleted in surface waters of the North Atlantic subtropical gyre (Gruber and Sarmiento 1997; Wu *et al.* 2000; Moore *et al.* 2009). Formation of enhanced N* are thought to come from a variety of sources, such as atmospheric deposition of high N:P nutrients (Gruber and Sarmiento 1997) and advection of high N:P DOM into the main thermocline (Michaels *et al.* 1996). Nitrogen fixation is also thought to influence the excess N accumulations, such as through the remineralisation of the high N:P biomass of nitrogen fixing organisms (Anderson and Sarmiento 1994; Hansell *et al.* 2004, 2007). Mechanisms by

which nitrogen fixation can contribute to the N* anomaly will be discussed further in Chapters 2, 3, 5, and 6.

1.4 Nitrogen Fixation

Nitrogen fixation is the conversion of inert N_2 to bioavailable ammonia (NH_3). The reaction (detailed in Table 1-1) is catalyzed by the nitrogenase enzyme. This enzyme has two subunits, an Fe-binding protein and an MoFe-binding protein. The Fe-binding subunit of the nitrogenase enzyme is coded for by the *nif*H gene (Young 1992). Diversity within this gene region allows delineation between various groups of *nif*H-containing organisms as indicated by Figure 1-3. Advances in molecular technologies have allowed for the identification of unique *nif*H phylotypes (taxon-neutral phylogenetic groups) and development of primers and probes for use in quantitative PCR (qPCR) assays (Zehr *et al*. 1997; 1998; 2003; Church *et al*. 2005a; 2005b, Foster *et al*. 2009, Moisander *et al*. 2010). This will be discussed in more detail in Chapter 2.

The nitrogenase enzyme is oxygen sensitive, so the nitrogen fixation reaction must be carried out anaerobically (Peters *et al*. 1995). The necessity for oxygen segregation from nitrogenase in diazotrophic cyanobacteria is enhanced due to the photosynthetic capability of these organisms resulting in oxygen production within their cells. Diazotrophic cyanobacteria have thus developed adaptive ways for segregating the nitrogen fixation process from oxygen exposure (Newton 2007). Some diazotrophic cyanobacteria overcome this segregation challenge spatially, such as through formation of a specialized cell known as a heterocyst where nitrogen fixation but not photosynthesis occurs (Fay 1992; Kumar *et al*. 2010), some separate nitrogen fixation and photosynthesis temporally (Toepel *et al*. 2008), while others do both (Bergman *et al*. 2013).

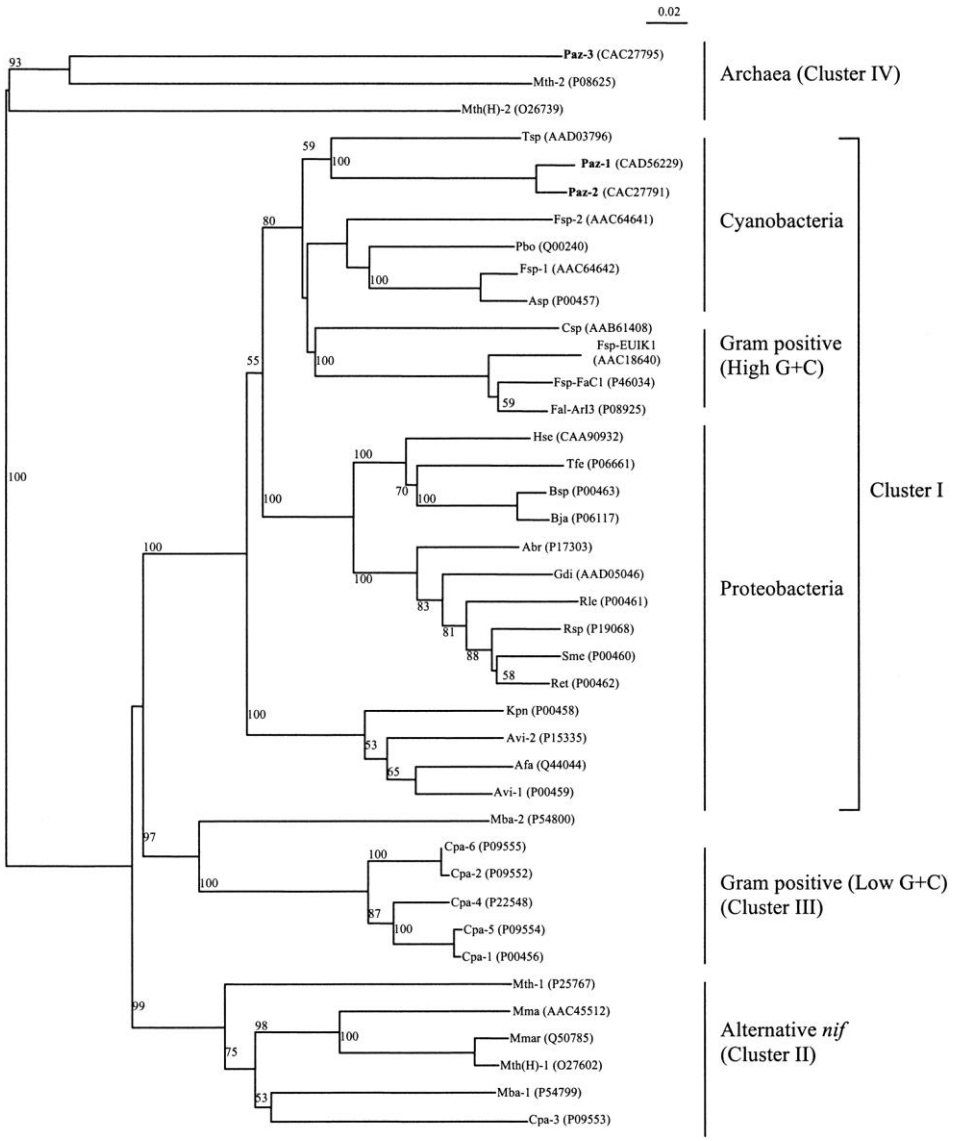

Figure 1-3. Phylogeny of *nif*H amino acid sequences from various *nif*H containing organisms. Note that *nif*H diversity within the cyanobacterial clade is high enough for targeted assessments of individual cyanobacterial species using qPCR of the *nif*H gene. Abbreviations of note include Csp: Cyanothece sp. strain ATCC 51142 a unicellular diazotroph, and Tsp: *Trichodesmium* sp. strain IMS101. Reproduced from Choo *et al*. (2003).

1.4.1 Importance of Nitrogen Fixation

The upper boundary of growth and productivity of marine photoautotrophs is constrained by nitrogen availability globally as many ocean regions are nitrogen limited (Falkowski 1997; Gruber and Galloway 2008; Moore *et al*. 2013). As nitrogen can be a limiting factor for growth, it is not surprising

that nitrogen fixing organisms are found in nearly all marine environments as they are not limited by nitrogen availability. Nitrogen fixing organism are present in the open ocean, deep sea, benthos/sediments, coral reefs, seagrass beds, intertidal areas, estuaries, other coastal areas (Carpenter and Capone 2008), and potentially even inside the guts of zooplankton (Braun *et al*. 1999). These organisms are often responsible for supporting the rest of the phytoplankton community via both the release of recently fixed nitrogen (discussed below) and through supply and recycling of that new nitrogen in the ocean. Gruber and Sarmiento (1997) postulated that the majority of fixed nitrogen in the surface oceans is diazotroph-derived, and thus these organisms play an integral role in ocean ecosystems. Fixed-nitrogen availability in the ocean is also coupled to the sequestration of atmospheric carbon and thus is not only an integral part of the nitrogen cycle, but also plays a role in the regulation of global biogeochemical cycles (Falkowski 1997). This is especially apparent over even longer timescales where changes in the fixed nitrogen inventory due to a variety of factors (such as changes in ocean circulation) are thought to cause glacial/interglacial changes in atmospheric carbon dioxide concentrations (Falkowski 1997; Broecker and Henderson 1998; Karl *et al*. 2002; Gruber and Galloway 2008; Straub *et al*. 2013). Although the full extent of the effect of continued global-scale anthropogenic perturbations of ocean biogeochemistry is currently unknown, it has been suggested that the geographical range of nitrogen fixers will expand in a future, warmer ocean (Boyd and Doney 2002), and that nitrogen fixation rates and carbon fixation by nitrogen fixing organisms are likely to increase as pCO_2 increases during the next century (Hutchins *et al*. 2007).

1.5 Marine Diazotrophs

There are three main cyanobacterial groups of nitrogen fixing organisms in the ocean: filamentous, heterocystous, and unicellular cyanobacteria (Zehr 2011). There are also heterotrophic diazotrophic organisms (Zehr *et al*. 1995).

1.5.1 Filamentous diazotrophs

The most widely studied marine diazotroph is the filamentous, non-heterocystous cyanobacterial genus *Trichodesmium*, members of which are considered to be the most abundant oceanic nitrogen fixers (Zehr 2011). *Trichodesmium* occurs throughout oligotrophic ocean regions (Capone *et al*. 1997; Sohm *et al*. 2011). The genus consists of six species (Hynes *et al*. 2012), which often exist in colonies of varying morphology, such as puffs, tufts or rafts, and nests (Figure 1-4). *Trichodesmium* is the main constituent of marine nitrogen fixation estimates in tropical and subtropical oligotrophic ocean regions (Capone *et al*. 2005).

Trichodesmium is buoyant and is typically constrained to the surface layer, but deeper (>50 m) populations of *Trichodesmium* are hypothesized to consist of vertically migrating colonies (Kromkamp and Walsby 1992; White et al. 2006). Buoyancy in *Trichodesmium* is provided by the presence of gas vacuoles (Walsby 1978), and is controlled by carbohydrate ballasting (Villareal and Carpenter 2003). Models of carbohydrate ballasting in *Trichodesmium* suggest that vertical migrations of large (≥1500 µm radius) colonies could span 200 m for nutrient mining and phosphorus acquisition (Kromkamp and Walsby 1992; White et al. 2006), but are realistically more likely to be confined to the upper 70 m of the water column (Villareal and Carpenter 2003). The morphology and physiology of *Trichodesmium* will be discussed in more detail in Chapters 3, 4, and 5.

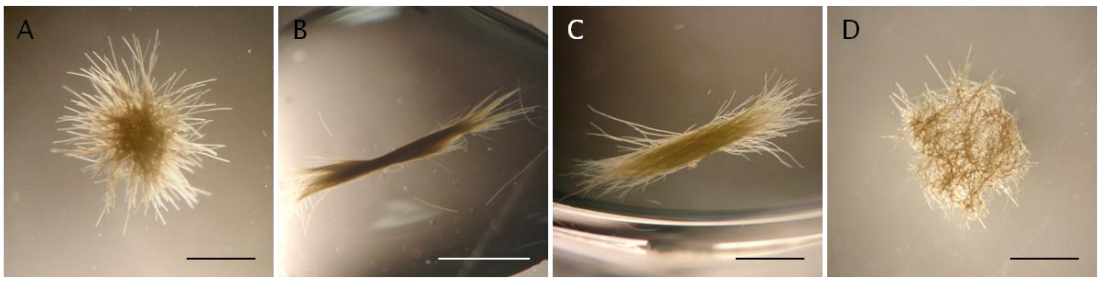

Figure 1-4. *Trichodesmium* colony morphology. Various colonial morphologies include (A) radial puffs, (B) twisted tufts, (C) rafts of trichomes arranged parallel to each other, and (D) flat, matted nests. *Trichodesmium* colonies typically consist of 100-200 trichomes (Carpenter *et al*. 2004). Scale bars represent 1 mm.

One of the six described *Trichodesmium* species falls under the antiquated genus *Katagnymene*. Members of this genus lack heterocysts and, in contrast to other *Trichodesmium* species, do not form colonies (Lundgren *et al*. 2001). *Katagnymene* spp. is present in warm, oligotrophic ocean regions globally, and has been successfully isolated into culture allowing for more thorough physiological investigations. Like other *Trichodesmium* species, *Katagnymene* only possess the nitrogenase enzyme in confined zones of cells along the trichome (Lundgren *et al*. 2001) now known as diazocytes (Berman-Frank *et al*. 2001). These diazocyte regions aide in the segregation of the nitrogenase enzyme from oxygen allowing for nitrogen fixation to occur during the light period when oxygen is also being produced via photosynthesis (Berman-Frank *et al*. 2001; Sandh *et al*. 2012). Although *Katagnymene* spp. is morphologically distinct from other *Trichodesmium* species, it is phylogenetically similar. The *nif*H gene region in both genera is nearly indistinguishable (Lundgren *et al*. 2001), and high similarity is also found within the internal transcribed spacer (ITS) region between the 16S and 23S rRNA genes (Orcutt *et al*. 2002) and the *het*R gene regions (Lundgren *et al*. 2005) prompting a call for reclassification and combination of *Katagnymene* into the *Trichodesmium* genus (Hynes *et al*. 2012).

1.5.2 Heterocystous diazotrophs

Heterocystous cyanobacteria possess specialized cells where nitrogen fixation, but not photosynthesis, occurs (Fay 1992), and compose the second group of marine diazotrophs, which include cyanobionts. Cyanobionts are cyanobacteria that are involved in symbiotic relationships with a eukaryotic host. In diazotrophic diatom associations (DDAs), the cyanobionts are nitrogen-fixing cyanobacteria, such as *Richelia intracellularis* and *Calothrix rhizosoleniae*. *R. intracellularis* was first described in an endosymbiotic relationship with the diatom *Rhizosolenia clevei* (Ostenfeld and Schmidt 1901) (Figure 1-5A); *R. intracellularis* has since been documented in similar consortia with the diatom species

Hemiaulus spp. (Heinbokel 1986; Villareal 1991; Kimor *et al*. 1992; Villareal 1994; Janson *et al*. 1999; Scharek *et al*. 1999; Foster and Zehr 2006; Bar-Zeev *et al*. 2008; Foster *et al*. 2009; Goebel *et al*. 2010; Padmakumar *et al*. 2010) (Figure 1-5B, C) and *Guinardia cylindrus* (a synonym of *Rhizosolenia cylindrus*) (Venrick 1974; Villareal 1992; Scharek *et al*. 1999).

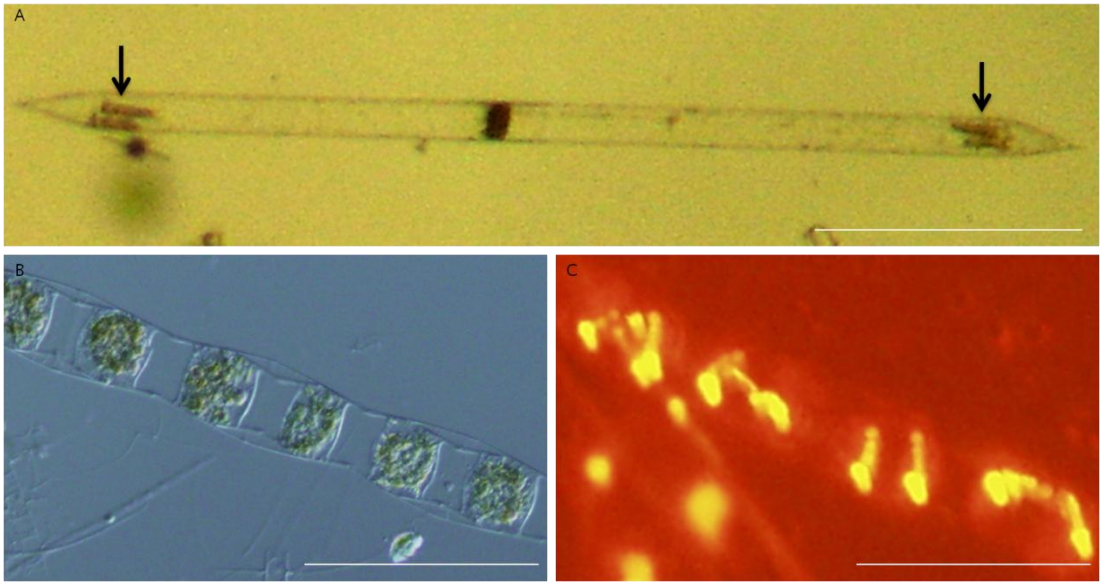

Figure 1-5. A diazotrophic diatom association (DDA). *Richelia intracellularis* associations with host diatoms. (A) *Richelia-Rhizosolenia* where *R. intracellularis* is confined to the apices of the host diatom (arrows), and (B) *Richelia-Hemiaulus* where cyanobionts are obscured by the cytoplasm unless they are (C) viewed under excitation of the phycoerythrin pigment which is not present in the host diatoms. Scale bars represent 100 µm.

R. intracellularis possesses a single terminal heterocyst and up to ten vegetative cells (Ostenfeld and Schmidt 1901); the heterocyst of this species is noticeably larger than the vegetative cells, which are uniform in size (Janson *et al*. 1999). *C. rhizosoleniae* was originally described as an epiphyte of the diatom *Chaetoceros compressum* (Lemmerman 1905). This cyanobacterium also consists of a single terminal heterocyst and multiple vegetative cells, but unlike *R. intracellularis*, the heterocyst of *C. rhizosoleniae* is smaller than the vegetative cells. Additionally, the vegetative cells are not uniform in size, and extend in a slightly tapered filament (Janson *et al*. 1999). *Calothrix* has been successfully cultured independent of a host diatom (Foster and Zehr 2006). Infrequently, *R. intracellularis* is reported as free-living (Weare *et al*. 1974; Goméz *et al*. 2005; White *et al*.

2007), but it has not yet been successfully cultured in this state and is assumed to be an obligate symbiont (Thompson and Zehr 2013). Janson *et al.* (1995) were unable to detect gas vesicles in both the heterocysts and vegetative cells of this species; they suggest that since all other marine cyanobacteria possess theses vesicles, the absence of gas vesicles in *R. intracellularis* may explain why the free-living form is such a rarity, as it may be unable to regulate its position in the water column (Janson *et al*. 1995), and would therefore be reliant on a host for buoyancy control.

1.5.3 Unicellular diazotrophs

The third group of diazotrophic cyanobacteria, unicellular diazotrophs, are vastly understudied in comparison to *Trichodesmium* and the DDAs, but are generally split into two categories: free living and symbiotic. Some of the unicellular diazotrophs are obligate symbionts, such as Group A cyanobacterium (*Candidatus Atelocyanobacterium thalassa)* (Thompson *et al*. 2012). This organism lacks photosystem II making it an obligate symbiont (Tripp *et al*. 2010), and it is thought to associate with a haptophyte host (Thompson *et al*. 2012). These organisms were first detected in open ocean water samples by nitrogenase gene analyses (Zehr *et al*. 1998), and it appears they are significant in contributing to oceanic fixed nitrogen on the global scale as recent phylogenetic surveys have revealed their prevalence in many marine environments (Church *et al*. 2005a; 2005b, Foster *et al*. 2009, Moisander *et al*. 2010). The geographical range of Group A cyanobacteria is also greater than that of *Trichodesmium* implying it may be the main contributor of new nitrogen at higher latitudes (Moisander 2010).

Group B cyanobacteria exist both as free living and in symbiosis with the diatom *Climacodium frauenfeldianum* (Carpenter and Janson 2000; Foster *et al*. 2011); Group B cyanobacteria are also capable of colonial aggregation (Foster *et al*. 2013). Group C cyanobacteria are free living, but little else is known about their physiology, and their taxonomic classification remains unclear (Taniuchi *et al*. 2012).

1.5.4 Heterotrophic Diazotrophs

Heterotrophic diazotrophs are distributed throughout the world's oceans, and unlike cyanobacterial diazotrophs, heterotrophic diazotrophs use organic carbon as an energy source. However, photoheterotrophy is also possible as is suggested for the Group A cyanobacterium, which lacks photosystem II (Zehr *et al*. 1998; Tripp *et al*. 2010). Heterotrophic bacteria were some of the first diazotrophic organisms described (Waksman *et al*. 1933), and non-cyanobacterial *nif*H is now known to compose the majority *nif*H community structure globally (Farnelid *et al*. 2011). Heterotrohpic diazotrophs also dominate nitrogen fixation in the South Pacific Gyre (Halm *et al*. 2012). There are multiple *nif*H clades of heterotrophic diazotrophs including proteobacteria and sulphate-reducing bacteria, which can exist free living, in association with microbial mats, and even in hydrothermal vent systems (Eckford *et al.* 2002; Steppe and Paerl 2002; Mehta *et al*. 2003; Halm *et al*. 2011). Active pelagic heterotrophic diazotrophs have also been detected via *nif*H assessments at and below 500 m (Hewson *et al*. 2007; Hamersley *et al.* 2011).

1.6 Ecology and Physiology of Marine Diazotrophs

1.6.1 Controls on Diazotrophy

The distribution of some diazotrophs appears to be restrained by temperature. *Trichodesmium* growth is most active above 20 ˚C (Carpenter 1983; Breitbarth *et al*. 2007), while the unicellular cyanobacteria display a tolerance for cooler water temperatures in temperate zones (Holl *et al*. 2007; Needoba *et al*. 2007; Langlois *et al*. 2008). Turbulence has also been hypothesised to adversely affect nitrogenase activity in *Trichodesmium* due to increased oxygen exposure (Carpenter and Price 1976), but the effect of turbulence on the nitrogen fixing capabilities of other diazotrophs is poorly

understood (Howarth *et al*. 1993). Nitrogen fixing organisms are not well described in higher latitudes, but *nif*H-containing organisms have been detected in the Arctic (Farnelid *et al*. 2011). As cyanobacterial nitrogen fixation has been observed in terrestrial and marine polar environments near 0 ˚C (Vincent 2002; Stall *et al*. 2003; Blais *et al*. 2012), and as actively growing populations of *Trichodesmium* and other diazotrophs are often observed in turbulent areas (Carpenter *et al*. 2004), it does not appear that activity of the nitrogenase enzyme itself is restricted by temperature and turbulence, but rather the physiology of individual diazotrophs limits their tolerances to these factors.

Trace metals, specifically iron, can be a primary limiting nutrient for diazotrophs as the nitrogenase enzyme requires both iron and molybdenum, and thus the iron requirements of diazotrophs can be an order of magnitude greater than the iron requirements of strict photoautotrophs (Berman-Frank *et al*. 2001; Kustka *et al*. 2003; Sañudo-Wilhelmy *et al*. 2001). This is especially apparent in the subtropical South Atlantic were phosphorus concentrations are in excess of the requirements for diazotrophic growth, but diazotrophy is minimal (Moore *et al*. 2009). In contrast, diazotrophy thrives in the subtropical North Atlantic where there is also an input of iron from atmospheric aerosols (Michaels *et al*. 1996; Wu *et al*. 2000; Mahaffey *et al*. 2003; Tyrrell *et al*. 2003; Moore *et al*. 2009). Iron has been observed to stimulate growth and nitrogen fixation in *Trichodesmium* both in culture and *in situ* (Rueter 1988; Paerl *et al*. 1994; Berman-Frank *et al*. 2001). As atmospheric dust deposition is low in many oligotrophic ocean regions where diazotrophs should otherwise flourish, iron limitation of nitrogen fixation has been proposed as a near global occurrence (Falkowski 1997; Berman-Frank *et al*. 2001; Moore *et al*. 2002).

Other nutrients, such as phosphorus can also limit diazotrophy, and co limitation of diazotrophy by iron and phosphorus is likely occurring in the subtropical North Atlantic (Mills *et al*. 2004; Ward *et al*. 2013). However, some diazotrophs, such as *Trichodesmium* are able to access organic pools of phosphorus allowing for continued growth even when phosphate is depleted (Mulholland *et al*. 2002; Dyhrman *et al*. 2006).

1.6.2 Grazing

Grazing of diazotrophs is not widely reported, but grazing deterrence by diazotrophs appears to be widespread. Depressed growth rates, egg production and biomass of zooplankton have been reported in the presence of cyanobacterial blooms (Heerkloss *et al*. 1984; Sellner *et al*. 1997), and some diazotrophs, such as *Trichodesmium*, are known to possess grazer-deterring toxins (Siddiqui 1992; Janson *et al*. 1995; O'Neil 1999; Kerbrat *et al*. 2010). However, modest grazing of *Trichodesmium* biomass has been reported in harpacticoid copepods (O'Neil and Roman 1994; O'Neil 1998; 1999), and isotopic assessments (see below) suggest that the transfer of diazotroph-derived new nitrogen to higher trophic levels does occur (O'Neil *et al*. 1996; Montoya *et al*. 2002; Loick-Wilde *et al*. 2012). Fish have also been observed to graze on *Trichodesmium* (Carpenter and Capone 2008 and references therein). Additionally, salp grazing on *Trichodesmium* has been theorised to occur following observations of negatively correlated salp and *Trichodesmium* abundances *in situ* (Carpenter and Capone 2008). Some coccoid cyanobacteria, as well as heterotrophic bacteria, are also directly grazed (Caron *et al*. 1991).

1.6.3 Nutrient Transfer

In heterocystous cyanobacteria the transfer of nutrients is essential, both along the trichome between the differentiated specialised cells and from symbiont to host. Only vegetative cells are able to perform photosynthesis, and therefore must supply the heterocyst(s) with the necessary sugars to support the energy demanding process of nitrogen fixation; in return, the heterocyst supplies the vegetative cells with fixed nitrogen (Golden and Yoon 2003; Foster *et al*. 2011). The mechanism for this transfer is described by Mullineaux *et al*. (2008), who showed diffusion of fluorescent molecules from a heterocyst cytoplasm to a vegetative cell cytoplasm, and vice versa, through intercellular channels, or microplasmodesmata, in the cyanobacterium *Anabaena cylindrical.*

Crucially, they showed that the exchange rate of fluorescent dye between vegetative cells significantly increases after 72 hours of nitrate deprivation, which suggests an increase in the number of connections between these cells after heterocyst differentiation thus facilitating a more efficient metabolite exchange pathway (Mullineaux *et al*. 2008). This also suggests that although nitrogen fixation takes place in the heterocysts, the vegetative cells of *R. intracellularis* could be responsible for nitrogen transfer from cyanobiont to host (Janson *et al*. 1995). Villareal (1990) cultured symbiotic *Rhizosolenia-Richelia* and asymbiotic *Rhizosolenia* in both nitrogen deplete and nitrogen replete medium, and found that both diatoms grew at comparable rates under replete conditions; conversely, under nitrogen deplete conditions *Rhizosolenia-Richelia* proliferated at a significantly higher rate, highlighting the benefits provided by this symbiotic association.

The dynamics of nutrient transfer and N release in *Trichodesmium* is slightly more complicated as *Trichodesmium* is free living and does not need to release N to support a host. However, release of DON and ammonia by *Trichodesmium* has been observed both *in situ* and in culture (Capone *et al*. 1994; Glibert and Bronk 1994; Mulholland *et al*. 2004). Potentially, *Trichodesmium* uses N release as a mechanism to ensure all cells have access to fixed nitrogen as only specialised cells along the trichome are able to fix nitrogen (Mulholland and Capone 2000; Berman-Frank 2001). Another potential explanation for new nitrogen exudation in *Trichodesmium* is support of associated organisms, such as epibionts, which may serve in a mutually beneficial partnership as these epibionts may aid in increasing *Trichodesmium*'s acquisition of phosphorus (Van Mooy *et al*. 2012).

The physiology and nutrient transfer dynamics of the unicellular cyanobacteria is less clear, but as with DDAs, it likely that the transfer of newly fixed N from the unicellular cyanobiont to host occurs. The unicellular *Crocosphaera watsonii* has been observed in close association with a diatom host, *Climacodium frauenfeldianum* lending some evidence to this theory (Foster *et al*. 2011).

1.6.4 Cell death

Cell death among diazotrophs can be a complicated, multi-pathway process. Programmed cell death (PCD), a self-initiated cell death mechanism, is common among eukaryotes (Jiménez *et al*. 2009), and has recently been described as a prominent cell death pathway among cyanobacteria (Sigee *et al*. 2007; Zheng *et al*. 2013), and appears to be the dominate cell death pathway in *Trichodesmium* (Bar-Zeev *et al*. 2013). Various cell death pathways in *Trichodesmium* have been previously assessed, and PCD appears to be a common pathway by which *Trichodesmium* dies (Berman-Frank *et al*. 2004; Bar-Zeev *et al*. 2013). PCD can occur with ageing or following exposure to a variety of physiological stressors, such as high irradiance, nutrient starvation, and temperature shock (Berman-Frank *et al*. 2004; Jiménez *et al*. 2009). Other cell death pathways among the cyanobacteria include autophagy, necrosis and autolysis (Zheng *et al*. 2013). The cell death pathways of *Trichodesmium* will be discussed further in Chapter 5.

1.7 Fate of Diazotrophic N

Nitrogen fixed by diazotrophs eventually becomes available to the wider phytoplankton community through the previously mentioned exudation of fixation products, grazing, or breakdown of diazotroph biomass (Capone *et al*. 1994; Glibert and Bronk 1994; O'Neil *et al*. 1996; Mulholland and Capone 2001; Berman-Frank *et al*. 2004; Mulholland *et al*. 2004; Hewson *et al*. 2004). This transfer of new nitrogen to other organisms can support their growth and productivity, and potentially facilitate enhanced export of other organisms (Capone *et al*. 1998; Carpenter *et al*. 1999; Ohlendieck *et al*. 2000). Mullholland (2007) theorised that diazotroph-derived new nitrogen, specifically that which is derived from *Trichodesmium*, is likely constrained to continuous recycling in the euphotic

zone through the microbial loop, where it may eventually contribute to export indirectly via the settling/sinking of biomass of other organisms. However Mulholland (2007) also postulated that there is the potential for direct export of diazotroph biomass following grazing (Figure 1-6).

More recently, species specific physiologies have been taken into account when considering organismal fate. Many now believe that programmed cell death plays a role in the demise of *Trichodesmium* blooms (Bar-Zeev et al. 2013; Chapter 5). The ever increasing *nif*H dataset has also provided new insights into species-specific vertical distributions (Church et al. 2005), and *in situ* camera systems have revealed diazotrophs, such as *Trichodesmium* can be evenly distributed as deep at 120m (the deepest depth assessed) (Davis and McGillicuddy 2006).

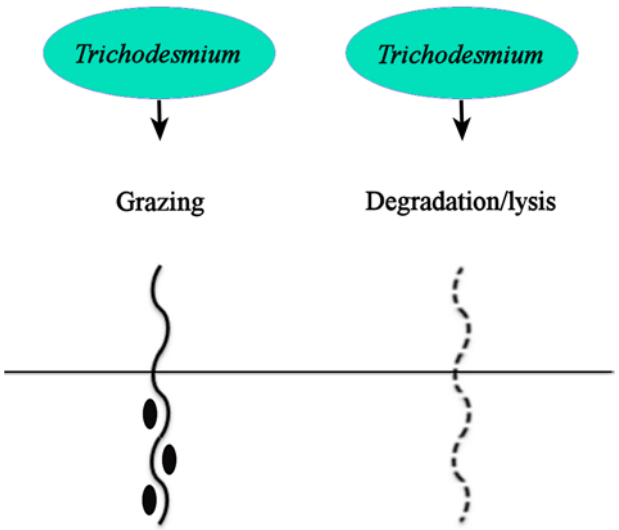

Figure 1-6. Schematic of some of the previously theorised export mechanisms for *Trichodesmium* and other diazotrophs including export of diazotroph biomass following incorporation into faecal material and secondary export following breaking down and recycling of diazotroph derived N, which is then available for incorporation into the biomass of other organisms (modified from Mulholland 2007).

1.7.1 Export of filamentous diazotrophs

Guidi *et al*. (2012) suggested that active export of *Trichodesmium* could be possible in association with downwelling eddies in the North Pacific Subtropical Gyre. Sweeping mechanisms where *Trichodesmium* would be caught up in the export of other organisms, such as diatoms, have also been used as an explanation for *Trichodesmium* presence at depth (Scharek *et al*. 1999b). Such occurrences are rarely observed, but this potenitally due to undersampling. The general consensus among the nitrogen fixation research community is that there is currently no evidence to suggest that *Trichodesmium* sinks below the euphotic zone unaided, and a recent review by Thompson and Zehr (2013) concluded that *Trichodesmium* is not likely to directly contribute to export of particulate organic matter (POM).

> "At this time there is no evidence that *Crocosphaera* or *Trichodesmium* cells sink beyond the euphotic zone, thus an oceanic regime dominated by these cell types would have patterns of C and N export very different from an ocean dominated by the symbiotic cyanobacterial N2 fixers and their hosts." –Thompson and Zehr (2013)

1.7.2 Export of heterocystous diazotrophs

Goldman (1993) hypothesized that diatom blooms resulting from new nitrogen inputs into the euphotic zone would be coupled with an export flux, specifically near the deep chlorophyll maximum (DCM). More recent data suggests larger diatoms, such as *Hemiaulus*, a known host of the diazotrophic *Richelia intracellularis*, are exported from the mixed layer, not the DCM (Scharek *et al*. 1999). Diatoms are historically important constituents of export events (Boyd and Newton 1995; Buesseler 1998; Boyd and Newton 1999; Kemp *et al*. 2000), and *Hemiaulus,* and other large autotrophs, can act as direct exporters of nitrogen, silica, and carbon to the deep sea (Scharek *et al*. 1999).

For direct export of new nitrogen out of the euphotic zone to occur, the cyanobionts, and any hosts, would need to remain intact, and their sinking rate would need to be rapid relative to the rate of remineralisation. Alldredge and Silver (1988) confirmed that diatoms are capable of reaching the sea floor intact following a bloom, but only when settling in aggregates 0.5mm or larger (Alldredge and Silver 1988). Alldredge and Gotschalk (1988) showed that the flocculation process was not only plausible, but highly likely; during diatom blooms they observed all visible diatoms aggregated into 0.1-1cm sized flocs between ten and 25m, and they additionally predicted that significant flocculation can occur in under 24 hours (Alldredge and Gotschalk 1988). Karl and others (2012) recently described an occurrence of DDAs constituting and causing the annual summer export pulse in the North Pacific Ocean over a 13- year study period (Karl *et al*. 2012), indicating that, at least in this ocean region, DDAs are integrally involved in the export of carbon and nitrogen into the oceans interior. Additionally, assessments of diazotrophic community structure and export in the Amazon River plume have revealed an association between DDA drawdown of CO_2 and increased export of POM in mesohaline environments (Subramaniam *et al.* 2008). Further, assessments of the fossil record suggest that historic diatom export was supported by diazotrophic cyanobacteria, and thus the potential for such associations is likely in a highly-stratified future ocean (Kemp and Villareal 2013).

1.7.3 Export of unicellular diazotrophs

There is no evidence that the free living unicellular diazotrophs contribute to the export of POM. However, as is seen in DDAs, the association with a host organism may increase the likelihood that these organisms contribute to export, such as following aggregation or grazing of the host.

1.8 Guide to this thesis

1.8.1 Ancillary data

The data discussed herein was collected and analysed by the author unless otherwise noted. Worthy of specific mention are the contributions of surface *nif*H abundances (Chapters 2, 4) carried out by Dr. Rebecca Langlois currently of Dalhousie University, nitrogen fixation rate measurements (Chapter 3) carried out by Dr. David Honey previously of the University of Southampton/National Oceanography Centre, Southampton, and SAPS deployment/^{234}Th measurements (Chapter 3) carried out by doctoral candidate Katsia Pabortsava of the University of Southampton/National Oceanography Centre, Southampton. Chlorophyll measurements and *Trichodesmium* cell counts for AMT17 and AMT 21 were provided by Dr. Mark Moore, and doctoral candidate Joe Snow respectively (Chapter 4).

1.8.2 Aims and objectives

Herein the role of these three groups of diazotrophs in export will be more thoroughly discussed with aims to elucidate species specific fates. In the next chapter molecular assessments are used to (1) determine if *Trichodesmium* is constrained to the upper ocean due to its innate buoyancy, (2) determine if unicellular diazotrophs are constrained to the euphotic zone due to their small size, and (3) determine if DDAs are escaping the mixed layer in the (sub-)tropical Atlantic and thus are contributing to export as is seen in the Pacific (Karl *et al.* 2012) and in river plumes (Subramaniam *et al.* 2008).

In Chapter 3 optical assessments are used to (1) determine whether *Trichodesmium* is contributing to the export flux of PON, (2) determine whether mechanisms of *Trichodesmium* export are restricted to

incorporation in faecal material, and (3) determine if remineralisation of *Trichodesmium* between the mixed layer and 500 m in the (sub-)tropical Atlantic Ocean is contributing to the N* anomaly seen in the thermocline in this region.

In Chapter 4 a combined assessment of molecular and optical cell counts was used to (1) confirm a discrepancy between *nif*H gene copies and cell counts in *Trichodesmium*, and (2) establish if polyploidy is present in this organism.

In Chapter 5 Transmission Electron Microscopy (TEM) was used to (1) determine if *Trichodesmium* is over ballasting in the surface layer, (2) determine if vertical migration is a plausible explanation for *Trichodesmium* colony presence below the mixed layer, and (3) establish whether other cell death pathways influence sinking in this organism.

1.8.3 Hypotheses

***H*$_1$**: *Trichodesmium* is not a likely constituent of export

i. Supporting evidence:
    1. *Trichodesmium* is a buoyant organism and has historically rarely been reported in sediment trap samples (Scharek et al. 1999; Chen et al. 2003).

***H*$_2$**: Remineralisation of *Trichodesmium* between the mixed layer and 500 m, north of the equator in the Atlantic, is contributing to the N* anomaly seen in the thermocline of the northern subtropical gyre, while DDA export likely results in sequestration of carbon and nitrogen rather than remineralisation.

i. Supporting evidence:
    1. The N* anomaly in the subtropical thermocline indicates excess nitrate accumulation in this region (Hansell et al. 2007).

2. Nitrogen fixation influence is assumed, but at current no mechanism is described for the transfer of diazotroph-derived new nitrogen to depth (Hansell et al. 2004).
3. DDAs have been seen intact in sediment traps up to 4000 m previously (Scharek et al. 1999; Karl et al. 2012).

H_3: There are multiple mechanisms by which diazotroph export occurs

i. Supporting evidence:
    1. *Trichodesmium* has been documented in association with a copepod that was observed to graze minimally upon it (Eberl and Carpenter 2007).
    2. Carbohydrate ballasting in *Trichodesmium* has been documented and vertical migration has been proposed as a mechanism by which the organism can access enhanced phosphate concentrations in deeper waters for nutrient mining (Villareal and Carpenter 2003); therefore, passive sedimentation is a potential export mechanism for this organism.
    3. *Trichodesmium* has been documented in sediment traps following diatom blooms (Scharek et al. 1999), which indicates a sweeping mechanism following incorporation in aggregates is a plausible mechanism of export.

H_4: Over ballasting of *Trichodesmium* in the surface layer is causing it to sink past phosphocline and terminating the ability for the colony to return to the surface.

i. Supporting evidence:

1. Models predict that ballasting for nutrient mining is feasible, but colonies could only reach depths of 150 m and maintain the ability to return to the surface if they were large (>1500um radius) (Kromkamp and Walsby 1992; White et al. 2006).

***H*$_5$**: If over ballasting is the mechanism by which *Trichodesmium* is exported, the intracellular POC/PON is high quality.

i. Supporting evidence:

1. Senescent *Trichodesmium* would not possess the ability to migrate (Villareal and Carpenter 2003).

***H*$_6$**: Gas vacuole collapse in colonies collected between 100 and 300 m guarantees sinking *Trichodesmium* at these depths lacks the ability to return to the surface.

i. Supporting evidence:

1. Depending on the species, *Trichodesmium* gas vessicles collapse between 100 and 300 m (Walsby 1978).

***H*$_7$**: Quantification of the *nif*H gene via qPCR can be directly related to cell number

i. Supporting evidence:

1. Amplification of *nif*H genes now frequently replaces optical cell counts as the method for diazotroph quantification on research cruises (Zehr et al. 1998; Langlois et al. 2008; Foster et al. 2009; Goebel et al. 2010). Luo et al (2012) acknowledged a discrepancy of an order of magnitude between gene copies and cell counts (Luo et al. 2012), but it was not pursued as 1:1 ratios of copies to counts have previously been observed in Crocosphaera watsonii (Langlois pers. comm.).

1.8.4 Thesis structure

The format of this thesis involves the presentation of chapters 2-5 as standalone pieces of work intended for submission as manuscripts. Chapter 6 is a synthesis of chapters 2-5 and discusses limitations of this study and recommendations for future work.

2. Novel molecular insights into the fate of N_2 fixed by diazotrophs

2.1 Abstract

The fate of diazotroph-derived new nitrogen and its role in marine biogeochemical cycles is not well understood. Sporadically, optical assessments of sinking particulate material have revealed the presence of two diazotrophic organisms, *Trichodesmium* spp. and *Richelia intracellularis*, outside of the mixed layer. However, assessments of diazotrophic organisms are traditionally constrained to the upper ocean; hence, the extent of diazotroph contribution to export is not clear. In an attempt to classify this occurrence, real-time quantitative PCR analysis with TaqMan probes was carried out on extracts of sinking particulate samples to 500 m to assess the presence of the *nif*H gene, which encodes the iron-binding subunit of the nitrogenase enzyme complex. Eight *nif*H phylotypes were assessed: a single filamentous cyanobacterial probe specific to *Trichodesmium*, two heterocystous cyanobacterial probes specific to *Richelia-Rhizosolenia* and *Richelia-Hemiaulus* (diazotrophic diatom associations), three unicellular cyanobacterial probes specific to *Crocosphaera watsonii* and the uncultured Group A and Group C cyanobacteria, and two non-cyanobacterial probes specific to the uncultured gammaproteobacterium Gamma A and the uncultured Cluster III. All but the Cluster III phylotype were detected in sinking particles below the mixed layer, which indicates previous assessments of the vertical distributions of these organisms may have overlooked the presence of multiple groups of diazotrophs at depth. Contrary to previous expectations, all three groups of marine diazotrophs were constituents of sinking material exported out of the euphotic zone in the subtropical and tropical Atlantic Ocean. This novel finding allows for comparisons of the distribution of *nif*H phylotypes in the surface and at depth, which aids in elucidation of species-specific fates. Quantifying the extent to which these groups are exporting provides new insight into the cycling of fixed nitrogen in the oligotrophic ocean.

2.2 Introduction

Marine diazotrophs play an important role in marine biogeochemical cycles by fixing N_2 into bioavailable forms, thus sustaining oceanic productivity over broad timescales through maintenance of bioavailable nitrogen stores. Historically, the two conspicuous groups of diazotrophs, non-heterocystous, filamentous cyanobacteria such as *Trichodesmium* and the heterocystous endosymbiotic cyanobacteria of diatoms (DDAs), were quantified optically, but the advent of molecular techniques, such as PCR, has resulted in a shift towards gene-based abundance assessments. It was not until this method became available that the unicellular nitrogen fixing Group A cyanobacterium was even detected (Zehr *et al*. 2001).

The ease of collection coupled with the large number of samples that can be analysed at once has resulted in a massive dataset of global diazotroph abundances, biomass, and nitrogen fixation rates, which continues to expand (Luo *et al*. 2012). Amplification of *nif*H, a highly conserved gene which codes for the iron binding component of the nitrogenase gene (Young 1992), allows detection of diverse groups of diazotrophs, including non-cyanobacterial *nif*H containing organisms, such as the gammaproteobacteria and green sulphur bacteria. These organisms were previously inaccessible via optical techniques, and their contribution to global nitrogen fixation remains unknown (Riemann *et al*., 2010). New *nif*H sequences are continuing to be detected (Langlois *et al*. 2005, Thompson *et al*. 2012)

Until recently, it was widely believed that *Trichodesmium* did not passively sediment out of the mixed layer, as it is buoyant, and typically occupies the surface layer in oligotrophic ocean regions (Carpenter and Price 1977, Carpenter *et al*. 2004). At least three mechanisms by which *Trichodesmium* contributes to export will be discussed in Chapter 3: free sinking, incorporation in faecal material, and incorporation in aggregates. The dominant mechanism appears to be free sinking followed by remineralisation in the upper twilight zone, which may contribute to the N* anomaly (Chapter 3) or following incorporation into the microbial loop

(Sellner 1992; Mulholland 2007). Additionally, physical mechanisms, such as eddies (Guidi *et al*. 2012) and particle sweeping (Scharek *et al*. 1999b), as well as physiological mechanisms, such as programmed cell death (PCD) (Bar-Zeev *et al*. 2013), have been described to drive and enhance *Trichodesmium* export. Any or all of these export mechanisms could potentially apply to all pelagic diazotrophic organisms (Mulholland 2007).

Many diatoms, including DDAs, are capable of contributing to export (Scharek *et al*. 1999a; 1999b, Karl *et al*. 2012). *Richelia* hosts *Rhizosolenia* and *Hemiaulus* flocculate when in dense concentrations (Alldredge and Gotschalk 1988, Villareal *et al*. 2011), and subsequently can directly export in fast sinking aggregations as Karl and others (2012) highlighted in the annual summer export pulse in the North Pacific Ocean. Karl *et al.* (2012) also speculated this occurrence may be specific to that region. What has yet to be assessed is what contribution DDAs and other diazotrophs are making to the direct export of carbon and nitrogen in other ocean regions.

Recent phylogenetic surveys of nitrogen fixers have revealed that previously undetected diazotrophs, unicellular nitrogen fixing cyanobacteria, are dominant in many marine environments (Church *et al*. 2005a; 2005b, Foster *et al*. 2009, Moisander *et al*. 2010). One such unicellular diazotroph, the Group A cyanobacterium (*Candidatus Atelocyanobacterium thalassa)* (Thompson *et al*. 2012), is an obligate symbiont, as it lacks photosystem II (Tripp *et al*. 2010). However, little is currently known about the physiology, ecology and fate of this Group A cyanobacterium. It displays similar *nif*H expression patterns to *Trichodesmium* and heterocystous cyanobacteria implying it is also an important contributor to newly fixed nitrogen into the upper ocean (Church *et al*. 2005b). Describing the presence or absence of Group A cyanobacteria in sinking material will provide vital insight into the cycling and fate of new nitrogen in this and other unicellular cyanobacterial groups.

To date, most studies of these three main groups of N_2-fixing organisms in the ocean have generally been limited to assessment of their presence and activity in the euphotic zone, while the role these organisms have in the export of material to the ocean's interior has seldom been addressed. In an attempt to track the fate of these nitrogen fixing

organisms we have quantified 4 *nif*H phylotypes in the surface and in sinking particles as deep as 500 m in the (sub-)tropical Atlantic Ocean attributable to the main diazotrophs: *Trichodesmium*, two groups of DDAs and the unicellular Group A cyanobacterium. We also amplified *nif*H from two other groups of unicellular cyanobacteria, Group B and Group C cyanobacteria, as well as two non-cyanobacterial *nif*H phylotypes, Cluster III and Gamma A, in this region.

These findings highlight that previous assessments of the vertical extent of marine diazotrophs has been under estimated, and that the fate of diazotrophic new nitrogen is not constrained to the surface layer. On the contrary, we propose that marine diazotrophs actively contribute to the export particulate organic material (POM) in the sub-tropical Atlantic Ocean. These observations of increased nitrate relative to phosphate beneath areas of high diazotroph abundance supports the potential for substantial remineralisation of diazotroph-derived organic material in the upper twilight zone along the northern part of the transect contributing to enhanced N* within the thermocline. This provides novel insight into the cycling and fate of fixed nitrogen in this region, and potentially throughout the global ocean.

2.3 Methods

2.3.1 Sample Collection

Samples for this study were collected in the (sub-)tropical Atlantic Ocean (Figure 2-1) on RRS *Discovery* D361 cruise (February and March 2011). All samples were collected using a conductivity, temperature, depth (CTD) rosette or *in situ* Stand Alone Pumping Systems (SAPS). See Table 2-1 for collection details.

During two-hour deployment, SAPS samples were collected on consecutively stacked 53 and 1 µm Nitex meshes in an attempt to separate the sinking portion of POM from suspended material. Samples were collected from depths ranging from 2 to 500 m. Upon retrieval, SAPS filters were carefully rinsed with 1L of filtered seawater to resuspend all collected material. Equal splits were the obtained using a folsom splitter. 25 mL of SAPS resuspension, representative of 47.9-85.5 L depending on total volume filtered (Table 2-1; Table A1), was filtered onto 0.7µm GF/F (Whatman) filters under low (2 mbar) vacuum pressure. To obtain surface reference samples, 2 L of CTD water was filtered onto 0.22 µm Durapore (Millipore) filters. After filtration, filters were flash frozen in liquid nitrogen and stored at -80˚C until DNA extraction.

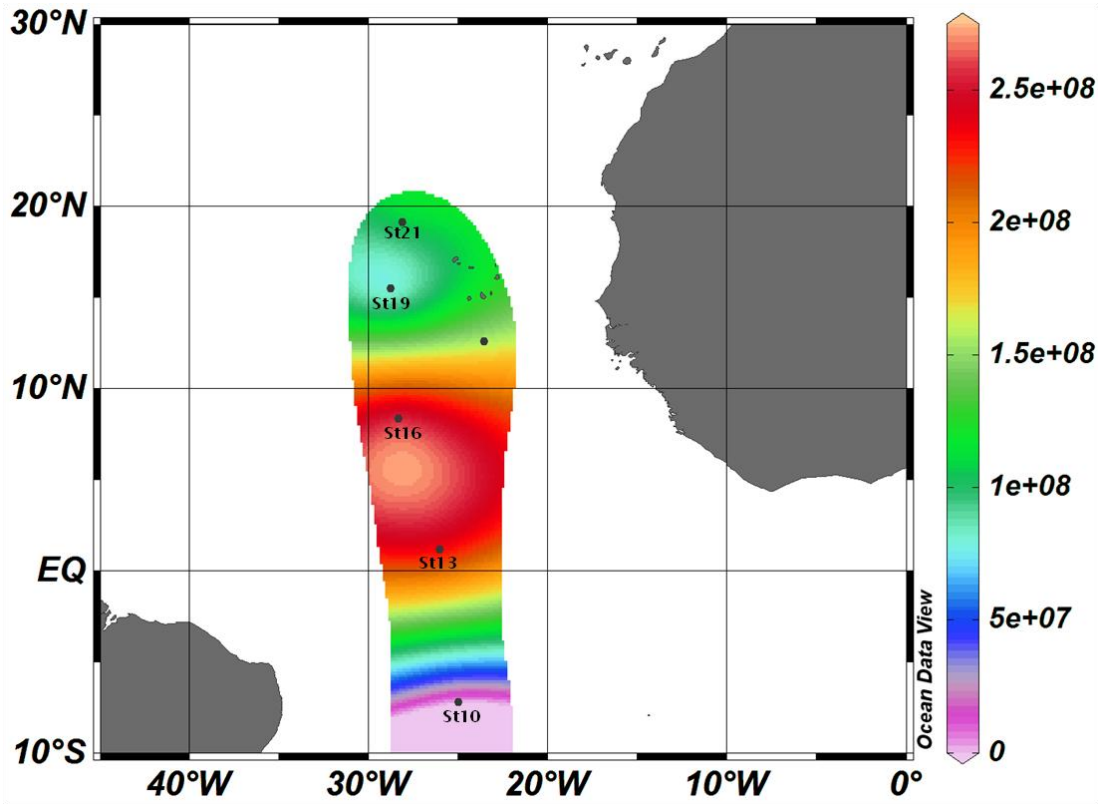

Figure 2-1. Stations sampled for *nif*H abundance on the D361. Total *nif*H abundance (gene copies m^{-3}) in surface samples reveals the peak of detectable diazotrophic *nif*H was located between the equator and 10˚N. Note that *nif*H was not detected in the surface at the southerly most station.

Table 2-1. Collection details and phylotype presence/absence

Station	Lat	Lon	Collection	Depth (m)	Size fraction (µm)	Extracted Volume (L)	Presence (+) / Absence (-) Fil	Het1	Het2	Group A	Group B	Group C	Cluster III	Gamma A
10	07˚13 S	25˚00 W	CTD	3.5	0.2	2	-	-	-	-	-	-	-	+
10	07˚13 S	25˚00 W	SAPS	70	53	51.7	+	-	-	-	-	-	-	+
10	07˚13 S	25˚00 W	SAPS	70	1	51.7	+	-	+	-	-	-	-	+
10	07˚13 S	25˚00 W	SAPS	170	53	58.6	-	-	-	-	-	-	-	-
10	07˚13 S	25˚00 W	SAPS	170	1	58.6	-	-	-	-	-	+	-	-
10	07˚13 S	25˚00 W	SAPS	500	53	54.4	-	+	+	-	+	-	-	-
13	01˚09 N	26˚02 W	CTD	21.5	0.2	2	+	+	-	+	-	+	-	+
13	01˚09 N	26˚02 W	SAPS	70	53	47.9	+	+	+	+	-	+	-	+
13	01˚09 N	26˚02 W	SAPS	70	1	47.9	-	+	+	-	-	+	-	+
13	01˚09 N	26˚02 W	SAPS	170	53	51	+	+	+	-	-	-	-	-
13	01˚09 N	26˚02 W	SAPS	170	1	51	-	+	-	-	-	+	-	-
13	01˚09 N	26˚02 W	SAPS	500	53	85.5	-	-	-	-	-	-	-	-
16	08˚20 N	28˚20 W	CTD	3	0.2	2	+	+	+	-	+	+	-	+
16	08˚20 N	28˚20 W	SAPS	70	53	50.6	+	+	+	+	+	+	-	+
16	08˚20 N	28˚20 W	SAPS	70	1	50.6	-	+	+	-	-	+	-	+
16	08˚20 N	28˚20 W	SAPS	170	53	51.3	+	-	-	-	-	-	-	-
16	08˚20 N	28˚20 W	SAPS	170	1	51.3	+	-	+	-	-	+	-	-
16	08˚20 N	28˚20 W	SAPS	500	53	53.7	+	-	-	-	-	-	-	-
19	15˚30 N	28˚23 W	CTD	1.2	0.2	2	+	+	+	+	+	+	-	+
19	15˚30 N	28˚23 W	SAPS	85	53	50.6	+	+	+	+	+	+	-	+
19	15˚30 N	28˚23 W	SAPS	85	1	50.6	-	+	+	+	+	+	-	+
19	15˚30 N	28˚23 W	SAPS	170	53	58.6	+	-	-	-	-	-	-	-

Table 2-1 continued

Station	Lat	Lon	Collection	Depth (m)	Size fraction (µm)	Extracted Volume (L)	Fil	Het1	Het2	Group A	**Group B**	**Group C**	**Cluster III**	**Gamma A**
19	15°30 N	28°23 W	SAPS	170	1	58.6	+	-	-	-	-	+	-	-
19	15°30 N	28°23 W	SAPS	500	53	52.9	+	-	-	+	-	-	-	+
21	19°10 N	28°07 W	CTD	6.2	0.2	2	+	+	+	+	+	-	-	+
21	19°10 N	28°07 W	SAPS	140	53	50.3	+	+	-	+	-	+	-	+
21	19°10 N	28°07 W	SAPS	140	1	50.3	+	-	-	+	+	+	-	-
21	19°10 N	28°07 W	SAPS	250	53	59.2	+	-	-	+	NA	NA	NA	NA
21	19°10 N	28°07 W	SAPS	250	1	59.2	-	-	-	+	NA	NA	NA	NA
21	19°10 N	28°07 W	SAPS	500	53	53.7	+	-	-	-	NA	NA	NA	NA

2.3.2 Sample Extraction and DNA Quantification

Frozen filters were manually crushed using a plastic pestle, and then samples were extracted using the Qiagen DNeasy mini plant kit according to the manufacturer's protocol. Following extraction, DNA concentrations were determined using the RediPlate 96 dsDNA Quantitation Kit (Molecular Probes). DNA concentrations were read on a Fluoroscan Ascent microplate reader.

2.3.3 *nif*H Quantification of *in situ* samples

Previously described primers and probes were chosen for amplification of 8 *nif*H phylotypes (Table 2-2). The qPCRs were run on an ABI Prism 7000 (Applied Biosystems) using cycling conditions of 2 minutes at 50˚C, 10 minutes at 95˚C, and 40 cycles of 95˚C for 15 seconds, followed by 1 minute at 60˚C. Each 25 µL qPCR reaction contained 10 pmol/µL each of the forward and reverse primers, 100 pmol/µL of the corresponding probe, 1 µL of bovine serum albumin, 5.25 µL of PCR water, 12.5 µL of TaqMan mix (Applied Biosystems), and 5 µL of template DNA from either a standard or an environmental sample (Langlois *et al.* 2008). The template DNA was equivalent to 1 to 5ng of DNA per reaction. Samples were run in duplicate and were quantified against serially diluted standards (10^7 to 10^1 gene copies). We considered C_t values, the cycle at which the amplification curve crosses the threshold of detection, above 37 to be detectable but not quantifiable (DNQ). Due to the different filter types used during collection and different volumes sampled (Table 2-1), we assume differences in collection and extraction efficiency were introduced between CTD and SAPS collected samples. Therefore, we consider this *in situ* data to be a qualitative assessment of *nif*H phylotype distribution in the study region and note that the SAPS-derived *nif*H values are likely underestimates of actual *nif*H abundance as a bias may have been introduced towards larger diazotrophs

due to prefiltration and loss during the rinsing and reconstituting of samples.

However, as our SAPS extractions are representative of much larger volumes of water than is traditionally assessed, our analyses allow for a lower limit of detection than is conventionally accepted. Gene based abundances are typically carried out on extracts derived from volumes ranging from 0.5-5 L (Langlois *et al.* 2008; Goebel *et al*. 2010; Moisander *et al*. 2010; Kong *et al.* 2011). When following a standard Qiagen DNeasy mini plant kit DNA extraction protocol, the final extract volume is typically 80 µL. 5µL of this extract is then typically added to a qPCR reaction for quantification of *nif*H. Although the assay is theoretically capable of detecting a single gene copy in the 5µL DNA template loaded, the actually volume represented would be 31.25-312.5 mL. Thus, in practice the detection limit when working with an example volume of 2L would be ≥8 copies per litre. These large volume SAPS extractions afford us a unique sensitivity of detection. The limit of detection for this study in SAPS samples representative of 47.9-85.5 L therefore ranges from being able to detect a single *nif*H copy in 3-5 L.

2.3.4 Statistical Assessments

Statistical assessments of *nif*H community structure were carried out in PRIMER v6 (PRIMER-E Ltd). Raw *nif*H phylotype data was normalised to percent of total *nif*H each sample to ensure assessments were reflective of similarity between community structure and that statistical groupings were not biased towards differences in absolute abundance. Bray-Curtis dissimilarity matrices were produced to assess the differences between samples and allow for dendrogram construction. An analysis of similarities (ANOSIM) was then performed within PRIMER to test for statistically significant difference between samples.

Table 2-2. qPCR primers and TaqMan probes used in this study

Target	Primer		Probe
	Forward	Reverse	
Filamentous	TGGCCGTGGTATTATTACTGCTATC (165-189)	GCAAATCCACCGCAAACAAC (275-256)	AAGGAGCTTATACAGATCTA (206-225)
Het-1	CGGTTTCCGTGGTGTACGTT (105–124)	AATACCACGACCCGCACAAC (158-177)	TCCGGTGGTCCTGAGCCTGGTGT (133-155)
Het-2	TGGTTACCGTGATGTACGTT (106-124)	AATGCCGCGACCAGCACAAC (158-177)	TCTGGTGGTCCTGAGCCTGGTGT (133-155)
UCYN-A	TAGCTGCAGAAAGAGGAACTGTAGAAG (50–76)	TCAGGACCACCGGACTCAAC (146–127)	TAATTCCTGGCTATAACAAC (98-117)
UCYN-B	TGCTGAAATGGGTTCTGTTGAA (54–75)	TCAGGACCACCAGATTCTACACACT (146–122)	CGAAGACGTAATGCTC (87–102)
UCYN-C	TCTACCCGTTTGATGCTACACACTAA (1–26)	GGTATCCTTCAAGTAGTACTTCGTCTAGCT (112–83)	AAACTACCATTCTTCACTTAGCAG (32–55)
Gamma A	TTATGATGTTCTAGGTGATGTG (240–266)	AACAATGTAGATTTCCTGAGCCTTATTC (321–294)	TTGCAATGCCTATTCG (275–290)
Cluster III	ACCTCGATCAACATGCTCGAA (175–195)	GCAGACCACGTCACCCAGTAC (267–247)	CCTGGACTACGCGTTC (225–240)

All sequences are 5' to 3' and relate to the 324-base *nif*H segment, and come from Langlois *et al.* 2008 and Foster *et al.* 2007

2.4 Results

2.4.1 *nif*H abundance of *in situ* samples

Apart from station 10 (Figure 2-2A-B, purple), where *nif*H was rarely detectable and surface abundance consisted solely of the non-cyanobacterial *nif*H phylotype Gamma A, total *nif*H detected below the mixed layer was consistently lower than surface *nif*H by at least an order of magnitude, and abundance generally decreased with depth at stations north of the equator.

As SAPS collected samples were originally prefiltered during collection onto 53 µm and 1 µm filters, thus excluding anything smaller than 1 µm for samples collected at 10 and 100 m below the mixed layer and anything smaller than 53µm for samples collected at 500 m, we can assume all SAPS collected samples are underestimations of actual *nif*H abundance, and that we have under sampled the unicellular cyanobacterial and non-cyanobacterial *nif*H. However, as the >53µm size fraction is considered to represent sinking material, we are confident that these samples have captured an accurate representation of the *nif*H associated with diazotrophs within this larger size fraction of POM, such as *Trichodesmium* and the DDAs.

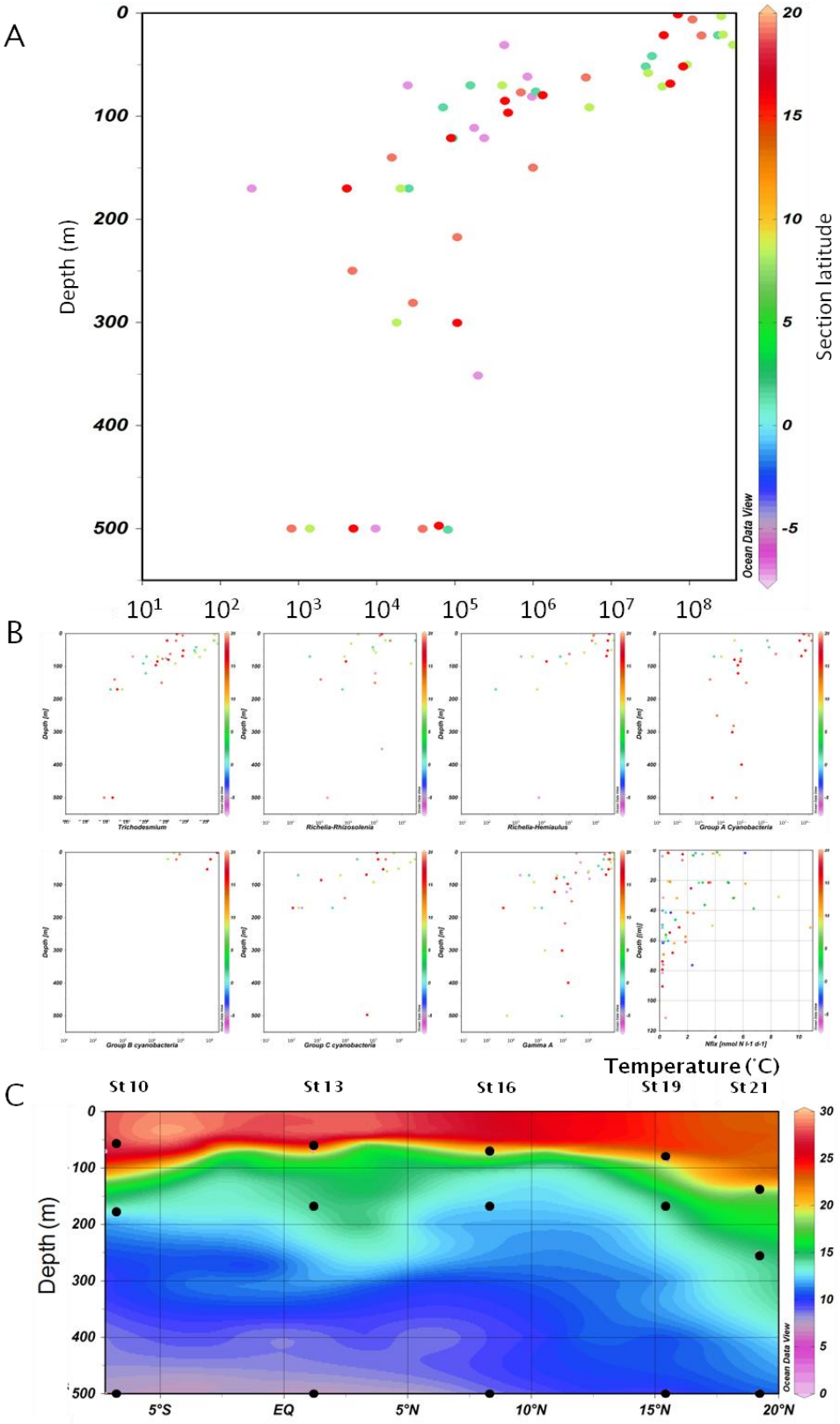

Figure 2-2. (A) Total *nif*H detected in each sample at each station (latitudinal color bar) along the north-south transect from 2 – 500 m illustrating rapid attenuation of *nif*H with depth. Note log scale. (B) Individual phylotype *nif*H detected at depth alongside water column nitrogen fixation rates. (C) Latitudinal section of temperature (˚C) along the north-south cruise transects demonstrating nearly all SAPS samples collected below 100 m were outside of the mixed layer.

2.4.2 Dominance and distribution all phylotypes

Gamma A non-cyanobacterial *nif*H and *Trichodesmium*-attributable *nif*H were ubiquitous in this study region with detectable *nif*H for these phylotypes at every station (Figure 2-4). Group B and C cyanobacteria *nif*H abundances were maximal at stations 19 (15˚30 N) and 16 (8˚20 N) respectively, but Group A and *Trichodesmium*-associated *nif*H dominated total *nif*H community structure at these stations (Figure 2-4).

The non-cyanobacterial *nif*H phylotype Cluster III was undetectable in all samples. As the standard curves were normal for this phylotype (Figure 2-3), we assume it was not present in this study region. All other phylotypes assessed were found outside of the mixed layer (60 - 130 m) at at least one station along the cruise transect. Excluding zero values, the abundance of total *nif*H detected in each sample varied from 253 gene copies m^{-3} in the 170 m sample at the southern most station, 7˚13 S (station 10), to 25.7 x 10^{7} gene copies m^{-3} in the surface sample at 8˚20 N (station 16) (Figure 2-4).

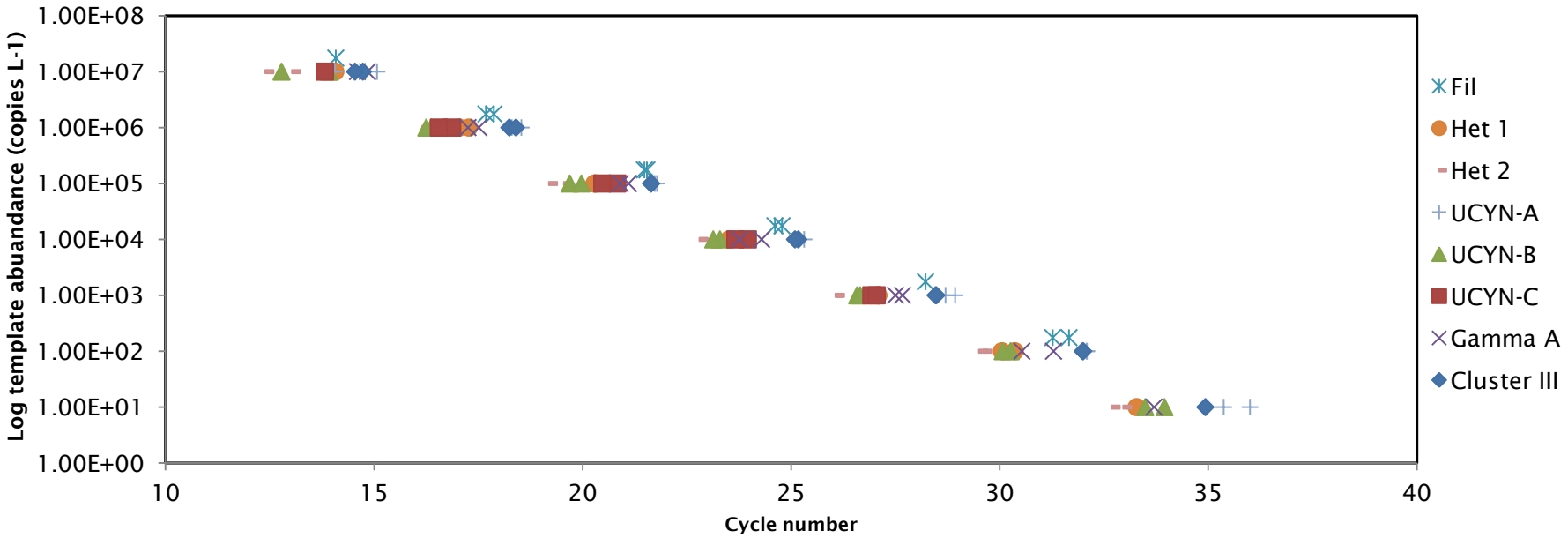

Figure 2-3. Standard curves for qPCR assessments of serially diluted standards for all eight phylotypes. $R^2 = 0.999$ for the filamentous standard (Fil, blue asterisks); $R^2 = 0.991$ for the *Richelia-Rhizosolenia* standard (Het1, orange circles); $R^2 = 0.999$ for the *Richelia-Hemiaulus* standard (Het2, pink rectangles); $R^2 = 0.999$ for the Group A cyanobacteria standard (UCYN-A, blue crosses); $R^2 = 0.998$ for the Group B cyanobacteria standard (UCYN-B, green triangles); $R^2 = 0.984$ for the Group C cyanobacteria standard (UCYN-C, red squares); $R^2 = 0.998$ for the Gamma A standard (purple crosses); $R^2 = 0.997$ for the Cluster III standard (blue diamonds).

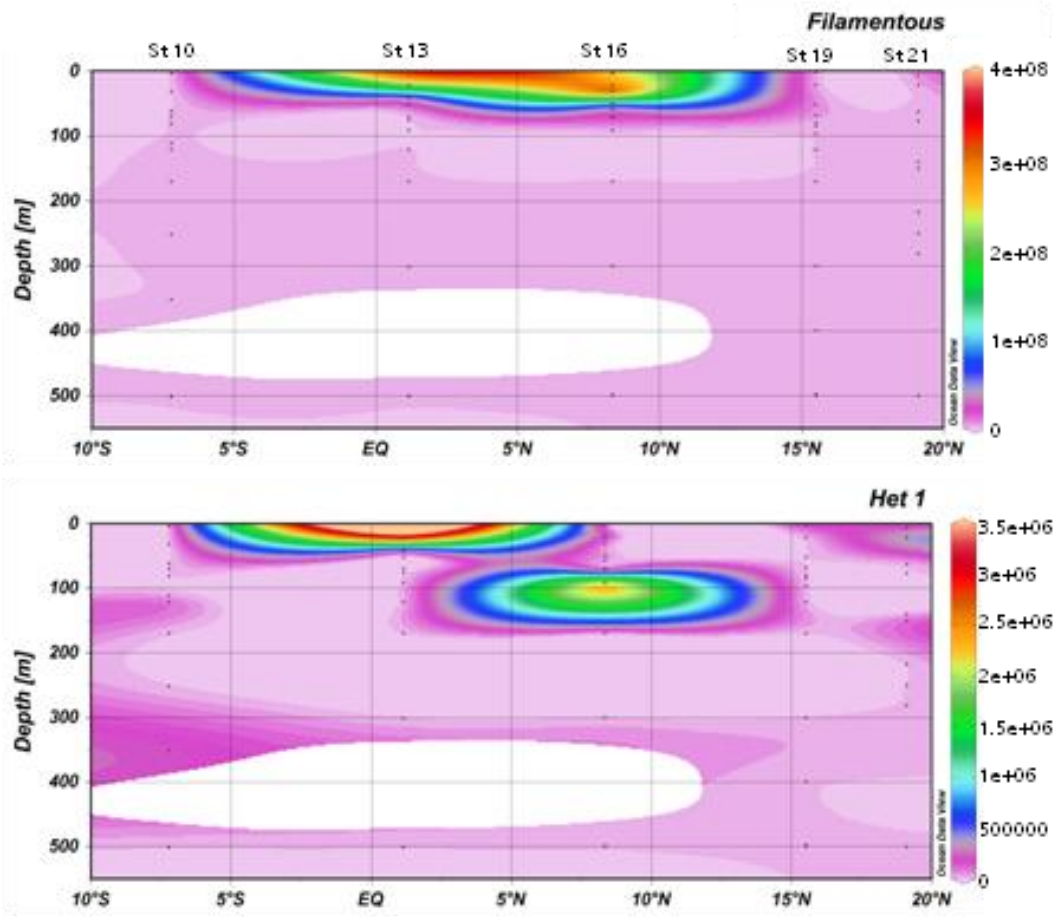

Figure 2-4. Latitudinal sections of absolute *nif*H phylotype abundance (gene copies m^{-3}) along the D361 transect demonstrating unicellular affinity for higher latitudes and cooler temperatures, filamentous *nif*H localisation just north of the equator, and the ubiquity of the non-cyanobacterial Gamma A *nif*H in the surface layer. Note varying scales.

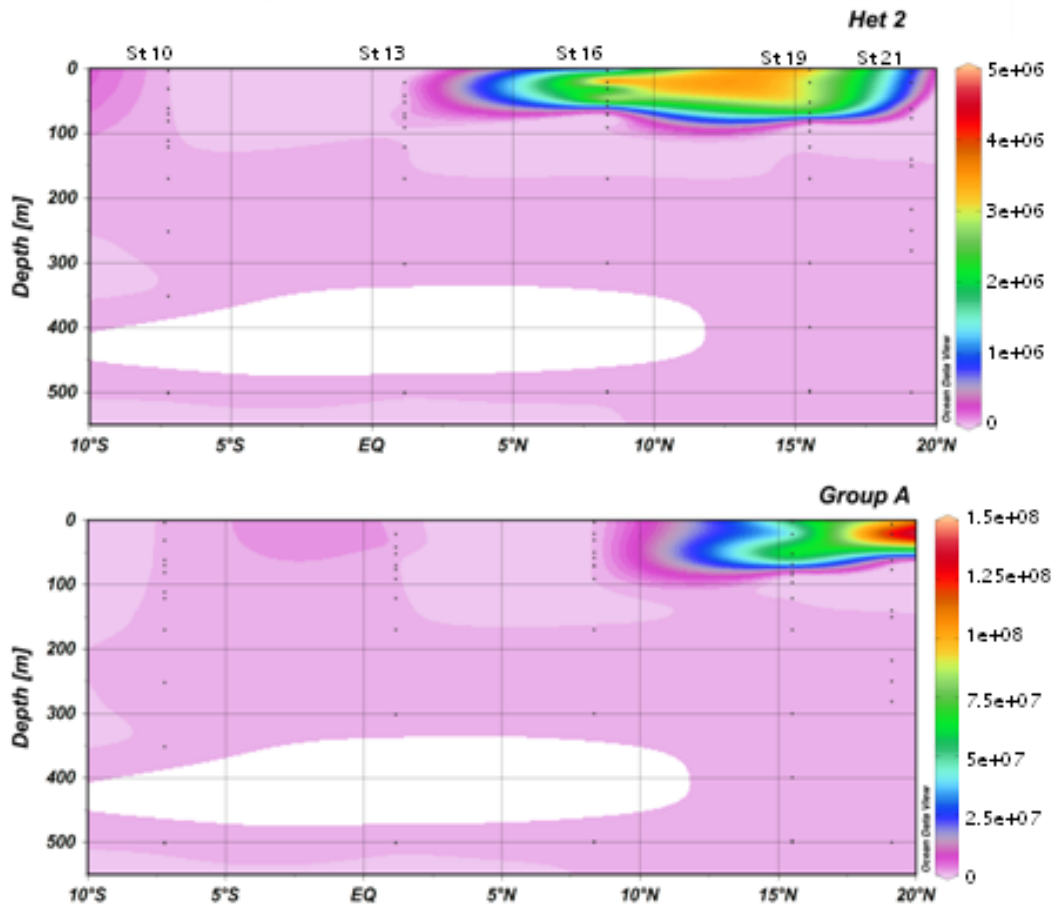

Figure 2-4 Continued. Latitudinal sections of absolute *nif*H phylotype abundance (gene copies m^{-3}) along the D361 transect demonstrating unicellular affinity for higher latitudes and cooler temperatures, filamentous *nif*H localisation just north of the equator, and the ubiquity of the non-cyanobacterial Gamma A *nif*H in the surface layer. Note varying scales.

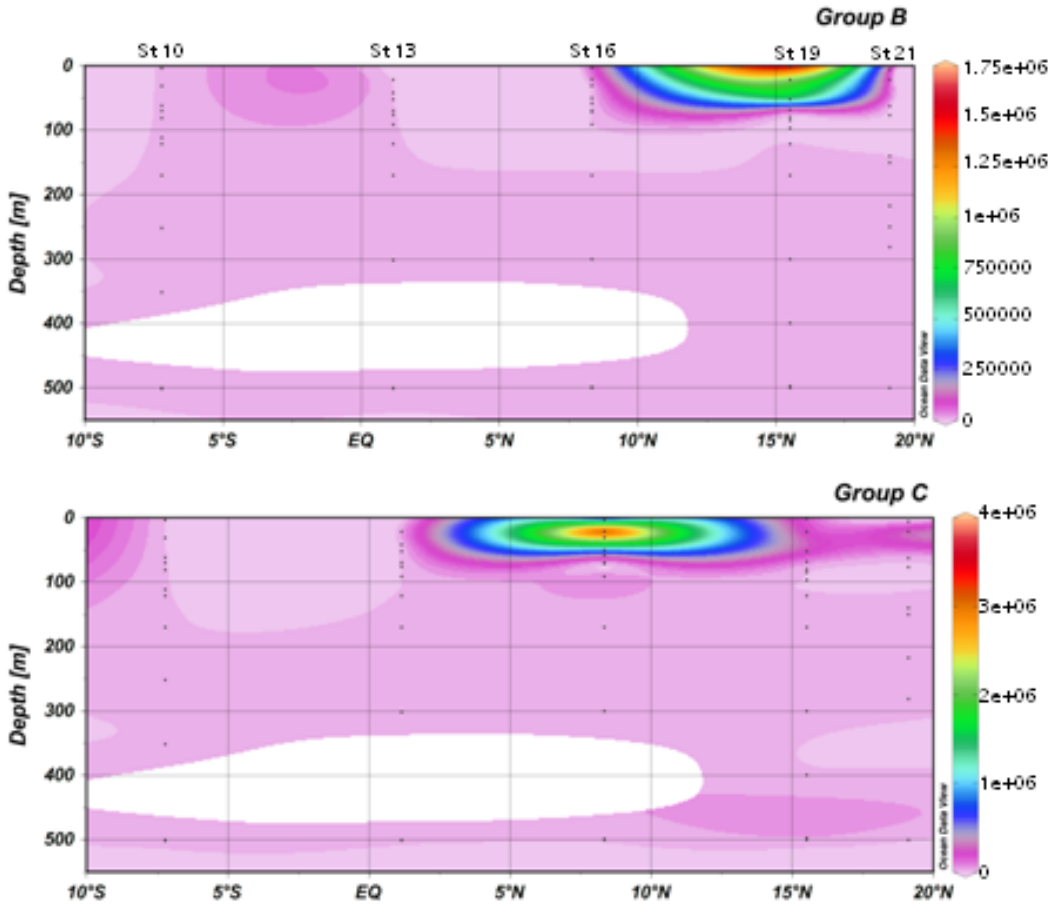

Figure 2-4 Continued. Latitudinal sections of absolute *nif*H phylotype abundance (gene copies m^{-3}) along the D361 transect demonstrating unicellular affinity for higher latitudes and cooler temperatures, filamentous *nif*H localisation just north of the equator, and the ubiquity of the non-cyanobacterial Gamma A *nif*H in the surface layer. Note varying scales.

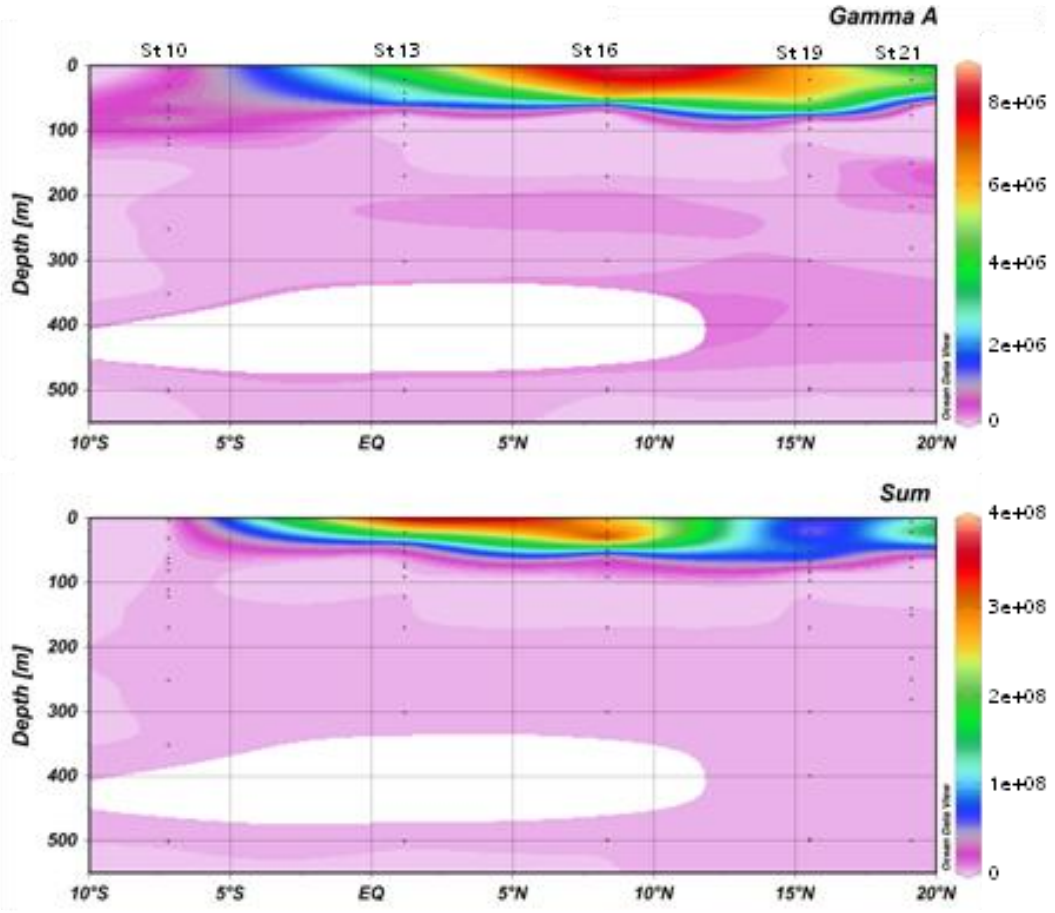

Figure 2-4 Continued. Latitudinal sections of absolute *nif*H phylotype abundance (gene copies m^{-3}) along the D361 transect demonstrating unicellular affinity for higher latitudes and cooler temperatures, filamentous *nif*H localisation just north of the equator, and the ubiquity of the non-cyanobacterial Gamma A *nif*H in the surface layer. Note varying scales.

2.4.3 *nif*H dominance and distribution of the four main diazotroph phylotypes

I was unable to detect *nif*H from any of the four main groups of cyanobacterial diazotrophs (Group A unicellular, filamentous, and both heterocystous phylotypes) in the 500 m sample at station 13 (1˚09N) and in the 2 m and 170 m samples at the southerly most station (station 10, 7˚13 S). All other samples had diazotrophic community structure which could be characterised by dominance by a single *nif*H phylotype.

Unicellular Group A cyanobacterial-attributable *nif*H was dominant in the surface samples at the northerly most stations 19 (15˚30 N) and 21

(19°10 N), while *Trichodesmium*-attributable *nif*H dominated the surface samples between the equator and 10° N. This relationship was not consistent in deeper samples, such as the northerly most station, station 21, where *Trichodesmium*-attributable *nif*H was the sole component of the 500 m sample (Table 2-1). Among the four main groups of cyanobacterial diazotrophs, Bray Curtis dissimilarity and ANOSIM assessments did not reveal any statistically significant grouping of *nif*H phylotype dominance with latitude (Figure 2-5). At all stations except for the southerly most station, station 10 (7°13 S), *nif*H phylotypes that were present in samples outside of the mixed layer were also present in the surface sample. However, the dominant *nif*H phylotype in a surface sample was not always the dominant *nif*H phylotype in the deeper samples at the same station, such as at stations 19 and 21 where Group A was dominant at the surface, while *Trichodesmium* was dominant below the mixed layer (Figure 2-5), and total *nif*H abundance was highly variable.

Trichodesmium-attributable *nif*H constituted the majority of detectable *nif*H in the surface layer between the equator and 10°N, where it composed 98.1 and 99.6% of total detectable *nif*H at stations 13 (1°09 N) and 16 (8°20 N), respectively. *Trichodesmium nif*H dominance was also echoed in deeper samples at these stations at 10 m below the mixed layer composing 66.2% of diazotroph community structure at station 13 and 94.7% at station 16. *Trichodesmium*'s surface dominance was replaced by unicellular diazotrophs to the north, where Group A cyanobacteria contributed 89.5 and 93.0% to total detectable *nif*H in the surface samples at stations 19 and 21 (Figure 2-5). *Trichodesmium nif*H was dominant in deeper samples at these stations at 10 m below the mixed layer composing 80.6% of *nif*H community structure at station 19 and 43.5% at station 21.

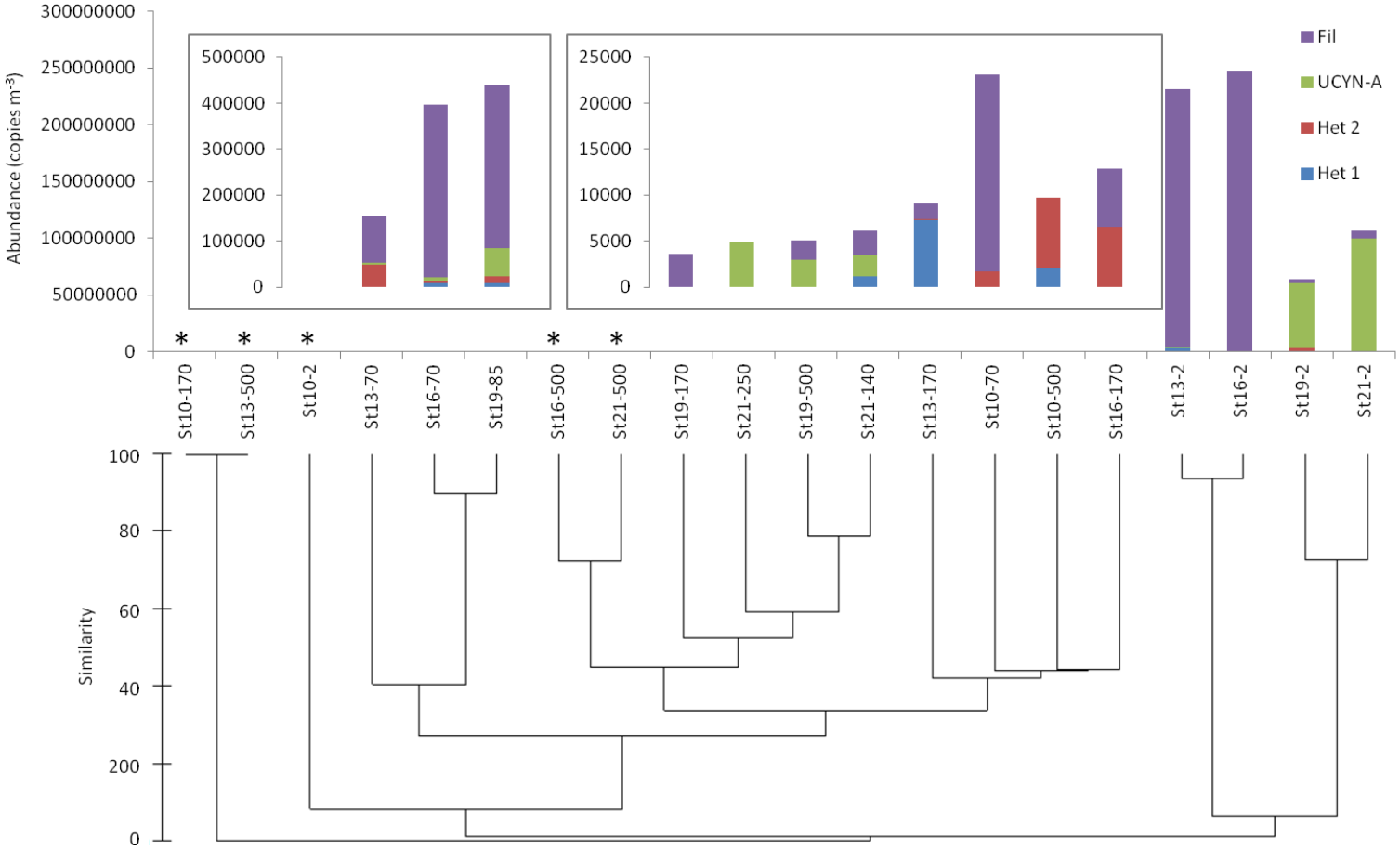

Figure 2-5. Bray Curtis dissimilarity dendrogram of *nif*H diversity normalised to total *nif*H in each sample. Relative proportions of *nif*H phylotypes within each sample are indicated by colour distributions in each bar: *Trichodesmium*-attributable *nif*H (purple), Group A Cyanobacteria-attributable *nif*H (green), *Hemiaulus-Richelia*-attributable *nif*H (red), and *Rhizosolenia-Richelia*-attributable *nif*H (blue); bar height represents absolute *nif*H abundance in each sample. Starred samples represent no *nif*H detection or absolute *nif*H abundance below 1000 copies m^{-3}. Sample labels are displayed at the station number followed by the depth of the sample.

2.5 Discussion

These results indicate that filamentous, heterocystous, and unicellular diazotrophs are escaping the surface layer and are all potentially contributing to particulate export in this study region. The mechanisms by which this is occurring are not well defined, but we speculate a cumulative influence of passive sedimentation, aggregation, and grazing, as is described for *Trichodesmium* via optical observations in Chapter 3. Guidi *et al*. (2012) have also suggested active export of *Trichodesmium* would be possible in association with eddies in the North Pacific Subtropical Gyre. This may also be important in this study region where enhancement of POC export by eddies has been previously observed (Sweeney *et al*. 2003, Davis and McGillicuddy 2006). We assume enhancement of diazotroph export by eddies would not be restricted to *Trichodesmium* and would likely influence the fate of all diazotroph-derived new nitrogen. Additionally, other mechanisms exist whereby diazotroph-derived N could contribute to export fluxes secondarily, following incorporation into other material, such as following viral lysis of the cells (Hewson *et al*. 2004) or extracellular release of fixation products (Glibert and Bronk 1994, Foster *et al*. 2011).

The symbiotic association between the Group A unicellular cyanobacterium, *A. thalassa,* and its haptophyte host (Thompson *et al*. 2012) implies there is also the potential for this group to contribute to export via a variety of mechanisms, such as 'export by association' if the host is apt to aggregation or is grazed upon. The host of *A. thalassa* is closely related to the heavily calcified coccolithophore genus *Braarudosphaera*, which is well documented in the fossil record (Kelly *et al*. 2003) suggesting its relatives may also be susceptible to sinking and thus contributing to export. This data revealed Group A specific *nif*H was present at 500 m in the open ocean, and *nif*H specific to Group A unicellular cyanobacteria has previously been amplified in coastal sediment samples (Thompson and Zehr 2013) suggesting the loss of new nitrogen within Group A from the euphotic zone is potentially a widespread occurrence. Similarly, some Group B unicellular cyanobacteria are known to associate with the diatom *Climacodium frauenfeldianum* (Carpenter

and Janson 2000; Foster *et al*. 2011), and may also be susceptible to export by association as is seen with the DDAs *Richelia-Rhizosolenia* and *Richelia-Hemiaulus* (Karl *et al*. 2012).

Historically, *Trichodesmium* is thought to be the dominant nitrogen fixing organism in this study area (Tyrrell *et al*. 2003, Moore *et al*. 2009, Zehr 2011, Groβkopf *et al*. 2012), and is potentially capable of accounting for the majority of the geochemically derived rates of nitrogen fixation inferred from the N* distributions in the North Atlantic (Gruber and Sarmiento 1997, Capone *et al*. 2005, Mahaffey *et al*. 2005, Hansell *et al*. 2004, 2007). These results indicate *Trichodesmium*'s dominance is restricted to the surface layer between the equator and 10°N. Farther to the north unicellular diazotrophs compose the majority of *nif*H community structure. This was not consistently echoed in deeper samples, which implies that *Trichodesmium* may be more likely to sink out of the mixed layer than Group A cyanobacterium. As only a >53 µm size fraction sample was taken at 500 m depth and the association between Group A and its host is known to be very weak (Tripp *et al*. 2010), the 500 m collections may have under sampled Group A, specifically at particle-light station 21, where turbulence from the pump could cause disassociation of the cyanobacterium from its host and loss of the former through the large mesh size. The presence of Group A in the 500m sample at station 19 highlights the potential for Group A to reach this depth and thus it's potential to transport new nitrogen out of the upper ocean. The 500 m sample at station 19 had nearly double the POC as the station 21 sample at the same depth (0.44 vs. 0.26 µgC L^{-1}) implying that even if Group A became detached from its host during collection, there may have been retention of the cyanobacterium on the filter by all of the other particulate material present. Future investigation of the diversity and abundance of *nif*H containing organisms at depth using a qPCR approach will require optimisation of the sampling procedures to ensure that larger volume collections are representative of an unbiased sample.

South of the equator at station 10, diazotroph abundance was minimal, and *nif*H was undetectable at the surface (Figure 2-4); this is likely to be due to the lack of the iron-rich aerosol deposition in this region, which is known to support diazotrophic growth north of the equator (Moore *et al*. 2009). At 10 m below the mixed layer, *nif*H from *Trichodesmium* and *Richelia-Hemiaulus* contributed 92.7% and 7.3% to diazotrophic community structure respectively.

The presence of these diazotrophs at depth, but not at the surface implies a temporal component to these findings; it is likely that in the days prior to the sampling these organisms were present in the surface, but sank or were otherwise transported to depth before we encountered them. In the 500 m sample at station 10 *Trichodesmium*-attributable *nif*H was undetectable, but *Richelia-Hemiaulus* and *Richelia-Rhizosolenia* attributable *nif*H, was present and composed 78.7% and 21.3% of diazotrophic community structure respectively.

The complete absence of the Cluster III *nif*H phylotype in this study region is unexpected. The Cluster III *nif*H phylotype may be particularly important in the oligotrophic North Pacific Ocean where it has been seen to dominate *nif*H communities in the lower photic zone (Church *et al*. 2005a) or in the western subtropical Atlantic Ocean where it has been observed previously (Langlois *et al*. 2008). However, previous reports of its distribution have documented an affinity for cooler temperatures than were observed in this study (Farnelid *et al*. 2011). Langlois *et al*. (2008) observed this phylotype to be associated with mean water temperatures of 18˚C, which is 5˚C cooler than the lowest temperature encountered on this transect. Cluster III specific *nif*H has also been found to dominate *nif*H community structure in the Arctic (Farnelid *et al*. 2011).

Furthermore, Cluster III anaerobes have previously been described to associate with zooplankton (Braun *et al*. 1999). The lack of Cluster III detection may be due to methodology as “swimmers” (zooplankton) were picked from SAPS filters following collection and were not subsequently included in DNA extraction. This zooplankton associated *nif*H is not well defined. If Cluster III *nif*H is expressed and nitrogen fixation is occurring inside zooplankton, this highlights an opportunity to explore whether faecal pellets contain new nitrogen, thus further contributing to export.

The majority of qPCR *nif*H assessments to date have come from small volume samples in the upper ocean, which may highlight an under-sampling bias both in vertical extent and sample volume. Church *et al*. (2005a) assessed *nif*H phylotype diversity in 1L samples as deep as 200 m, and found that Group B and Cluster III *nif*H was still detectable in the deepest samples while Group A and *Trichodesmium nif*H was not. Potentially these phylotypes were present, but under the detection limit, and would have been revealed with larger

volume sampling. This idea is supported by optical observations of *Trichodesmium* in the 150 to 200 m depth range and below in this (Chapter 3) and other studies (Carpenter and Price 1977; Scharek *et al*. 1999b). Additionally, the detection of *Trichodesmium* and Group A associated *nif*H in larger volume samples in this study provides further support for the idea that previous assessments have under-evaluated *nif*H presence at depth.

2.6 Conclusion

These results suggest that filamentous, heterocystous, and unicellular diazotrophs are all being removed from the mixed layer and are likely to be involved in the export of PON through a variety of potential mechanisms. Previously *Trichodesmium* and *R. intracellularis* have only been observed to contribute to export following incorporation in fecal pellets or following surface blooms (Scharek *et al*. 1999a; 1999b, Mulholland 2007), and it has only recently been suggested that Group A unicellular cyanobacteria could contribute to export by association with their host (Thompson and Zehr 2013). Further investigation of the mechanisms contributing to diazotroph presence in sinking material will give a clearer idea of the fate of the nitrogen fixed by these organisms and hence expand the definition of their biogeochemical roles.

Quantitative PCR of the *nif*H gene is clearly a fundamental tool in the study of marine diazotrophs and comparison of the distributions of various *nif*H phylotypes in the surface and at depth will aid in the elucidation of species specific fates. This work represents some of the first comprehensive qPCR analyses of *nif*H in marine snow and other sinking particulate material and thus provides vital insight into the contribution *nif*H containing organisms are making to export.

Quantifying the extent to which these groups are exporting will provide novel insight into the cycling of fixed nitrogen in the oligotrophic ocean and determining the fate of newly fixed nitrogen by nitrogen fixers will provide insight to the nitrogen budget through delineation of utilised, remineralised,

and deep-ocean-sequestered fixation products. Contrary to previous expectations, results suggest that all three groups of marine diazotrophs are constituents of sinking material and are exported out of the euphotic zone in the subtropical and tropical Atlantic Ocean. Diazotrophs play a vital role in global biogeochemical cycles by providing significant amounts of newly fixed nitrogen to surface ocean globally. As we assume for *Trichodesmium* (Chapter 3), some of that new nitrogen could potentially be injected into the water column below the mixed layer following remineralisation, which in turn could contribute to the N* anomaly.

3. Describing the presence of *Trichodesmium* spp. in sinking material

3.1 Abstract

Trichodesmium plays a major role in ocean biogeochemical cycling through supplying fixed nitrogen to the warm surface ocean. However, the subsequent fate of the nitrogen fixed by *Trichodesmium* and its role in the biogeochemistry of deeper waters has yet to be established. We examined the loss of *Trichodesmium* derived organic carbon and nitrogen from the surface ocean to the ocean interior through sinking/settling. Sinking particles were collected and assessed for *Trichodesmium* presence in the subtropical and tropical Atlantic Ocean. *Trichodesmium* was commonly present below 100 m in three forms: tufted colonies, free filaments, and free filaments associated with aggregations of other organisms and faecal matter. We collected negatively buoyant *Trichodesmium* colonies sinking at 12 - 120 m d^{-1} between depths of 80-250 m in all regions where *Trichodesmium* was a significant component of the surface population. Free filaments were also observed in low concentrations as deep as 500 m. Contrary to the previous belief that *Trichodesmium* was constrained to the surface layer and did directly contribute to export, these results suggest that despite its buoyancy during active growth, *Trichodesmium* can be an important constituent of sinking material with an average of 8.8% of the surface *Trichodesmium* standing stock leaving the mixed layer each day. Biomass estimates suggest that *Trichodesmium* contributes 0.4-3% of the total particulate organic nitrogen (PON) standing stock directly beyond the mixed layer and an average of 5.6% of the total PON flux leaving the mixed layer along a latitudinal transect in the Atlantic Ocean. These results provide some of the first characterizations of the mechanisms by which *Trichodesmium* (and diazotrophs in general) could contribute to the N* anomaly observed in the thermocline in the North Atlantic sub-tropical gyre.

3.2 Introduction

Dinitrogen fixation by marine diazotrophs constitutes the leading source of external nitrogen to the ocean (Zehr and Kudela 2011). However, with a few notable exceptions (Karl *et al*. 2012), we lack knowledge of the short term fate of the newly fixed nitrogen contributed to the surface ocean microbial community by these organisms, which limits our understanding of their integrated biogeochemical role. *Trichodesmium* is a buoyant, filamentous cyanobacterium that is found in warm oligotrophic oceans in colonial aggregations and as free trichomes (Capone *et al*. 1997), and is the most conspicuous marine diazotroph. The highest abundances of *Trichodesmium* in the Atlantic have historically been observed to correlate with shallow mixed layer depth and areas estimated to have high iron deposition (i.e. between 0 and 15˚N) (Tyrrell *et al*. 2003; this study), although this relationship appears to breakdown north of this latitudinal range where *Trichodesmium* abundance has been observed to correlate more closely with temperature (Agawin *et al*. 2013).

Actively growing *Trichodesmium* populations are predominantly observed in the upper portion (0 to ~50 m) of the water column (Carpenter and Price 1977; Carpenter *et al*. 2004). Recent work has documented that *Trichodesmium* colonies can also be well distributed down to ~120 m in some regions (Davis and McGillicuddy Jr. 2006). Deeper (>50 m) populations of *Trichodesmium* have frequently been hypothesized to consist of vertically migrating colonies (Kromkamp and Walsby 1992; White *et al*. 2006). Buoyancy in *Trichodesmium* is provided by the presence of gas vacuoles (Walsby 1978), and is controlled by carbohydrate ballasting (Villareal and Carpenter 2003). Models of carbohydrate ballasting in *Trichodesmium* suggest that vertical migrations of large (≥1500 µm radius) colonies could span 200 m for nutrient mining (e.g. phosphorus acquisition) (Kromkamp and Walsby 1992; White *et al*. 2006), but are realistically more likely confined to the upper 70 m of the water column (Villareal and Carpenter 2003).

Unlike diazotrophic diatom assemblages (DDAs), which have been observed to predominate sediment trap collections in regions where both DDAs and *Trichodesmium* are present in the surface layer (Scharek *et al*. 1999b; Karl *et al*. 2012), *Trichodesmium* has rarely been reported to reach the deep ocean (>1 km) intact. Consequently, *Trichodesmium* is not thought be an important component of direct export.

The relative abundances of the macronutrients nitrate and phosphate can be used to infer inputs and loss of nitrogen through the biological processes of nitrogen fixation and denitrification respectively (Gruber and Sarmiento 1997). The derived N* tracer (Chapter 1, equation 1) (Gruber and Sarmiento 1997; Hansell *et al*. 2004, 2007; Moore *et al*. 2009), indicates deviation of the local nitrate and phosphate pools from the N:P ratio of typical particulate organic matter (POM), assumed to have a canonical value of 16:1 (Redfield 1934). Gradients of increasing N* can hence be used to infer a net gain of nitrogen through nitrogen fixation or other sources (Gruber and Sarmiento 1997; Hansell *et al*. 2004, 2007), which are discussed in more detail in Chapter 1. Throughout the majority of the global ocean, N* is negative within the thermocline and in deeper waters (Gruber and Sarmiento 1997; Moore *et al*. 2009). However, north of the equator in the Atlantic there is a positive N* anomaly in the subtropical thermocline to ~1100 m (Hansell *et al*. 2007) (Figure 3-1). Moreover the isotopic signature of the nitrate pool in the subtropical North Atlantic thermocline indicates that newly fixed nitrogen is contributing to this N* anomaly (Gruber and Sarmiento 1997; Karl *et al*. 2002; Knapp *et al*. 2008).

Various studies have inferred nitrogen fixation rates in the Atlantic on the basis of both the N* anomaly (Gruber and Sarmiento 1997; Hansell *et al*. 2004, 2007) and the isotopic anomaly of the nitrate pool (Knapp *et al*. 2008), with the range of recent estimates spanning 0.4 – 2 Tmol N year $^{-1}$ (Gruber and Sarmiento 1997; Hansell *et al*. 2004, 2007; Knapp *et al*. 2008). *Trichodesmium* appears to be the dominant nitrogen fixing organism in the tropical and sub-tropical North Atlantic (Tyrrell *et al*. 2003; Moore *et al*. 2009; Groβkopf *et al*. 2012) potentially fixing around 1.6 Tmol N year^{-1} (Capone *et al*. 2005).

Consequently this organism may contribute a significant, if not the dominant fraction of the geochemically derived estimates of nitrogen fixation in the region (Capone *et al*. 2005; Mahaffey *et al*. 2005).

For nitrogen fixation to be capable of explaining some of the anomaly in N* within the North Atlantic thermocline, a mechanism is required for newly fixed nitrogen to be transferred to depth (Hansell *et al*. 2004, 2007), such as remineralisation of diazotroph biomass and advection of resultant nutrients (Yoshikawa *et al*. 2013) or active transport of diazotroph biomass to depth via eddies (Guidi *et al*. 2012). If nitrogen fixation by *Trichodesmium* is to be capable of contributing significantly to the anomaly in N* within the North Atlantic thermocline and consequential phosphate depletion in surface waters of the gyre (Wu *et al*. 2000; Moore *et al*. 2009), such mechanisms require further investigation. Mulholland (2007) suggested *Trichodesmium*-derived material is likely recycled in the euphotic zone through the microbial loop, but could also be exported in faecal material following grazing with release of *Trichodesmium*-derived nutrients into the water column during sloppy feeding or microbial break down of faecal material (Sellner 1992). Other potential fates of *Trichodesmium*-derived newly-fixed nitrogen could follow cellular lysis, autocatalytic programmed cell death (PCD), or extracellular release of fixation products, but all previous assessment of these processes have occurred in near-surface collected or cultured samples (Capone *et al*., 1994; Glibert and Bronk, 1994; Hewson *et al*., 2004; Mulholland *et al*., 2004, 2007; Bar-Zeev *et al*. 2013). This highlights an unexplored area of the fate *Trichodesmium* in deeper waters.

The current study focuses on tracing the fate of *Trichodesmium*-derived new nitrogen through the assessment of multiple export mechanisms along a transect in the (sub-)tropical Atlantic. Determining the fate of newly fixed nitrogen by diazotrophs provides insight into nitrogen cycling through delineation of shallow, remineralised, and deep-ocean-sequestered fixation products. We document evidence of grazing on *Trichodesmium* and detail the presence of *Trichodesmium* outside of the euphotic zone as both free trichomes incorporated in sinking aggregates and unincorporated sinking colonies. When combined with ^{234}Th derived PON fluxes, observations of sinking *Trichodesmium* allow us to estimate this organism's contribution to

export fluxes. Overall, this data suggests substantial remineralisation of *Trichodesmium*-derived organic material between 100 and 500 m, which we suggest contributes to the N* anomaly observed in the thermocline of the sub-tropical gyre further to the north.

3.3 Methods

3.3.1 Sample Collection

Sampling was carried out in February-March 2011 (D361; 03 Feb 2011 – 19 March 2011) on the *RRS Discovery* during a transect spanning the (sub-)tropical Atlantic Ocean (Figure 3-1). The Marine Snow Catcher (MSC) and *in situ* Stand Alone Pumping Systems (SAPS) were used to collect sinking particles from below the Deep Chlorophyll Maximum (DCM) at the base of the euphotic zone. Hydrographic data and the depth of the DCM were determined using a CTD interfaced with a Chelsea MKIII Aquatracka fluorometer. Water column oxygen profiles were determined using a CTD mounted Sea-Bird 43 oxygen sensor. Additional measurements of *Trichodesmium* colony sinking speeds were undertaken in July 2011 (CH0711; 04 July 2011 – 27 July 2011) on the *RV Cape Hatteras* in the Gulf of Mexico.

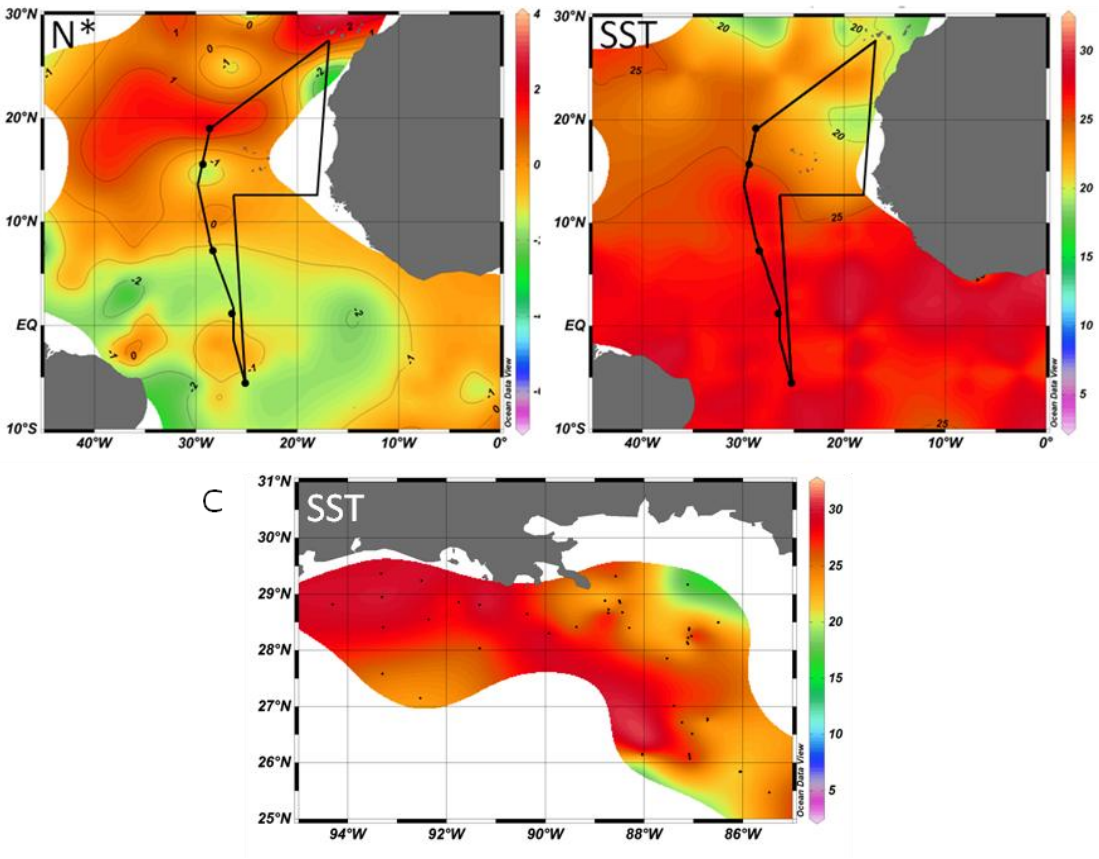

Figure 3-1. Sampling locations. (A) D361 cruise track overlain on N* (μmol kg^{-1}) along the 26.8σθ and (B) SST (degC). Data from Key *et al*. (2004). (C) CH0711 stations overlain on SST (degC) from shipboard measurements.

3.3.2 Marine Snow Catcher Deployment

The MSC (Figure 3-2A), a messenger-operated PVC closing water bottle, samples 100 L of seawater during deployment, and allows for collection of sinking particles with minimal turbulent agitation (Lampitt *et al*. 1993). The MSC allows for the separation of fast and slow sinking particulate material (Riley *et al*. 2012). After each of 9 deployments to 10 m below the DCM on D361 (35-100 m), the MSC was recovered and lashed upright on deck for 2-3 hours to allow particles to settle into a 7 L 'aquarium' chamber at the bottom of the sample column. The top 93 L of water was then drained through a 20 μm mesh and the concentrate was resuspended and preserved in 2% acidic Lugol's iodine to allow for *Trichodesmium* trichome and total cell enumeration. Once the top column was empty, it was detached from the

aquarium and any particles which had sunk to the bottom were collected from the base.

Figure 3-2. The 100L Marine Snow Catcher (A) and the particle collection technique (B): each particle was transferred from the aquarium to an individual well in a welled plate using a glass Pasteur pipette.

3.3.3 Particle Collection

Individual aggregates, faecal pellets, and whole colonies of *Trichodesmium* were picked out of the base unit using a glass Pasteur pipette and were transferred to welled plates for observation and imaging under an optical microscope and/or for use in sinking rate experiments (Figure 3-2B). Each aggregate was picked from the aquarium chamber and was immediately transferred into an individual well of a 24-well culture plate

containing 1mL of 0.2µm filtered seawater. This was done in an attempt to ensure artificial aggregation would not occur between free filaments and aggregates during storage and transfer as trichomes were observed unentangled in MSC collections in both the top column and in the aquarium chamber following the two hour settling period. *Trichodesmium* colony length was measured on a millimetre-scale ocular micrometer under a dissecting microscope at 10x magnification, with measurements were documented to the nearest 0.5 mm. Particles that were not mounted for shipboard microscope observations were preserved in either 2% acidic Lugol's iodine or 5% buffered formalin for post cruise image analysis. Handling and transfer of particles was kept to a minimum as morphological alteration of particles through physical manipulation could affect sinking rates and imaging. The water remaining in the aquarium after all visible particles had been picked out was drained through a 20 µm mesh and the concentrate was resuspended and preserved in acidic Lugol's iodine to allow for trichome and total *Trichodesmium* cell enumeration.

3.3.4 Sinking Rates

Sinking rate data was combined from the two cruises. During D361, 4 colonies collected from below 100m were used in sinking rate experiments. During the separate cruise in July 2011 (Gulf of Mexico), sinking rates for 24 additional *Trichodesmium* colonies collected between 100 and 250 m were calculated in a 2 L graduated cylinder filled with surface seawater at ambient temperature. Colonies were transferred into the measuring cylinder using a Pasteur pipette, or inoculation loop depending on *Trichodesmium* colony size. Colonies were placed just below the water surface in the settling column (Martin *et al*. 2010), then monitored settling over the 0.5m length of the column for 60 minutes, with observations performed at 5, 6, 7.5 and 10 minutes from the start of the experiment, and every 5 minutes after that. Sinking rates were then calculated based on the maximum time interval at which individual colonies reached the bottom of the cylinder. Duplicate measurements of sinking rates were made for 17 colonies, the remaining 11

colonies disassociated into free filaments between the first and second measurement.

3.3.5 SAPS Deployment

During deployment on D361 the SAPS pumped between 1000-2000 L of seawater through size fractionated (53 µm and 1 µm) Nitex meshes at 10 m, 100 m and 500 m below the base of the mixed layer (determined from temperature profiles) for sinking particle collection (collection details: Chapter 2, Table 3-1). Once recovered, particles were rinsed off the meshes with 1 L of filtered seawater and the resuspension was split into four equal parts with a Folsom splitter, one of which was preserved in 2% acidic Lugol's iodine for microscope counts. Another split was filtered onto pre-combusted (450˚C for 12 hours) 25 mm diameter, 0.7 µm pore size Whatman GF/F for particulate organic carbon and nitrogen (POC/PON) analysis post-cruise. POC/PON samples were fumed with 37% HCl for 24hrs, dried, pelleted in pre-combusted aluminium capsules and analyzed for organic carbon and nitrogen with a CHN analyzer (Thermo Finnigan EA 1112 Series Flash Elemental Analyzer).

3.3.6 *Trichodesmium* Enumeration and Biomass Estimation

Colony and trichome counts were performed on preserved samples. Cell abundance was directly measured for free trichomes as the number of cells per trichome was easily quantifiable, while the lengths of free trichomes were variable (Figure 3-3). When *Trichodesmium* was present in aggregates and faecal pellets, cell counts were performed for visible material only. Surface abundances of *Trichodesmium* were determined by gravity filtering a 20 L CTD surface bottle through a 47 mm diameter 10 µm pore size, polycarbonate filter. The resultant concentrate was rinsed and

resuspsended in 30-45 mL filtered seawater and preserved in 2% acidic Lugol's iodine.

To facilitate comparison against measured standing stock of POC/PON of SAPS collected material, *Trichodesmium* biomass was estimated assuming 166 pgC per cell, which was determined assuming 10 µm x 10 µm cell size applied to the protocol of Kovala and Larrence (1966). The estimated carbon content per cell, 166 pgC $cell^{-1}$, was then converted to PON using the average C:N ratio of *Trichodesmium* biomass, 6.3 (Mulholland 2007). The calculated carbon content per *Trichodesmium* cell falls within colonial carbon content observed by Carpenter *et al*. (2004) and within the range for the dominant *Trichodesmium* species in the Atlantic, *T. thiebautii* (O'Neil 1998; Carpenter *et al*. 2004; Capone *et al*. 2005). Luo *et al*.(2012) reported a carbon content of 120 ± 57 pgC per cell for *T. thiebautii*, which was calculated from biovolume data derived from Hynes *et al*. (2012) applied to a carbon content model described by Verity (1992); the 166 pgC per cell assumption was outside of the range determined by Luo *et al*. (2012) for *T. erythraeum* (65 ± 32 pgC per cell), which is another common Atlantic *Trichodesmium* species (O'Neil 1998; Carpenter *et al*. 2004; Capone *et al*. 2005).

Figure 3-3. Forms of *Trichodesmium* collected. Colonial puff (A) and colonial tuft (D), as was quantified in the Gulf of Mexico collections, and free trichomes (B, C), which vary in length, as were quantified in the Atlantic. Scale bars represent 100µm.

3.3.7 Nitrogen Fixation Rates

N_2 fixation rate data for the D361 cruise was provided by Dr. David Honey. It was determined from incorporation of $^{15}N_2$ gas assimilation as previously described (Montoya *et al*. 1996; Moore *et al*. 2009). Briefly, 4.5 L polycarbonate bottles with screw cap seals and silicon septa were completely filled with CTD captured seawater so that no air bubbles remained. Each bottle was then injected with 4 mL $^{15}N_2$ gas using the method described by Montoya *et al*. (1996). The spiked bottles were then placed in deck incubators cooled to sea surface temperature using running seawater and at light levels shaded to approximate *in situ* conditions using blue and natural density filters. After 24 hours the contents of each bottle were filtered onto pre-ashed glass-fibre filters (Whatman GF/F or Fisherbrand MF300), which were subsequently folded into eppendorf tubes and dried for 24 hours at 40°C. After drying samples were stored in a cool, dry environment until analysis by isotope ratio mass spectrometry on a Thermo Finnigan EA 1112 Series Flash Elemental Analyzer. Use of the bubble injection technique potentially led to systematic underestimation of actual rates by up to 50% (Groβkopf *et al*. 2012; Wilson *et al*. 2012). Rates were integrated over the upper 20 to 50 m of the water column at each station.

3.3.8 ^{234}Th-derived PON Fluxes

The thorium-derived PON flux data for D361 was provided by Katsia Pabortsava. To determine total ^{234}Th activity in seawater, the 'small volume' technique (Pike *et al*. 2005) was used. Within ~1 hour of collection, seawater samples were acidified to a pH of 1-2 with concentrated nitric acid at 1.5ml/L to separate ^{234}Th from parental ^{238}Uranium and shaken vigorously. 50µl (0.35Bq/g) of ^{230}Th yield tracer was then added. The samples were vigorously shaken again and left to equilibrate for 6-8hrs. After equilibration, 7-8ml of ammonium hydroxide was added per sample to bring the pH to 8.0-8.1. To form suspension of manganese oxide, 50µl (7.5mg/L)

of potassium permanganate and 50µl (7.5mg/L) of manganese chloride were subsequently added to seawater samples. The manganese oxide precipitate was then allowed to scavenge ^{234}Th for 6-8hrs. The contents were then filtered onto ashed 25mm QMA (Whatman) filters. Filter precipitates were dried for 12-24hrs at 60˚C and then mounted onto Risø beta-counter filter holder under a layer of Mylar film and aluminium foil in order to shield alpha-particles and low energy beta-emitters. ^{234}Th was quantified by counting daughter ^{234m}Protactinium ($t_{1/2}$=1.2 min) on a low-level Argon gas-flow 5-sample GM-25 beta-counter manufactured by Risø National Laboratories (Roskilde, Denmark). The unit was completely shielded by lead bricks to reduce background count rates. To assess efficiency of beta-counting, deep water (from >1000 m depth) was collected and analyzed for ^{234}Th activity. The activity of parental ^{238}U was calculated from salinity according to Chen *et al*. (1986). Initial counting was followed by a final background radiation count after >7 half-lives of ^{238}Th decay (~6 months).

3.4 Results

3.4.1 Spatial Distribution

Sampling spanning depths of 2-500 m in the subtropical and tropical Atlantic Ocean, demonstrated that *Trichodesmium* was a major component of surface community structure relative to other diastrophic organisms (Chapter 2). *Trichodesmium* was also present below 100 m in three forms: tufted colonies, free filaments (Figure 3-3), and free filaments included in aggregations with other organisms/faecal matter. Intact colonies of *Trichodesmium* were observed as deep as 300 m, although free filaments dominated the collections below 150 m, and were observed as deep as 500 m within SAPS deployments (the maximum depth assessed).

Surface *Trichodesmium* abundance varied along a latitudinal transect in the Atlantic ranging from 48 x 10^3 – 19 x 10^6 cells m^{-3} under varying colonial morphology (Figure 3-4A) Total cell abundance consistently decreased with depth below the mixed layer (Figure 3-4B), ranging from 4.5-74% of the surface abundance at 10 m below the DCM, <1-63% 100 m below the mixed layer, and 0-0.8% of the surface abundance at 500 m respectively. Colony morphology was mixed at the surface with similar ratios of tufts and puffs at all stations (Figure 3-4A).

In contrast, all the negatively buoyant colonies collected below the DCM using the MSC were of the tuft morphology (Figure 3-3D). Negatively buoyant colonies were consistently small, and total colony length did not exceed 2000 µm in any of the colonies collected below the DCM. However, larger colonies were observed near the surface. Sinking rates of negatively buoyant colonies between 100 and 250 m averaged 62.1 ± 39.7 m d^{-1}, ranging from 12-120 m d^{-1} (Figure 3-5).

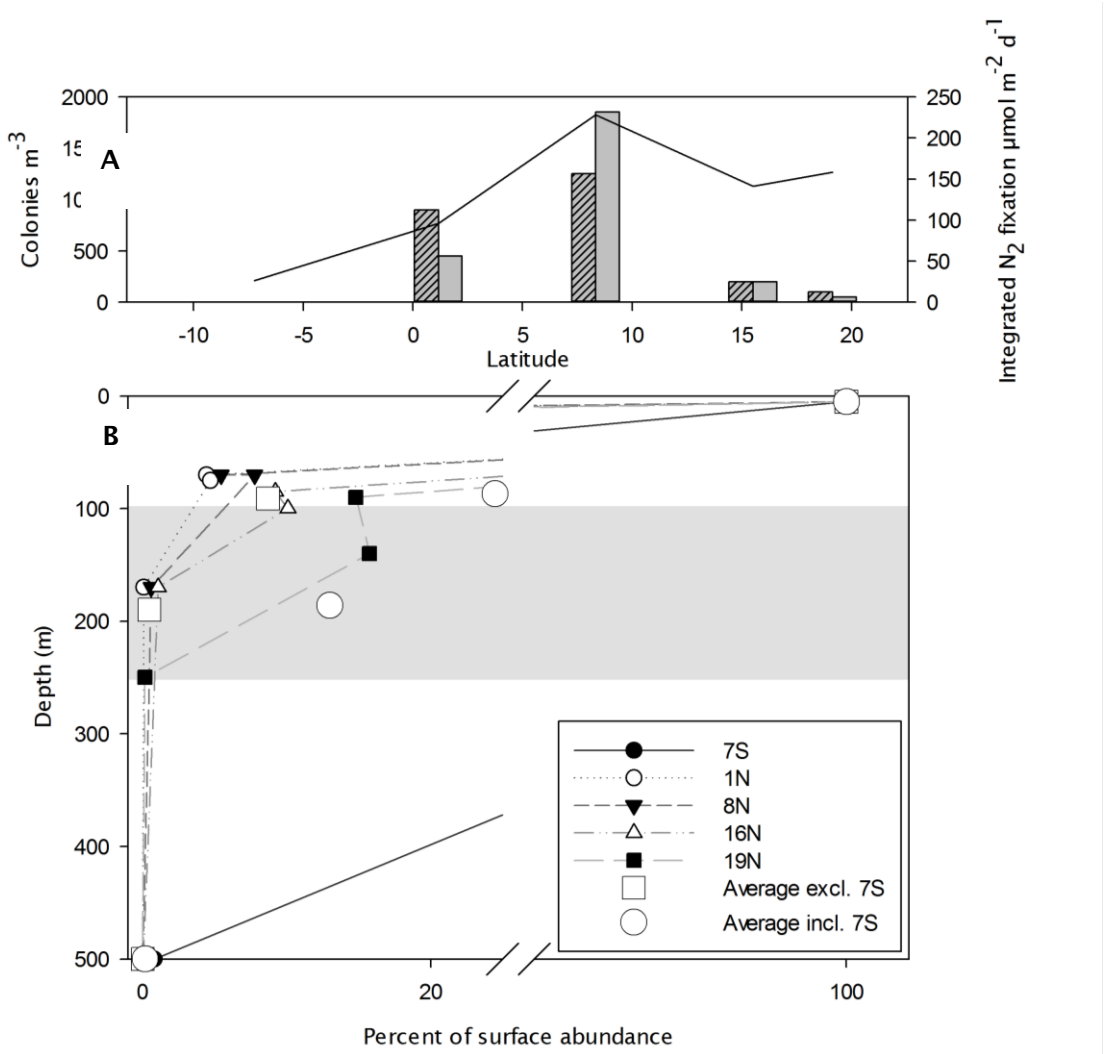

Figure 3-4. *Trichodesmium* abundance in the (sub-)tropical Atlantic. Nitrogen fixation rates and surface colonial morphology of *Trichodesmium* (A). Percentages of *Trichodesmium* surface abundance at depth; shaded area represents depths over which remineralisation is assumed to occur (B).

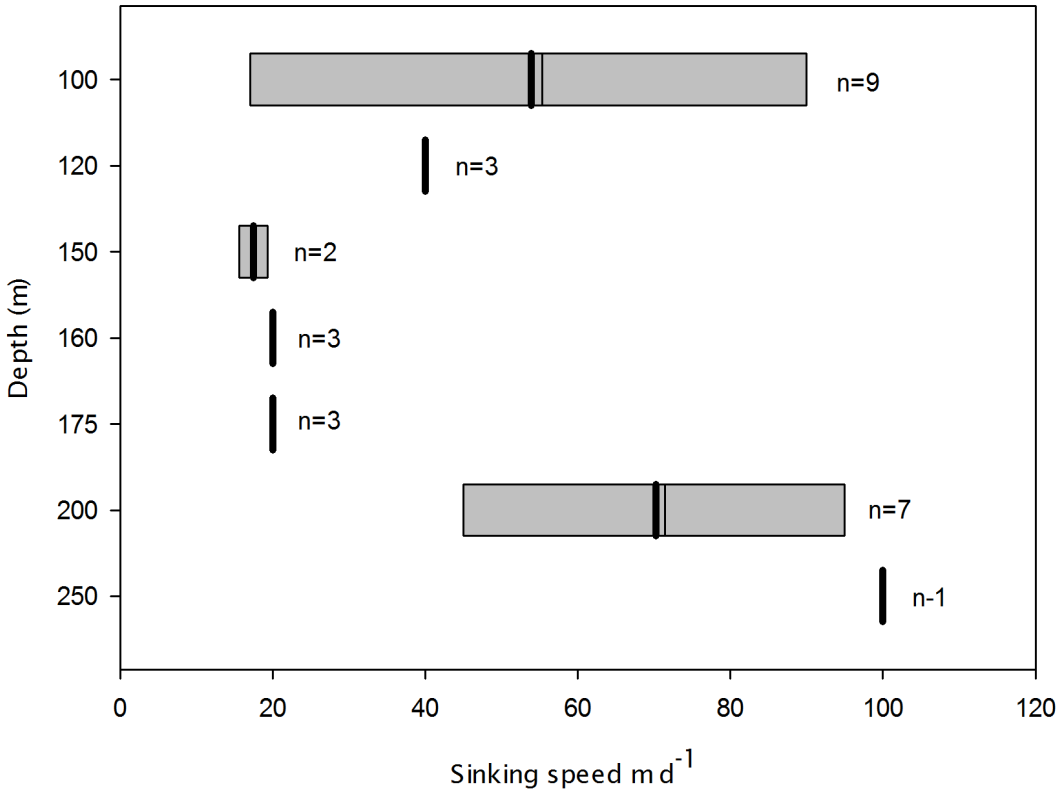

Figure 3-5. Sinking speeds of *Trichodesmium* colonies in the Gulf of Mexico and in the Atlantic collected between 100 and 250 m. Solid black lines represent he average sinking speed for each depth, which ranged from 19 to 100 m day^{-1}. Replicates for each depth are as noted above.

3.4.2 Aggregates

Free trichomes of *Trichodesmium* were present at all depths assessed except the deepest sample at the most northerly station. Trichomes varied in length from 15-177 cells. Aggregate isolation from MSC collections revealed trichomes were consistently present in aggregations with radiolarians in varying abundances (Figure 3-6). Trichomes incorporated in aggregates were intact, and both phycoerythrin (Figure 3-6C) and chlorophyll fluorescence were consistently observed under epifluorescence microscopy immediately following collection and isolation. Infrequently (at one station each), both intact (Figure 3-7C) and degraded trichomes (Figure 3-6A) were observed incorporated into faecal pellets (Figure 3-7B, D) in material collected in MSC deployments as deep as 250 m.

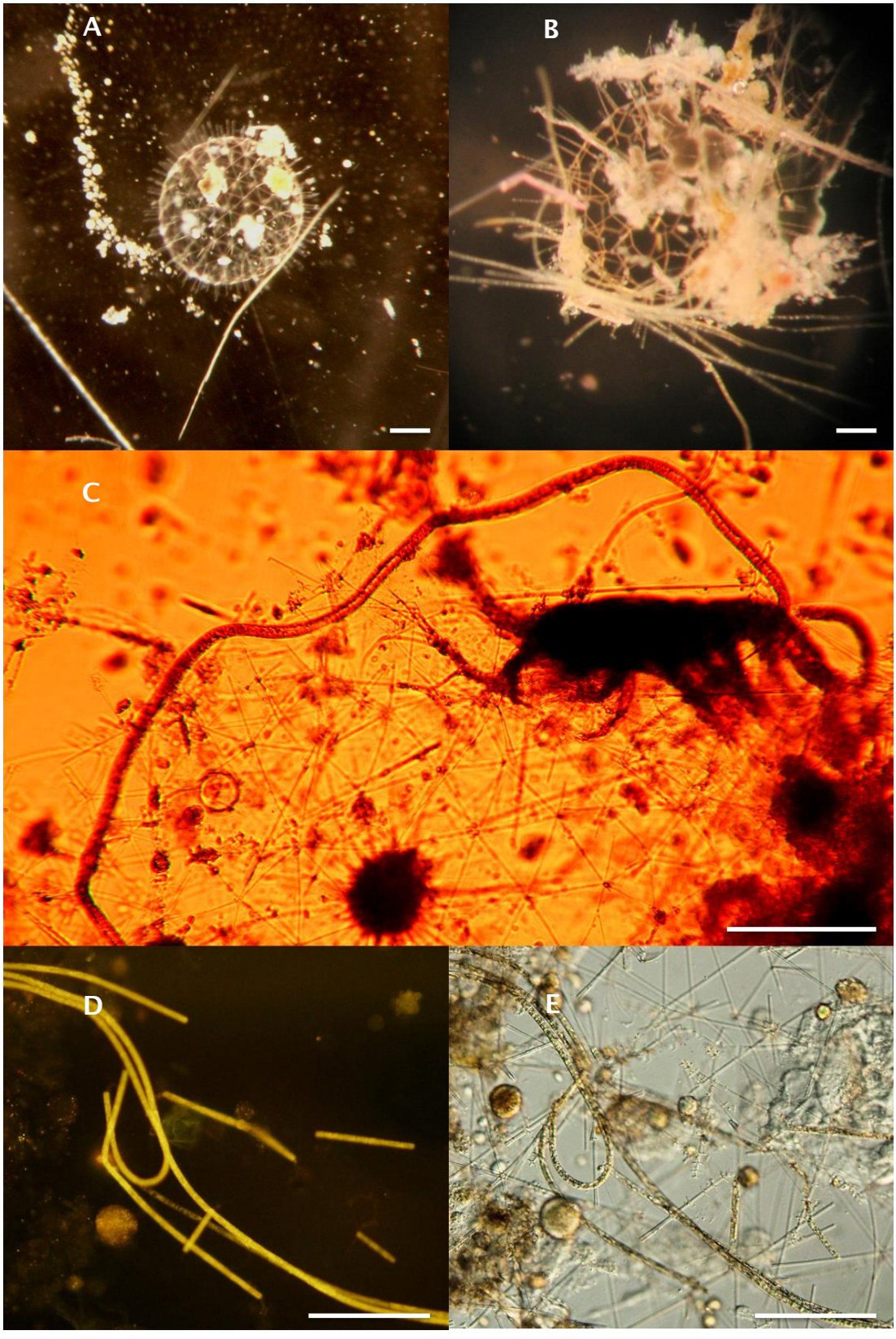

Figure 3-6. Plate of photomicrographs of *Trichodesmium* in aggregates. (A, B, C, E) Trichomes in conjunction with radiolarians. (D) Active phycoerythrin fluorescence of the trichome from panel E. Scale bars represent 100µm.

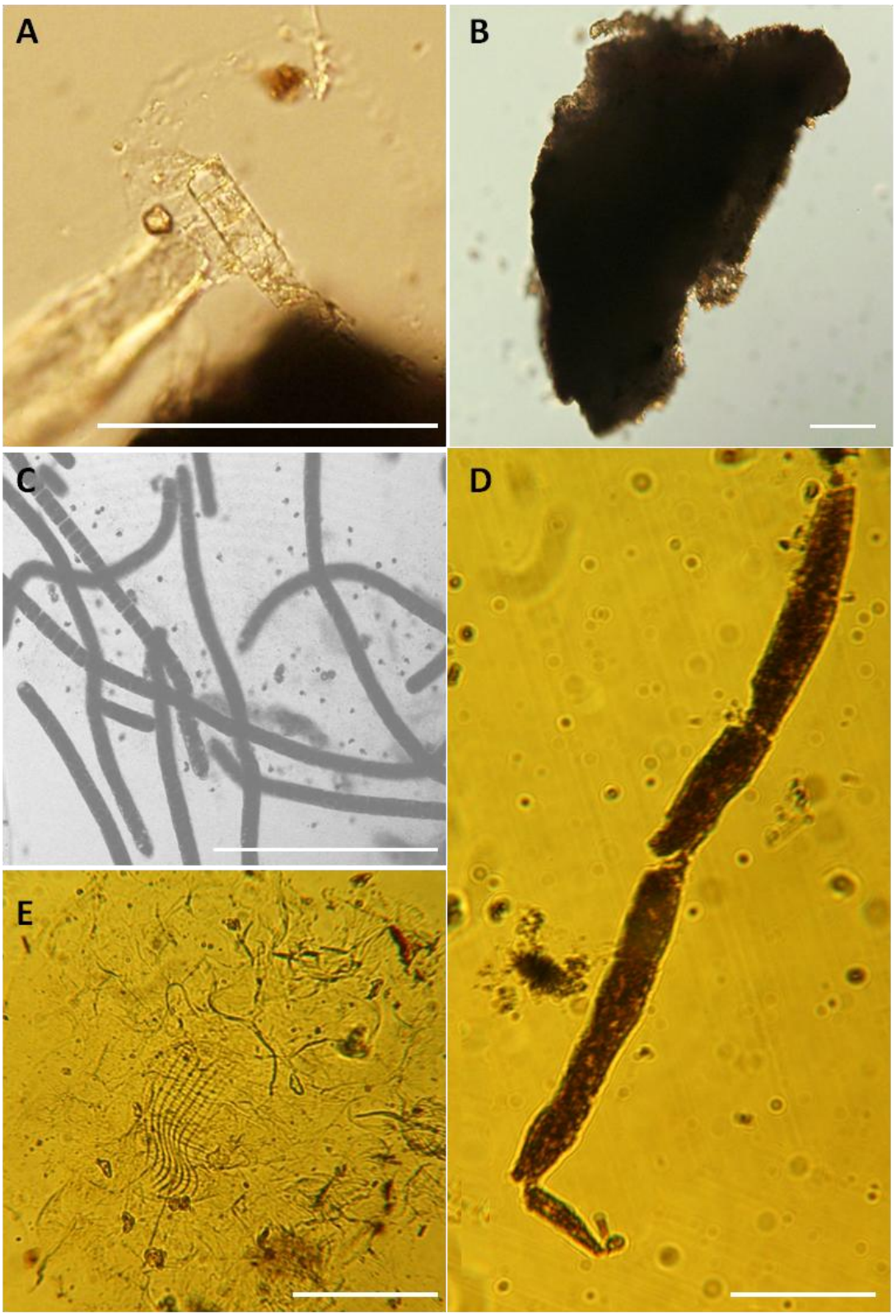

Figure 3-7. Plate of photomicrographs of *Trichodesmium* in faecal pellets. (A) Partially degraded trichomes incorporated in (B) faecal pellets from CH0711; (C) Confocal micrograph of seemingly intact trichomes from (D) faecal pellet of unknown origin; (E) pteropod food web from same collection as pellet with intact trichomes from D361. Scale bars represent 100µm.

3.4.3 *Trichodesmium* Biomass and Contribution to Fluxes

The proportion of PON collected by SAPS deployments which could be directly attributed to *Trichodesmium*-derived PON calculated from visible *Trichodesmium* cells in SAPS collections ranged from 0.4-3% at 10 m below the mixed layer, 0.03-1% at 100 m below the mixed layer, and from 0-0.4% at 500 m (Table 3-1).

When combined with sinking rates measured for colonies (Figure 3-5), the estimated visible *Trichodesmium*-attributable PON flux leaving the mixed layer averaged 32.9 (5.0 – 99.6) μmol m^{-2} d^{-1}, which accounts for an average of 5.6% (1– 17.5%), of the total PON flux independently derived from ^{234}Th (Table 3-1).

Measured N_2 fixation rates varied along the transect, ranging from 26-228 μmol m^{-2} d^{-1} (Figure 3-4A). Consequently, when compared to surface nitrogen fixation rates, exported (visible) *Trichodesmium*-derived PON accounted for an average of 23% of the daily nitrogen fixation in the upper water column (Table 3-1). If all the newly fixed nitrogen in the surface were contributing to organic nitrogen export, estimated surface-N_2-fixation rates could have supported 20% of the ^{234}Th-derived PON flux at 10 m below the mixed layer (Table 3-1).

Table 3-1. Estimated *Trichodesmium*-derived PON contribution and fluxes

Depth (m)	*Trichodesmium* Abundance (cells x 10^3 m^{-3})	% Surface Abundance	Contribution to PON Standing Stock (%)	Potential Contribution of N_2 Fixation to PON Flux (%)	*Trichodesmium* PON Flux (µmol m^{-2} d^{-1})	*Trichodesmium* Contribution to Total PON Flux (%)	*Trichodesmium* PON Flux as % N_2 Fixation
70-140 (mixed layer +10 m)	240 ± 280	21.9 ± 29.5*	1.18 ± 0.85	20.3 ± 13.2	32.9 ± 29	5.6 ± 7.0	23.1 ± 16.2
170 (mixed layer +100 m)	20 ± 22	13 ± 28.0*	0.40 ± 0.46	12.3 ± 6.8	2.8 ± 3.1	0.43 ± 0.36	4.3 ± 6.7
500	0.45 ± 0.47	0.2 ± 0.4	0.02 ± 0.02	7.4 ± 5.4	0.01 ± 0.01†	<0.01	0.01 ± 0.02

*Cell abundance calculated based on trichome counts. These ranges include abundance data from a station with particularly low surface abundance. Excluding this station the range maximum at 70-140 m, 170-250 m, and 500 m were 13.99%, 1.02%, and 0.05% respectively. Flux contributions were calculated from biomass estimates and sinking rates compared to Thorium derived PON flux measurements from SAPS deployments. †Calculated assuming a single trichome sinking rate of <0.5 m d^{-1}.

3.5 Discussion

3.5.1 *Trichodesmium*-derived Fluxes of PON

The current study presents some of the first evidence that *Trichodesmium* contributes to PON export through passive sedimentation. Previously, only active transport (Guidi 2012) and sweeping mechanisms (Scharek *et al*. 1999b), or aggregation, have been suggested to account for *Trichodesmium* presence at depth. Guidi *et al*. (2012) suggested that active export of *Trichodesmium* could be possible through downwelling associated with eddies in the North Pacific Subtropical Gyre. Such enhancement of POC export by eddies has also been observed in the Sargasso Sea (Sweeney *et al*. 2003; Davis and McGillicuddy 2006).

Based on the biomass estimates and sinking rates, up to 74% of surface *Trichodesmium* standing stock could leave the mixed layer each day. Moreover, visible *Trichodesmium* cells likely composed up to 3% of the standing stock of PON at depth (Table 3-1). When *Trichodesmium* biomass estimates were combined with colonial sinking rates, the visible *Trichodesmium*-attributable PON flux composed an average of 5.6% of the ^{234}Th derived PON flux at 10 m below the mixed layer (Table 3-1). This indicates that intact *Trichodesmium* cells are making a contribution to PON leaving the mixed layer, potentially through a combination of relatively high sinking speeds and enhanced nitrogen content compared to the other sinking particulate organic material. The maximum contribution to the PON flux was observed below the maximum surface abundance of *Trichodesmium* encountered along the transect (8.3°N, 28.3°W). At this station *Trichodesmium* contributed an estimated 17.5% of the exported PON flux. Such a contribution is comparable to, although still less than, previous estimates of the proportional contribution of *Trichodesmium* to total new production in regions of high *Trichodesmium* abundance (Capone *et al*. 2005). Observations under regions of high *Trichodesmium* surface abundance, where standing stocks and nitrogen fixation rates can be an order of magnitude higher than we observed (Carpenter *et al*. 2004; Capone *et al*.

2005) would be required to examine whether the potential for increased *Trichodesmium* contribution to PON flux continues to scale with increasing surface biomass. A recent study of an artificial bloom of *Trichodesmium* IMS 101 suggests this is a plausible scenario, as the collapse of the artificial bloom resulted in enhanced PON export (Bar-Zeev *et al*. 2013).

The estimated contribution of *Trichodesmium* PON export herein are likely conservative as we could only attribute the flux associated with intact, microscopically visable cells. Although the intact nature of the cells may not be preserved, and therefore not easily quantified, there remains the potential for the packaging of *Trichodesmium* into faecal material beyond that observed visibly, which could increase the *Trichodesmium*-attributable PON flux estimates. Additionally, other mechanisms exist whereby *Trichodesmium*-derived N could contribute to export fluxes secondarily, following incorporation into other material, such as following viral lysis of cells (Hewson *et al*. 2004), extracellular release of fixation products (Glibert and Bronk 1994), or following PCD (Bar-Zeev *et al*. 2013).

N_2-fixation, which appeared to be dominated by *Trichodesmium* between the equator and 10°N (Chapter 2), could potentially have supported 20% of the ^{234}Th-derived PON flux at 10 m below the mixed layer (Table 3-1). There is the potential for a much larger diazotroph contribution to PON export yet to be described, which could contribute to the transfer of new nitrogen to depth. If consistent with these observations for sinking *Trichodesmium*, this PON could then be available for remineralisation and integration into the thermocline. The possibility that the measured surface rates are systematic underestimates (Wilson 2012; Groβkopf *et al*. 2012) also requires consideration. An average doubling of surface rates (Wilson 2012; Groβkopf *et al*. 2012) would mean that surface N_2 fixation had the potential to contribute to 40% of the total PON flux, while visible *Trichodesmium*-derived PON flux would be reduced to around 12% of the surface N_2 fixation.

3.5.2 Mechanisms of Export of *Trichodesmium*

Preliminary results suggest that despite its archetypal surface distribution and buoyant properties, *Trichodesmium* is a standard constituent of sinking material and is directly involved in the export of POC/PON through a variety of mechanisms (Figure 3-8). Deep colonial distributions of *Trichodesmium* are largely unreported, and reports of its presence in sediment traps are a rarity (Scharek *et al*. 1999b; Chen *et al*. 2003). Below the euphotic zone, *Trichodesmium* cannot photosynthesize, and is unlikely to be actively fixing N_2. This was confirmed by *nif*H expression collected on this cruise (Langlois 2011 pers. comm.). This study thus provides evidence that while not diazotrophically active, *Trichodesmium* is likely a regular constituent of sinking material, and previous assessments have overlooked or underestimated *Trichodesmium*'s presence at depth.

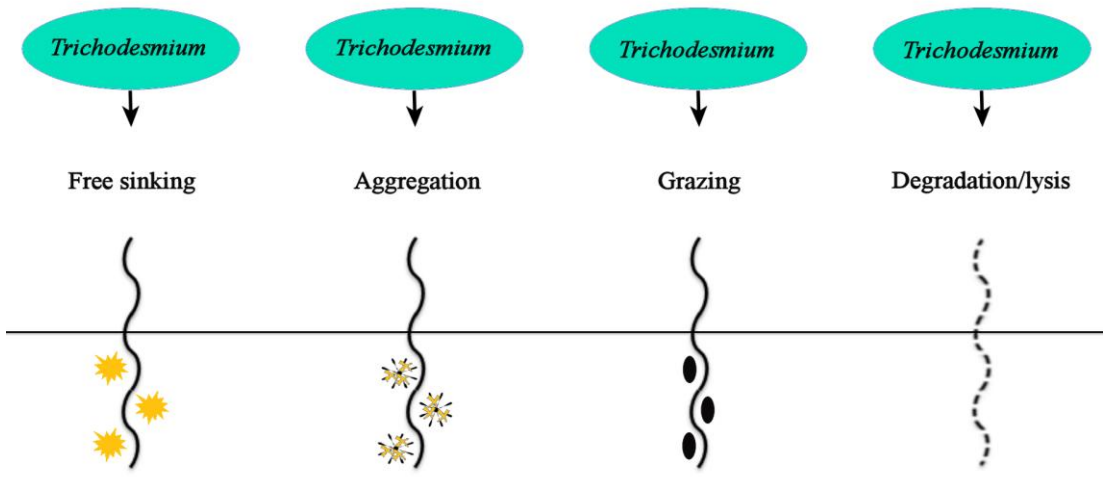

Figure 3-8. Schematic of possible export mechanisms for *Trichodesmium* (modified from Mulholland 2007).

There are number of potential mechanisms that could explain *Trichodesmium*'s presence below the depth where it can photosynthetically fix carbon and nitrogen. The vertical migration of colonies provides a potential mechanism for transport of *Trichodesmium* to depth. This theory assumes that

after fixing carbon near the surface, colonies become laden down with carbohydrates, overcoming their positive, gas vesicle supplied buoyancy, which causes them to sink. As they do so they respire allowing them to 'burn-off' the excess ballast, which decreases the colony sinking rate (Villareal and Carpenter 2003). In an optimal system, once a colony reaches the phosphocline, it would be neutrally buoyant, and would be able to absorb nutrients for a few hours before regaining positive buoyancy and returning to the surface (Villareal and Carpenter 2003). This nutrient mining hypothesis is a potential explanation for the location of the colonies collected at depth. The colonies collected between 120 and 175 m had much slower, and less variable, sinking rates than colonies distributed above and below these depths (Figure 3-5). These decreased sinking rates observed between 120 and 175 m correspond with the depth range of enhanced phosphorus concentrations along both of the cruise tracks (Figure 3-9) indicating these colonies could be in the process of reversing buoyancy in an effort to return to the surface following nutrient acquisition.

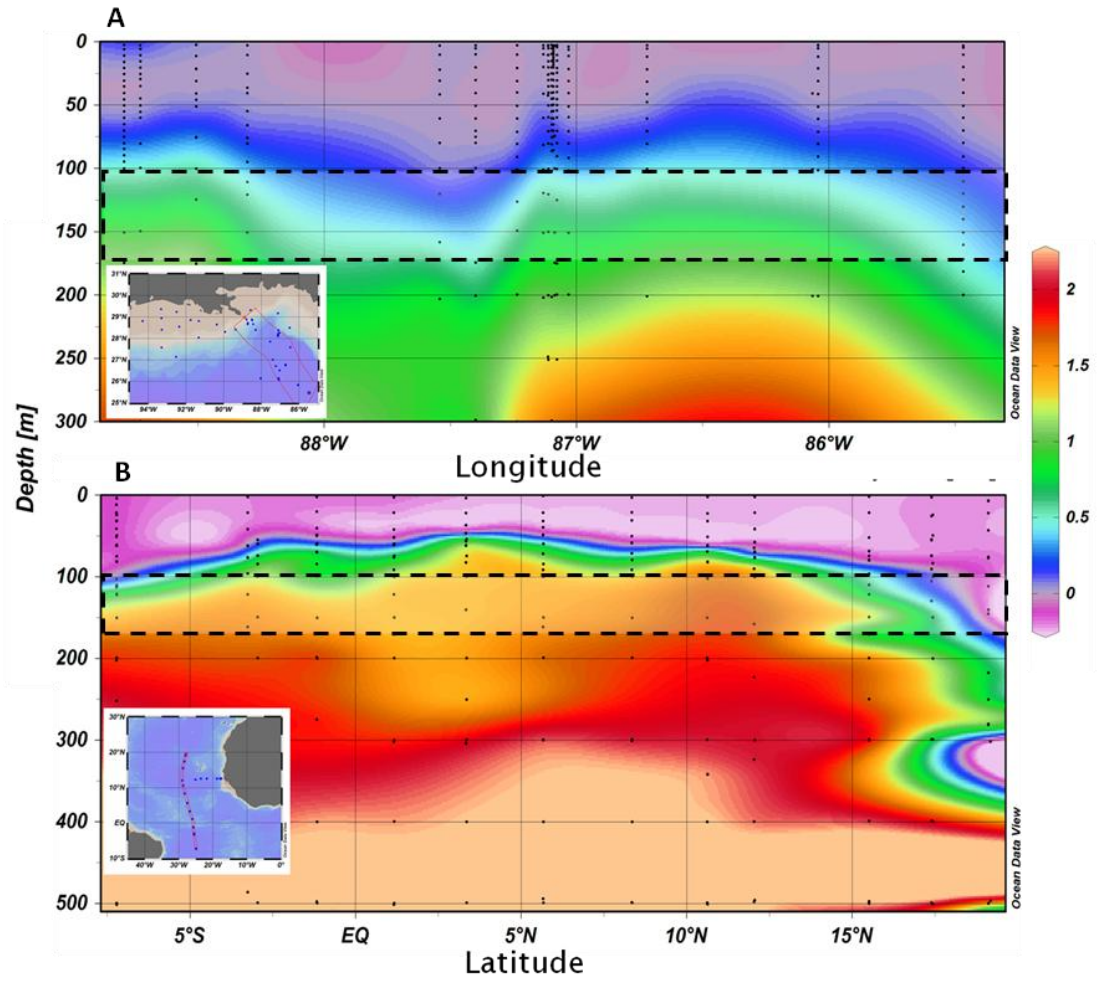

Figure 3-9. Longitudinal section of Phosphate (µM) along a pelagic transect during CHO711 (A) and a latitudinal section of phosphate (µM) along the north-south transect of D361 (B) illustrating enhanced phosphate concentrations within the depth range of potential nutrient mining (dashed boxes).

However, colony size and sinking rate did not appear to be correlated in this study (R^2<0.1) (CH0711, n = 24; D361, n=4). Previous models considering cell size, gas vacuole content and carbohydrate ballast potential suggest that only large (>1500 µm radius) colonies would possess the capability to carry out vertical migrations beyond 100 m (Kromkamp and Walsby 1992; White *et al*. 2006), suggesting that such a mechanism is insufficient to account for colonies collected in this study, which were consistently less than 1000 µm in length. However, these models did not incorporate any cellular components other than carbohydrates into cellular density analyses, and also did not include physical influences on colony transport in the water column. Therefore, colony size cannot be used as a strict determinant for colony ability to return to the surface from depth.

Colony collections included cells which were morphologically variable, but phylogenetic analyses are necessary to determine whether multiple species of *Trichodesmium* are depth distributed as interspecific cryptic diversity can make morphological identification difficult (Hynes *et al*. 2012). Determining species type would give insight into species-specific physiologies, which could influence the assumptions of gas vacuole dynamics. The dominant *Trichodesmium* species in this study region, *T. thiebautii* (O'Neil 1998; Carpenter *et al*. 2004; Capone *et al*. 2005), have previously been shown to suffer only a 10% gas vacuole loss through collapse at 200 m depth, with 100% of gas vacuoles collapsing by 350 m (Walsby 1978). The other common *Trichodesmium* species in the Atlantic, *T. erythraeum* has been observed to suffer 100% gas vacuole collapse at a much shallower depth, between 105 and 120 m. If sinking colonies consist of *T. erythraeum*, their fate is likely locked below 100 m, but if the species is *T. thiebautii*, as is suggested by ultrastructural assessments of sinking colonies in a different study region (Chapter 5), we must consider the potential for these colonies to reverse buoyancy. Regardless of species type, small, fast sinking colonies present below 100 m would be locked in a persistent and irreversible downward trajectory. With maximum sinking rates of 120 m d^{-1} it is plausible that these colonies would reach depths potentially complete gas vacuole collapse (>300 m) within 1-2 days whereby it would be impossible to reverse direction.

There was no correlation between sinking rate and depth in this study. When gas vacuoles were manually pressure-destroyed colonial sinking rates varied between 43 and 255 m d^{-1} (Walsby 1978). Most colonial sinking rates from both cruises fell within this range (Figure 3-5), but species identifications were not carried out in this study and sample size below 100 m was relatively small (n=19). Additional assessments of species-specific sinking rates would be beneficial to expanding the understanding of the mechanism of sinking in *Trichodesmium* colonies.

The deepest colonies were present to 300 m, but a switch from colony to trichome dominated samples occurred below 150 m. Colonies likely begin to disassociate into free trichomes with depth as free trichomes should be unable to sink to these depths unaided by incorporation into large, fast sinking particles; colonial sinking rates were markedly faster than that of free filaments as MSC settling indicated free filaments were in low abundance, and were part

of the slow sinking/suspended pool of particulate material. It is also possible that colonial associations become more fragile as they sink, as the disassociation of some negatively buoyant colonies into filaments during sinking rate experiments was observed. This observation supports the idea that the deep free filaments we observed originated in colonies and were transported to depth in that morphology, but that some other, likely physical force caused them to disassociate. For the SAPS collected samples, the filtration process would certainly have disturbed morphological features.

Moreover, partial cell breakage during SAPS filtration could also contribute to the estimated contribution of *Trichodesmium* to PON flux being an underestimate due to the potential loss of visually distinguishable trichomes. The deepest colony reported here, which represents the deepest report of a colony to date, was collected at 300 m using the CTD, but free trichomes were distributed as deep as 500 m along the latitudinal transect in the Atlantic, albeit sampled using SAPS. Previously *Trichodesmium* colonies have been observed to 200 m (Carpenter and Price 1977; Tyrrell *et al*. 2003) and free filaments have been reported deeper in the South China Sea in a sediment trap at 925 m (Chen *et al*. 2003), and at station ALOHA in the Pacific in a sediment trap at 2800 m (Scharek *et al*. 1999b).

Factors causing colonies to disassociate into free filaments at depth greater than 100 m could greatly decrease the sinking rate of *Trichodesmium*, potentially enhancing susceptibility to remineralisation in the twilight zone (200-1000 m). Additionally, the significance of the observed morphological bias, where mixed colony morphology at the surface was absent at depth remains to be investigated. As all negatively buoyant colonies collected below the mixed layer were in tuft form, enhanced fragility and disassociation of puff colonies could explain the disproportional morphological sampling below the mixed layer. Alternatively, it remains to be explored whether physiological or species specificity of *Trichodesmium* sinking, such as epibiont communities unique to different morphologies, plays a role in the morphological characteristics of sinking *Trichodesmium* colonies.

The presence of *Trichodesmium* trichomes in aggregates with other organisms, such as radiolarians (Figure 3-6), and/or detrital material was encountered in most collections and increased with depth, denoting alternative

pathways of export for this organism. Due to the method of SAPS collection, a bias towards entanglement could have been introduced during pumping and conglomeration of material on the filter, so it is possible that free trichomes are more common at these depths than observed. Phycoerythrin and chlorophyll fluorescence of cells at depth indicated that cells were reasonably un-degraded, but cells were not particularly stable. Multiple observations of trichome degradation were observed during imaging implying these trichomes may have been on the verge of apoptosis when collected (Figure 3-10); potentially the stress of collection and/or imaging may have induced the observed apoptosis. If this process were to occur while the aggregates were sinking it would represent a mechanism of direct release of *Trichodesmium* intracellular contents into the water column at depth.

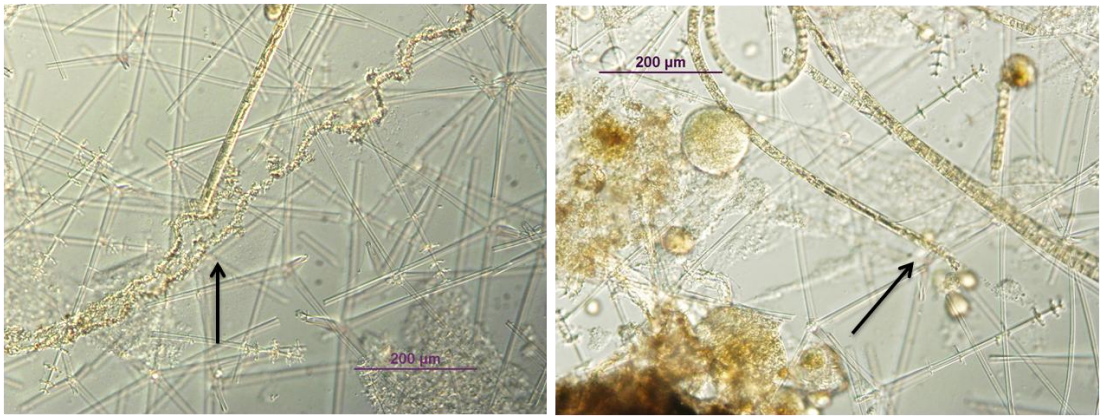

Figure 3-10. Light micrographs of *Trichodesmium* spp. in association with aggregates within the hour following collection showing apoptosis of trichomes in progress. Scale bars represent 200µm as indicated.

Additionally, one of the negatively buoyant colonies collected using the MSC in the Gulf of Mexico was found to still exhibit variable chlorophyll fluorescence, indicating a retained degree of photosynthetic competence. If these trichomes remain intact while sinking after being caught in associations with other organisms, they would likely retain their cell matter and transport it out of the euphotic zone where it could then be remineralised. Further, as phycoerythrin has been previously shown to be a nitrogen storage mechanism in *Synechococcus* (Kirchman and Alberte 1985), its maintained presence here represents a concentrated nitrogen pool exported within *Trichodesmium*.

Previous reports have rarely documented grazing on *Trichodesmium*, so the observed sporadic presence of this organism in faecal material is significant. Trichomes of *Trichodesmium* were observed to be relatively intact in faecal matter (Figure 3-7C). Trichomes of *Trichodesmium* were observed in faecal matter both partially degraded, and seemingly intact. The latter situation implies accidental feeding by an organism not capable of digesting *Trichodesmium.* Faecal pellets containing intact trichomes shared characteristics with pteropod waste material. As pteropods are non-selective web feeders that passively capture their prey through filtration into mucous sheets (Silver and Bruland 1981), *Trichodesmium* could have become entangled in the feeding mesh and consumed unintentionally. Such an incidence would preserve intact trichomes in a compact, fast-sinking pellet that would transport trichomes to depth much quicker than if they were free-sinking. Intact, previously ingested organisms in pteropod waste is common (Silver and Bruland 1981), providing a transport mechanism for all *Trichodesmium* cell matter. The fecal pellet containing intact *Trichodesmium* also shared characteristics with euphausiid waste material (Yoon *et al*. 2001). Further investigation of the occurrence of krill grazing on filamentous cyanobacteria is warranted to assess whether these organisms may also unintentionally or incompletely ingest *Trichodesmium*. The frequency of occurrence of unintentional digestion is currently unknown, and was only encountered at one station on D361 where pteropods were noted in the surface samples.

Partial degradation of trichomes in faecal matter suggests digestion is taking place. In the present study this was only seen once in a pellet of unknown origin. Trichome abundance was very low in this pellet compared to the pellet with intact trichomes indicating it may be possible for some feeders to breakdown and digest *Trichodesmium* in low quantities. Again, this could contribute to quick sequestration of cell matter to depth. A more thorough assessment of faecal material is needed to approximate the frequency of this occurrence as packaging of fresh trichomes in large faecal pellets could transport the associated newly fixed nitrogen to depth more efficiently than if they were free-sinking, and could potentially make a large contribution to total *Trichodesmium* export.

3.5.3 Fate of *Trichodesmium*-derived Nitrogen

When *Trichodesmium* cell abundance is combined from colonies, free trichomes, and trichomes incorporated in aggregates, it represents a significant fraction of PON at depth, and the spatial consistency of the values indicates the potential for significant episodic export following surface blooms via the mechanisms we have previously described. Moreover, the occurrence of Programmed cell death (PCD) during bloom collapse can significantly increase transparent exopolymer particle (TEP) production, thereby enhancing export of *Trichodesmium*-derived POM, such that after 5 days, ~0.08 mg N m^{-2} was present at the bottom of the artificial bloom settling column when initial surface concentrations were ~0.13 mg N m^{-2} (Bar-Zeev *et al*. 2013).

These results suggest that despite its archetypal surface distribution and buoyant properties, *Trichodesmium* is a standard constituent of sinking material in these (sub-)tropical waters and is directly involved in the export of PON through a variety of mechanisms. Previously *Trichodesmium* was only believed to export in fecal pellets on a small scale as well as secondarily by cycling through the microbial loop in the euphotic zone resulting in eventual loss of *Trichodesmium*-derived new nitrogen following incorporation into the biomass of other organism and their subsequent export (Mulholland 2007). The current study confirms that *Trichodesmium* export does occur following grazing and repackaging in fecal material, but also documents two novel mechanisms by which *Trichodesmium* exports (i.e. freely sinking and incorporation in aggregates). *Trichodesmium* does not appear to be a major contributor to total PON export under the observed moderate abundance conditions in the Atlantic (Table 3-1), where surface abundance rarely exceeded 5 colonies per litre.

However, the contribution to PON export and total new N production in the surface (Capone *et al*. 2005; Mourino-Carballido 2011) may be more significant under conditions of higher abundance of both *Trichodesmium* (Carpenter *et al*. 2004) and other diazotrophs. Scharek and others (1999b) attributed *Trichodesmium* presence in sediments traps to be a consequence of a sweeping mechanism whereby trichomes were caught up in the flux of larger, stickier diatom aggregates. The sweeping mechanism could also

explain the observation of trichome incorporation in aggregates. Continued observation of trichome incorporation in aggregates and fecal pellets suggests a previously overlooked involvement in export that remains to be more comprehensively explored. Further investigation of *Trichodesmium*'s presence in sinking material will give a clearer idea of this organism's contribution to export fluxes allowing us to better constrain the fate of the nitrogen fixed by this organism and hence it's detailed biogeochemical role.

Trichodesmium is the dominant nitrogen fixing organism in this study area (Tyrrell *et al*. 2003; Moore *et al*. 2009; Zehr 2011; Groβkopf *et al*. 2012), and is potentially capable of accounting for the majority of the geochemically derived rates of nitrogen fixation inferred from the N* distributions in the North Atlantic (Gruber and Sarmiento 1997; Capone *et al*. 2005; Mahaffey *et al*. 2005; Hansell *et al*. 2004, 2007). The spatial consistency and continuous decrease in cell abundance with depth below the mixed layer along the transect is indicative of remineralisation between 100 and 500 m (Figure 3-4B). The water column oxygen minima and region of maximum apparent oxygen utilization was located between 150 and 750 m within our (sub-)tropical Atlantic transect (Figure 3-11), suggesting that the majority of the total export of organic material is also likely remineralised within this same depth. The depth range of likely remineralisation also partially overlaps with the density surfaces within which remineralisation of diazotroph-derived material could contribute to N* (Figure 3-11).

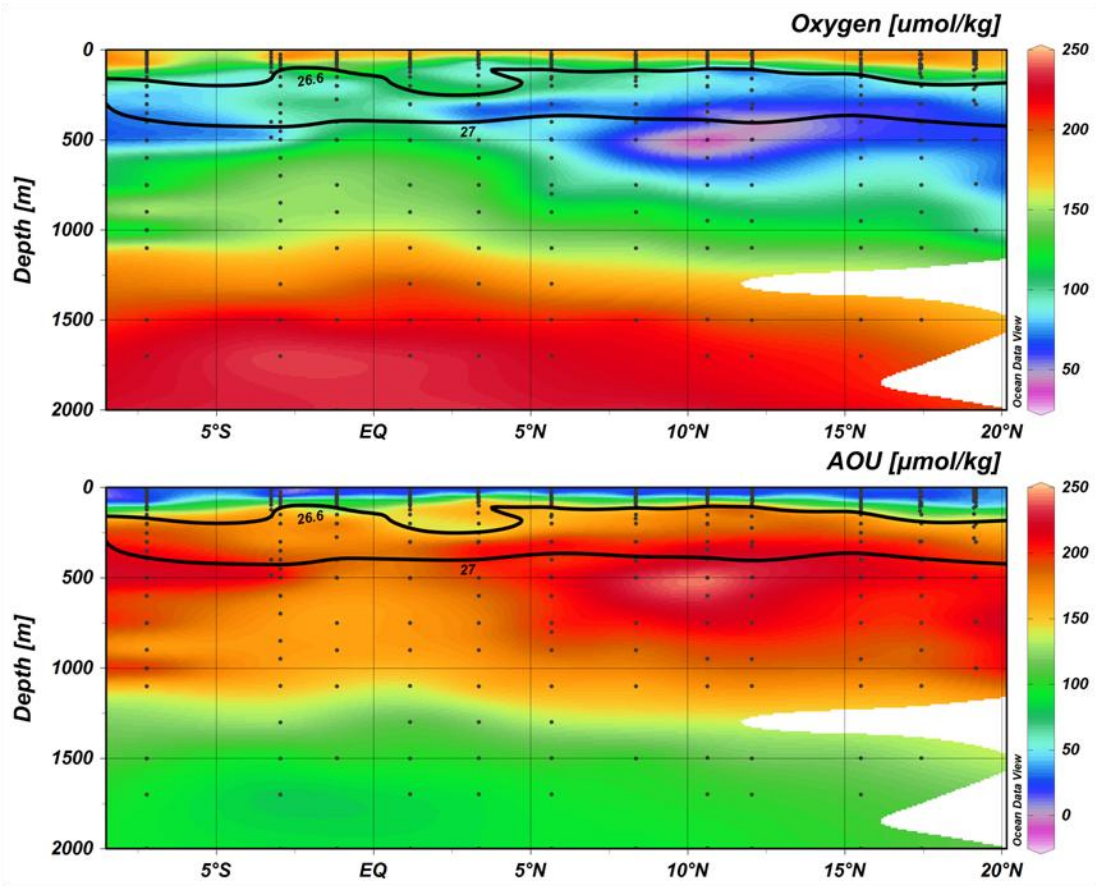

Figure 3-11. Latitudinal section of oxygen along the south-north transect on D361 showing decreased water column oxygen in the depth range where remineralisation of *Trichodesmium* is assumed (100-250 m), and alignment with the density surfaces within which remineralisation of diazotroph derived material could contribute to N*. Oxygen saturation was calculated from the method described by Garcia and Gordon (1992) and AOU was subsequently derived from the equation provided by Sarmiento and Gruber (2006).

Maximum N* anomalies in the North Atlantic gyre are associated with a potential density interval in the σ_θ = 26.1-27.1 range (Gruber and Sarmiento 1997; Hansell *et al*. 2007). Due to the shoaling of the permanent thermocline at low latitudes near the equator (Sarmiento *et al*. 2004), this potential density interval was shallower than 500 m along the Atlantic transect. Consequently, release of *Trichodesmium*-derived exported material into the upper twilight zone remineralisation region (100-500 m), provides a mechanism for generating at least a portion of the N* anomaly observed within the σ_θ = 26.1-27.1 range. Direct export of *Trichodesmium* thus potentially resolves one of the pathways by which the North Atlantic N* anomaly develops (Hansell *et al*. 2007).

3.6 Conclusion

Trichodesmium provides a significant amount of newly fixed nitrogen to the warm surface ocean in many oligotrophic regions thereby indirectly supporting the growth and export of non-diazotrophic organisms (Carpenter and Capone 2008). Conservative estimates that an average of 8.8% (excluding the southerly most station, otherwise average of 22%) of the surface standing stock of *Trichodesmium* is vertically leaving the mixed layer each day contributing an average of 5.6% to the total PON flux, provides insight into the biogeochemical fate of a significant proportion of the nitrogen fixed by this organism. The decrease in *Trichodesmium* biomass from 10 m below the mixed layer to 500 m suggests that *Trichodesmium* is remineralised within the twilight zone and hence contributes diazotroph-derived new nitrogen to the thermocline of the (sub-)tropical Atlantic Ocean. When coupled with the potential for enhanced export following surface blooms, such a previously undescribed mechanism could export newly fixed nitrogen to depths facilitating accumulation along the isopycnals associated with the thermocline of the sub-tropical gyre, thus contributing to the N* anomaly in these waters (Gruber and Sarmiento 1997; Hansell *et al*. 2007). Consequently nitrogen fixation by *Trichodesmium* in the low latitude Atlantic is not only an important contributor of new nitrogen in the euphotic zone (Capone *et al*. 2005), but may also be important in the supply of nutrients to the thermocline. In turn these nutrients could sustain productivity on longer time scales, through eventual resupply to the surface ocean, while also potentially contributing to the deficiency of phosphorus downstream within the surface waters of the gyre.

4. An exploration of the significance of polyploidy in *Trichodesmium*

4.1 Abstract

Quantitative PCR of the *nif*H gene is commonly used to assess the biogeography and relative abundance of diazotrophic species in the global oceans, and was employed in Chapter 2 to gauge the fate of a variety of diazotrophic groups. However, discrepancies between *nif*H-based and optical abundance data have been previously acknowledged, often citing an order of magnitude higher *nif*H-based than cell-count-based abundance for *Trichodesmium* indicating the potential for extreme overestimation of biomass when converting between the two methodologies. As DNA extraction efficiency is variable between species, and can be less than 100% efficient, the discrepancy between *nif*H gene copies and cell counts is potentially even larger. Similar discrepancies have also been noted for heterocystous, diazotrophic cyanobacteria. Herein we endeavour to explain the discrepancy between detectable *nif*H gene copies and optical cell counts through an investigation of polyploidy in *Trichodesmium*. Polyploidy, or the condition of having more than one genome per cell, is well described in prokaryotic organisms and it present in many cyanobacterial groups. *R*esults suggest polyploidy in *Trichodesmium* could result in inflated detectable *nif*H relative to cell abundance. If *Trichodesmium* is polyploid, this has implications for the interpretation of qPCR data globally, and thus we caution against any use of direct conversion from detectable *nif*H gene copies to cell numbers, especially in *Trichodesmium*.

4.2 Introduction

The development of molecular technologies has resulted in a near universal switch from microscopy (hereafter optical) cells counts to qPCR of the *nif*H gene (hereafter gene-based abundances) to understand the distribution and abundance of diazotrophs in the global ocean. This switch from optical to gene-based abundance methodologies is striking with 40 studies spanning 49 years resulting in 5191 data points from optical abundance data, while 19 gene-based abundance studies have resulted in 3201 data points in just 7 years (Luo *et al*. 2012).

As previously discussed in Chapter 2, the *nif*H gene is a highly conserved gene which codes for the iron binding component of the nitrogenase enzyme (Young 1992). Sequence diversity of *nif*H is variable enough between genera of diazotrophs that the technique has been used to detect and quantify diverse groups of *nif*H-containing organisms (Zehr *et al*. 1997), including non-cyanobacterial *nif*H-containing organisms, such as the gammaproteobacteria and green sulphur bacteria whose contribution to global nitrogen fixation remains unknown (Riemann *et al*., 2010). This influx of data derived from gene-based abundances has substantially contributed to the expansion of our knowledge of the diversity and biogeography of *nif*H-containing organisms, and use of the procedures has been crucial to increased understanding of the intricacies of the marine nitrogen cycle (Zehr 2011; Thompson and Zehr 2013).

Without the advent of gene-based abundance technologies we would essentially know nothing about some of the unicellular nitrogen fixing cyanobacteria, such as Group A and Group C cyanobacteria. Group A cyanobacteria have proven to be dominant in many marine environments (Church *et al*. 2005a; 2005b, Foster *et al*. 2009, Moisander *et al*. 2010) and may be quite a significant contributor of new nitrogen in these regions (Church *et al*. 2005b). Gene-based technologies have also helped to elucidate the ecological significance of these unicellular cyanobacterial groups, and have expanded our understanding of the role of unicellular,

filamentous and heterocystous cyanobacteria in the global oceans (Thompson and Zehr 2013).

However, there are discrepancies between gene-based and optical abundance data. Often an order of magnitude higher gene-based abundance is reported for *Trichodesmium* than can be accounted for by optically enumerated cells (Luo *et al*. 2012). This is troubling when considering biomass estimations derived from gene-based abundance data, as it would likely be an overestimation of actual biomass, and could result in an inaccurate representation of dominant biomass when assessing total *nif*H community structure. This of course also has knock on effects when comparing gene-based abundance data with nitrogen fixation rate measurements and other parameters.

This study compares gene-based abundance data alongside optical abundance data for both *in situ* and culture experiments. Herein, we endeavour to explain the higher abundance of detectable *nif*H gene copies relative to optical cell counts through an investigation of polyploidy in *Trichodesmium*. In the case of prokaryotes, polyploidy is the condition of containing more than one genome per cell. Polyploidy is known to be present in other cyanobacterial groups such as *Synechocystis* and *Anabaena,* and known polyploid prokaryotes actually outnumber known monoploid prokaryotes (Griese *et al*. 2011). This suggests polyploidy may be the norm for prokaryotic organisms and thus the investigation of this condition in *Trichodesmium* is warranted.

Results from comparisons of gene-based and optical abundances, assessments of the potential contribution *Trichodesmium* would make to *in situ* chlorophyll derived from gene-based abundances if assuming a single gene copy per cell, and microscopic assessments of intracellular DNA distribution in *Trichodesmium* all suggest polyploidy is a reasonable explanation for the aforementioned discrepancy. Gene-based technologies are still a useful tool for assessing the diversity and biogeography of *nif*H-containing organisms, but we caution against any use of direct conversion from detectable *nif*H gene copies to cell numbers, and call for reintroduction of optical based cell counts when conducting assessments of

Trichodesmium biomass *in situ* until a suitable conversion metric can be established, should this even be possible.

4.3 Methods

4.3.1 Investigation of ploidy in *Trichodesmium*

Surface cell counts for *Trichodesmium* (Chapter 3) were compared with surface *nif*H gene copy abundance using the filamentous probe (Chapter 2). Following detection of an enhanced gene-based abundance relative to cell counts, samples were obtained from *Trichodesmium erythraeum* IMS 101 cell cultures to conduct a side by side analysis of the two abundance methodologies. Ten millilitres of four different cultures grown under varying phosphorus sources were filtered in triplicate onto 0.22 µm Durapore (Millipore) filters under low (2 mbar) vacuum pressure. Testing of the different phosphorus conditions was opportunistic, but was later used to determine if differences in gene and optical abundances were affected by the phosphorus source or ages of cultures. After filtration, filters were flash frozen in liquid nitrogen and stored at -80˚C until DNA extraction as described previously (Chapter 2.3.2). Primers and probes were chosen for amplification of the filamentous *nif*H phylotypes and qPCR was run as described above (Chapter 2.3.3) by Dr. Rebecca Langlois at the Leibniz Institute for Marine Sciences, in Kiel, Germany; Dr. Langlois is now located at Dalhousie University in Halifax, Nova Scotia, Canada.

Cell counts were performed in triplicate on 10 mL sub-samples of the *Trichodesmium erythraeum* IMS 101 cultures, which were preserved in 2% acidic Lugol's iodine (Throndsen 1978). Cell abundance was directly measured from free trichomes via light microscopy at 200x magnification. A 10 mL sub-sample was also filtered onto a 25mm GF/F, 0.7µm poresize filter, which was frozen until acetone extraction and fluorometric chlorophyll determination.

4.3.2 Genome Copy Determination

Theoretical genome copies per cell were determined for *in situ* and culture samples. Following qPCR, the calculated gene copies per litre were divided by optically determined cells L^{-1} to give an upper threshold for potential genome copies per cell as described by Pecoraro *et al*. (2011).

4.3.3 DAPI staining and Imaging

Trichodesmium erythraeum IMS 101 was examined under epifluorescent microscopy following DAPI staining to assess intracellular DNA distribution. Following gravitational settling and aspiration of five millilitres of media, *Trichodesmium* biomass was fixed with 1% glutaraldehyde, 3% formaldehyde, and 14% sucrose in PIPES buffer. After 20 minutes at 4 ˚C, samples were filtered onto 0.8µm polycarbonate black filters, transferred to microscope slides, and were mounted with **VECTASHIELD HardSet Mounting Medium with DAPI at 1**.5 µg mL^{-1} (Vector Laboratories). Slides were allowed to set overnight at 4 ˚C. Samples were imaged on a Leica SP5 confocal microscope under UV and 488nm excitation, which excites DAPI, chlorophyll *a*, and phycoerythrin fluorescence. The method used to process and acquire the transmission electron micrographs is discussed thoroughly in Chapter 5.3.

4.4 Results

4.4.1 Discrepancy between cell counts and gene copies

A large discrepancy between the abundance of gene copies and cell numbers is apparent when comparing cell counts and gene copies from *in situ* data. Abundances from gene copies consistently exceed cell count abundances by one to two orders of magnitude except at the lowest end of abundance where under sampling may have contributed to non-representative DNA extractions, and gene copies below the detection limit of the qPCR assay resulted in cells counts exceeding gene copies (Figure 4-1A). For culture samples, the discrepancy between gene copies and cell counts consistently span two orders of magnitude (Figure 4-1B). The trend of gene copies exceeding cell counts is consistent for all data, and the two abundance methodologies correlate strongly (R^2=0.89) (Figure 4.2).

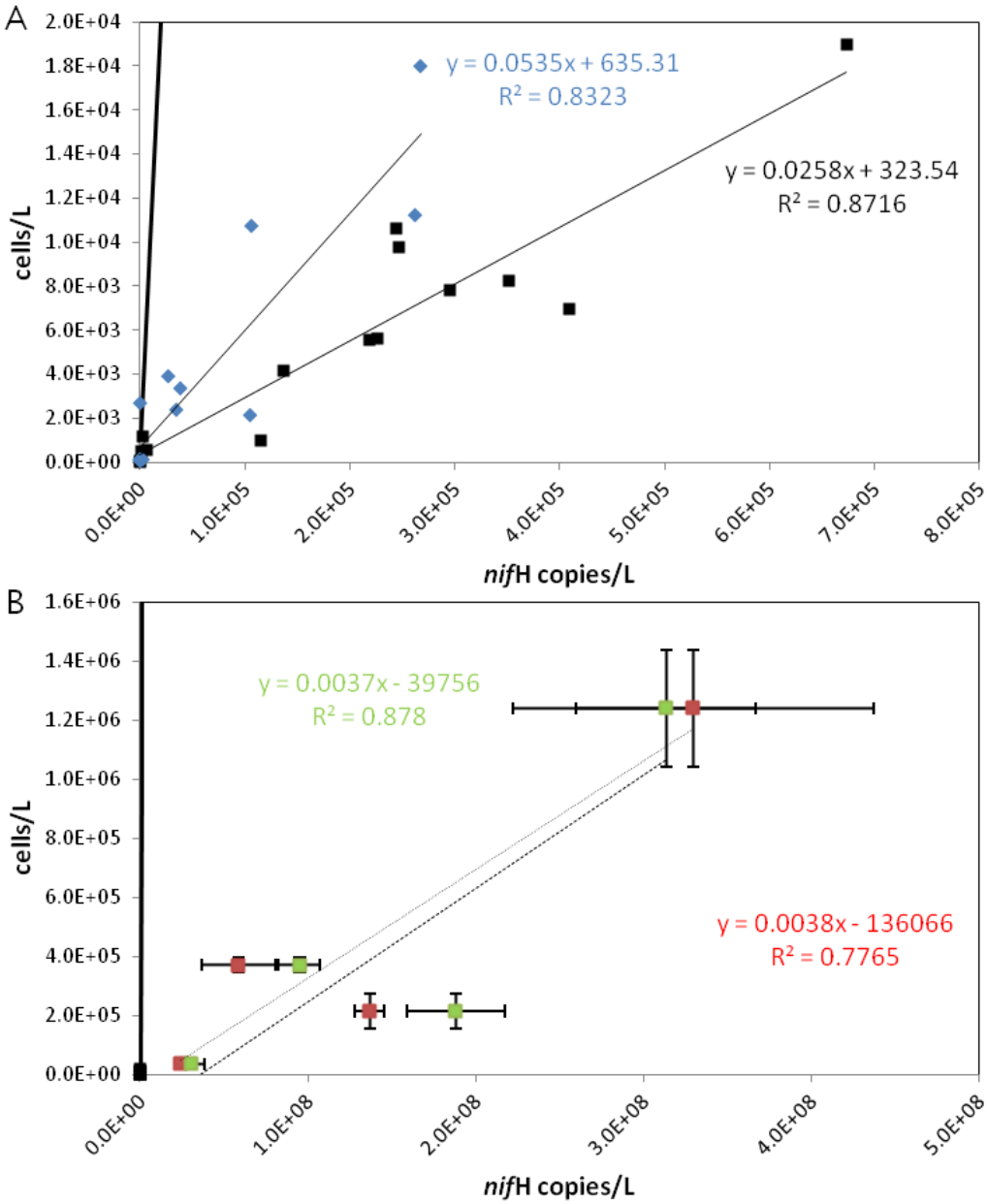

Figure 4-1. Raw Discrepancy between *Trichodesmium* cell counts and *nif*H gene copies. (A) *in situ* data from surface samples along the D361 transect (black), R^2=0.87, and AMT17 transect (blue), R^2= 0.83, and (B) *Trichodesmium erythraeum* IMS101 culture samples extracted from Durapore (red), R^2=0.78, and polycarbonate (green), R^2=0.88, filters. Gene copies consistently exceed cell counts by one to two orders of magnitude ($p<0.01$), except at and below the limit of detection for the qPCR assay. Theoretical genome copies per cell derived from this discrepancy (gene copies/L divided by cells/L; Pecoraro *et al.* 2011) range from 1-119 for *in situ* data and from 159-698 for *Trichodesmium erythraeum* IMS 101. The solid black lines represent a 1:1 ratio between cell counts and gene copies.

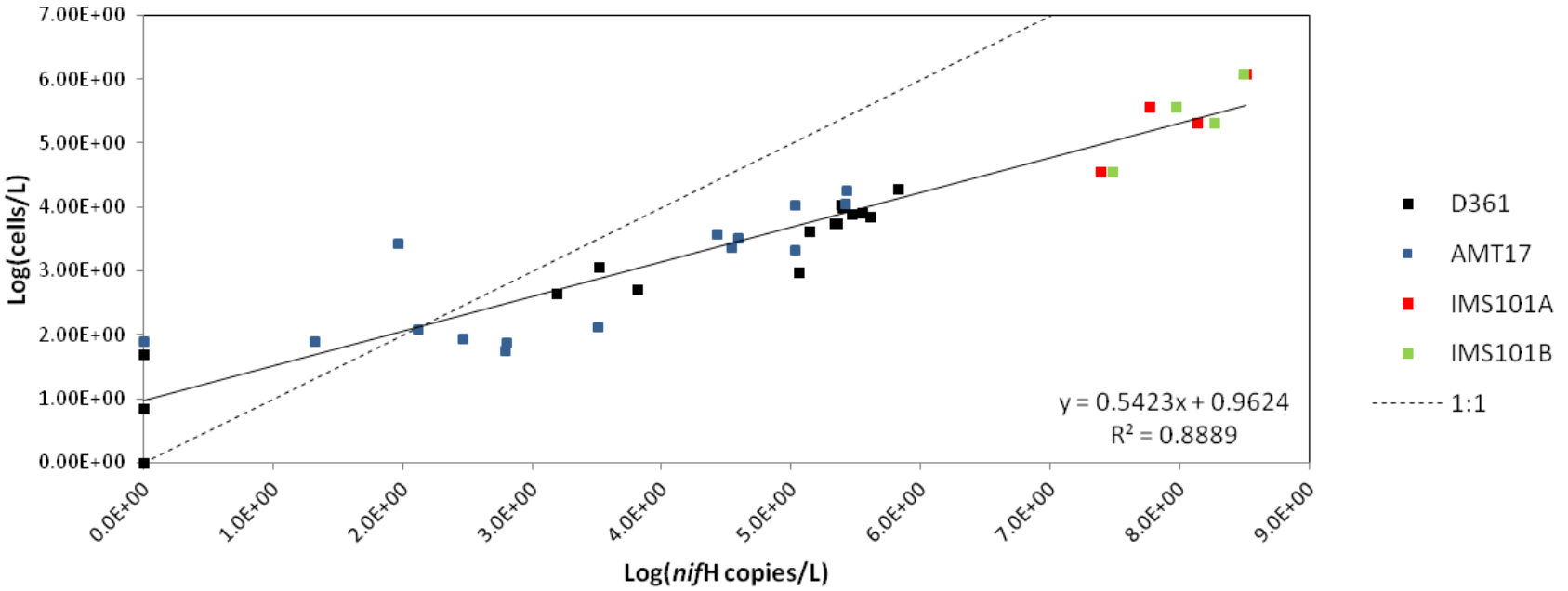

Figure 4-2. A combined assessment of log transformed cell count and gene copy abundances to illustrate the sustained discrepancy across all samples, except at and below the limit of detection for the qPCR assay.

4.4.2 Ploidy assessment

In *Trichodesmium* IMS101, estimated genome copies per cell ranged from an average of 159 ± 59 to 698 ± 100 (Table 4-1), while the ploidy level of *Trichodesmium* spp. collected *in* situ averaged 12 ± 13 (1 - 50) on AMT17 and 31 ± 30 (1 - 120) on D361.

Table 4-1. Estimated genome copies in *T. erythraeum* IMS 101 under varying phosphorus conditions calculated by division of gene copies/L by cells/L as described by Pecoraro *et al*. 2011).

Culture (phosphorus source)	**Cell count (cells/L)**	**Potential genome copies**
T. erythraeum IMS 101 (PO4 exponential)	213967 ± 59800	639.4 ± 41.3
T. erythraeum IMS 101 (PO4 senescent)	35367 ± 2201	697.5 ± 100.1
T. erythraeum IMS 101 (Glycerol)	1239533 ± 195725	265.9 ± 86.8
T. erythraeum IMS 101 (Methyl)	370000 ± 25662	158.7 ± 59.2

4.4.3 Intracellular DNA distribution

All stained *Trichodesmium* cells revealed a markedly segregated DAPI staining throughout the entirety of the cell in which the pattern of distribution was unique along the z plane (i.e. through the depth of the cell), implying intracellular DNA distribution in *Trichodesmium* IMS101 is scattered and extensive (Figure 4-3). Chlorophyll and phycoerythrin were predominantly constrained to the thylakoid lamellae (Figure 4-4A). Transmission electron microscopy (TEM) of the same culture revealed that ultrastructure alone cannot account for the observed scattering as intracellular organic matter is not segregated in the same manner as is observed by DAPI fluorescence (Figure 4-4B).

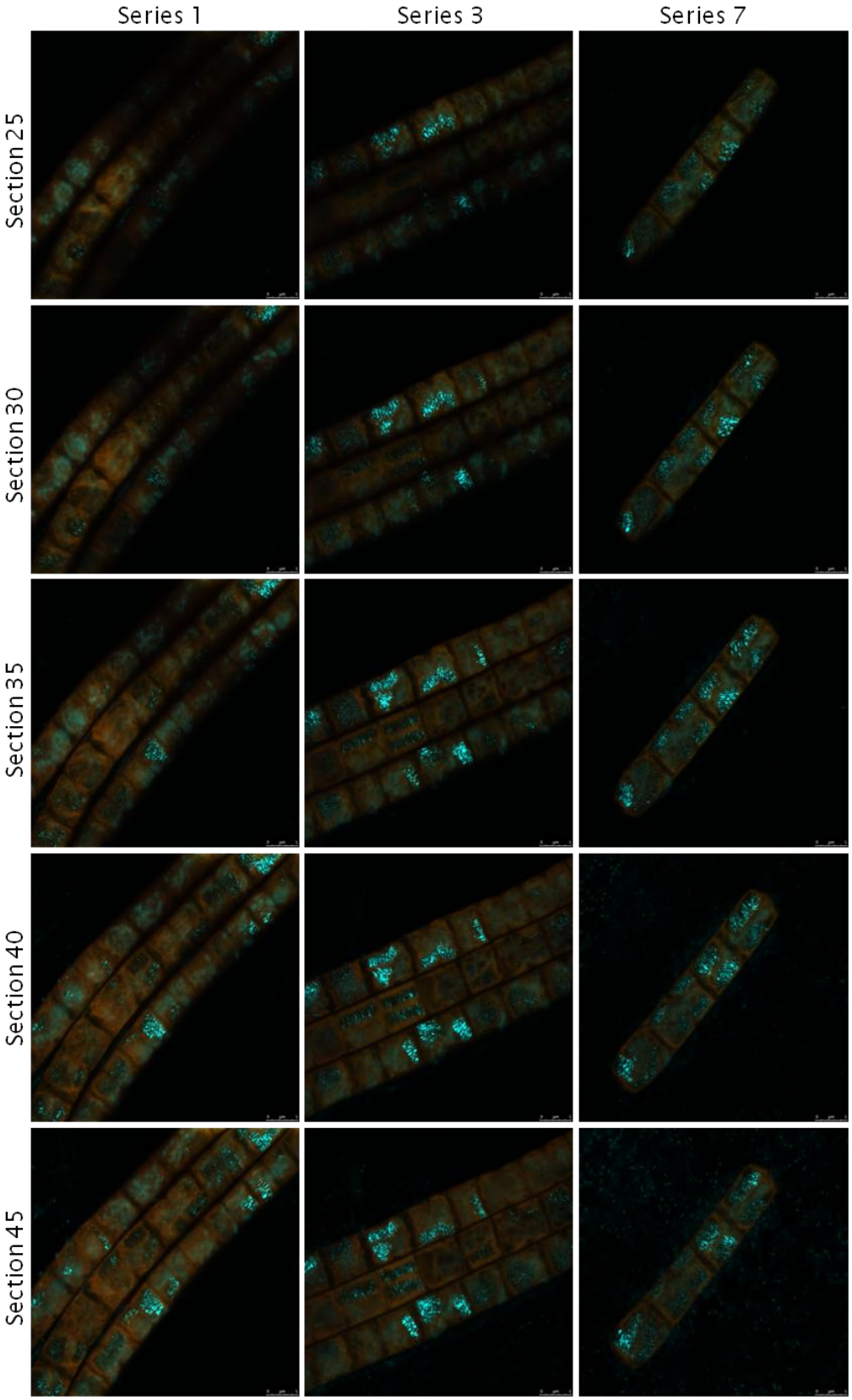

Figure 4-3. Multiple sections of 3 series (out of 11) of DAPI staining assessments in *Trichodesmium* IMS101 showcasing the DNA distribution within each cell is not uniform along the z plane (sections). The distance between each panel is approximately 55nm. Scale bars represent 5 µm.

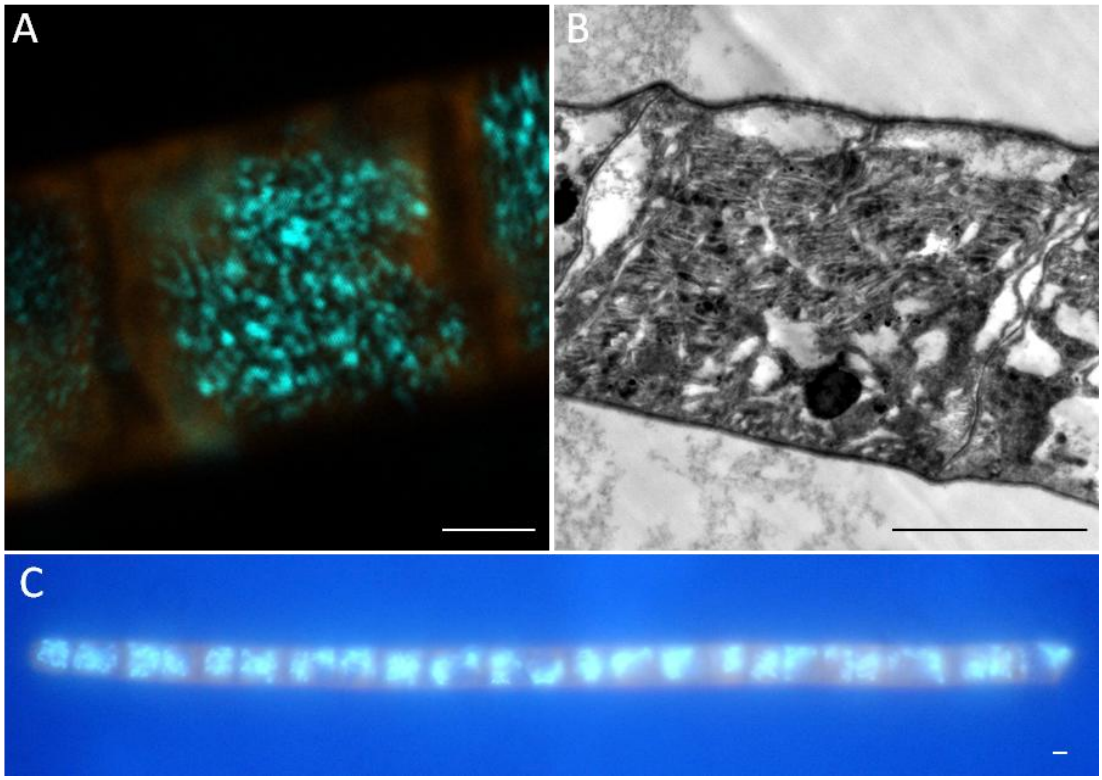

Figure 4-4. DNA distribution in *Trichodesmium erythraeum* IMS 101. (A) DAPI (blue) and autofluorescence (orange) illustrate marked segregation of DNA staining within the cell. (B) Transmission electron micrograph illustrating that ultrastructure alone doesn't account for DAPI staining patchiness as intracellular organic matter is not segregated in the same manner as is observed by DAPI fluorescence. (C) Such DNA segregation is not as readily visible as lower resolutions. Scale bars represent 2µm.

4.4.4 Chlorophyll

The chlorophyll content of individual *Trichodesmium* IMS 101 derived from cell counts and from qPCR of the *nif*H gene in extracts was highly variable. Cellular chlorophyll content derived from cell counts was on the pictogram scale as is consistent with the literature, while cellular chlorophyll content derived from assumptions that a single *nif*H gene copy is equal to a single cell was on the femtogram scale, three orders of magnitude below cellular chlorophyll levels reported in the literature (Figure 4-5).

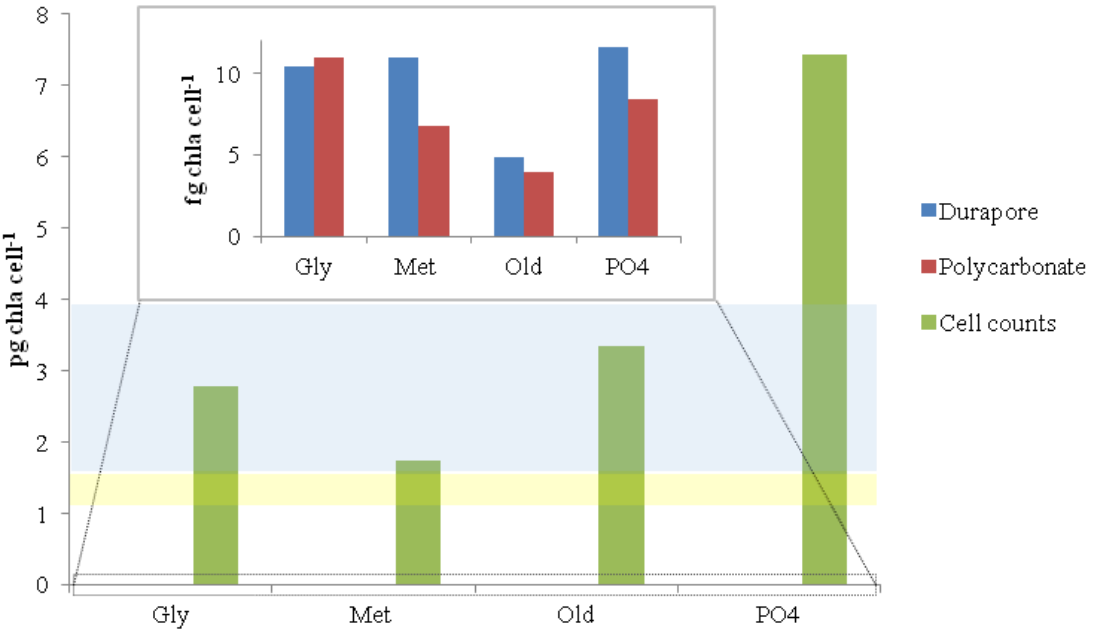

Figure 4-5. Theoretical chlorophyll content of individual *Trichodesmium* IMS 101 cells derived from cell counts (green) and from qPCR of the *nif*H gene in extracts from Durapore (blue) and polycarbonate (red) filters over the four cultures of varying age and phosphorus source. The femtogram scale of chla per cell derived from qPCR abundances implies gene copies are not an accurate representation of cell number as cellular chlorophyll content derived from these abundances results in 3 orders of magnitude less chlorophyll per cell than is reported in the literature. Literature values for *Trichodesmium* cellular chlorophyll content are represented by the yellow box, 1.1-1.5 pg chla cell^{-1} (La Roche and Breitbarth 2005), and the blue box, 1.56-3.9 pg chla cell^{-1} (Carpenter *et al.* 2004); it should be noted that these cellular chlorophyll content values are derived from field samples, which may contain less chlorophyll per cell than observed in the phosphate culture.

4.5 Discussion

This data suggests that the greater abundance of gene copies relative to cells counts is not due to a deficit in cell counts, but rather is due to the presence of more than one copy of the genome in each *Trichodesmium* cell. *T. erythraeum* IMS101 only has a single copy of the *nif*H gene in its genome (Genbank accession NC_008312), but the number of genome copies per cell has yet to be evaluated. If *Trichodesmium* is polyploid, this could explain the discrepancy between *nif*H-based and cell count-based abundances. The marked segregation of nuclear material hints at the possibility for multiple

individual genomes to be scattered throughout *Trichodesmium* cells (Figure 4-4). Scattering of nuclear material has been previously highlighted by Siddiqui *et al*. (1992) who noted a difference in DNA distribution between *T. erythraeum* and *T. thiebautii* cells where the latter showed a scattered pattern. The nuclear material in *T. erythraeum* on the other hand is more centrally located (Van Baalen and Brown 1969). However, both of these studies assessed *Trichodesmium* DAPI stains under epifluorescence microscopy where the resolution is 200 nm, the confocal microscopes assessments herein allowed for resolution of 80 nm, and thus may have revealed this segregatory DNA pattern in *Trichodesmium* more clearly (Figure 4-4A, C). Other ultrastructural characteristics of *Trichodesmium*, including DNA distribution, will be discussed further in Chapter 5.

Some other species of cyanobacteria are polyploid (Table 4-2), such as species of the freshwater diazotrophic genus *Anabaena*, which can contain 8-25 genome copies per cell (Simon 1977, 1980) and a motile wild-type strain of the marine cyanobacterium *Synechocystis* (PCC 6803) which can contain up to 210-226 genome copies per cell during exponential growth and 53-59 genome copies per cell during stationary phase (Griese *et al*. 2011). Ploidy in cyanobacteria is often determined by comparing gene-based and optical-based abundance data, but this argument has not yet been adopted to explain the discrepancies commonly observed between quantification of *Trichodesmium* spp. via optical cell counts and gene copies (Luo *et al*. 2012).

There are many advantages to being polyploid, such as insurance of chromosome presence in daughter cells (Schneider *et al*. 2007). Differing DNA concentrations in daughter cells of *Synechocystis* has been previously observed (Schneider *et al*. 2007). This could be a particular advantage for *Trichodesmium* as the cells are large, and genetic material could be more easily distributed throughout the cell. Similarly, although intracellular transport is not well described in *Trichodesmium*, multiple genome copies distributed throughout each cell could allow for transcription and protein expression in a localised area of the cell.

Table 4-2. Experimentally determined ploidy levels of marine and aquatic cyanobacterial species (Amended from Griese *et al*. 2011)

Species	Physiology	Cell size (μm)	Genome size (Mbp)	Average ploidy level	Ploidy	Reference
Anabaena cylindrica	Aquatic	10	-	25	Polyploid	Simon (1977)
Anabaena variabilis	Aquatic	10	7.1	5-8	Oligoploid	Simon (1980)
10 Microcystis strains	Aquatic	5	-	1-10	Oligoploid	Kurmayer & Kutzenberger (2003)
Anabaena sp. PCC 7120	Aquatic	10	7.2	8.2	Oligoploid	Hu *et al*. (2007)
Prochlorococcus	Marine	1	1.7	-	Monoploid	Vaulot *et al*. (1995)
Synechococcus elongatus PCC 7942	Marine	0.8-1.5	2.8	3.9/3.3*	Oligoploid	Griese *et al*. (2011)
S. elongatus PCC 7942	Marine	0.8-1.5	2.8	3-5	Oligoploid	Mori *et al*. (1996)
Synechococcus sp. PCC 6301	Marine	0.8-1.5	2.7	2-6	Oligoploid	Binder & Chisholm (1990)
Synechococcus sp. WH 7803	Marine	0.8-1.5	2.4	3.6	Oligoploid	Griese *et al*. (2011)
Synechococcus sp. WH 7803	Marine	0.8-1.5	2.4	2-4	Oligoploid	Binder & Chisholm (1995)
Synechococcus sp. WH 7805	Marine	0.8-1.5	2.6	1	Monoploid	Binder & Chisholm (1995)
Synechococcus sp. WH 8101	Marine	0.8-1.5	3.2	1	Monoploid	Armbrust *et al*. (1989)
Synechococcus sp. WH 8103	Marine	0.8-1.5	2.7	1-2	Monoploid	Binder & Chisholm (1995)
Synechocystis sp. PCC 6803 (motile)	Aquatic	2-5	3.6	218/58/58*	Polyploid	Griese *et al*. (2011)
Synechocystis sp. PCC 6803 (GT)	Aquatic	2-5	3.6	142/47/43*	Polyploid	Griese *et al*. (2011)
Synechocystis sp. PCC 6803 ('Kazusa')	Aquatic	2-5	3.6	12	Polyploid	Labarre *et al*. (1989)
Trichodesmium erythraeum IMS101	Marine	10	7.75	440	Polyploid	This study
Trichodesmium spp.	Marine	10	-	12, 50	Polyploid	This study (AMT17 and D361 respectively)

*Exponential phase/linear phase/stationary phase.

As the ploidy level of *Trichodesmium* is previously unconfirmed, and as we are unable to distinguish between *nif*H gene copies present inside living diazotrophs from extracellular *nif*H gene copies in the water column or in association with other material following grazing or apoptosis, we must consider whether the discrepancy between gene-based abundances and cell counts can be attributable to artefact. Nucleic acids are a well described component of the dissolved organic matter pool (Karl and Bailiff 1989), which can bind to particulate material in the water column and in sediments and resist degradation (Lorenz and Wackernagel 1987; Corinaldesi *et al*. 2011), but if extracellular DNA was providing additional template for *nif*H amplification, we would have expected to see a larger disproportion of gene copies to cell counts in the older [culture] samples and/or between filter types. As no significant difference ($p=0.7$) in potential genome copies was observed between active (639 ± 41.3) and senescent (697.5 ± 100.1) cultures (Table 4-1) we do not feel extracellular DNA could account for the entirety of the gene-based versus optical-based abundance discrepancy. Additionally, Durapore filters are used most frequently in qPCR work as they are known not to bind nucleic acids. If extracellular DNA was contributing to the enhanced *nif*H abundances we observed, we would have expected to detect more gene copies in samples taken onto polycarbonate filters as they may have bound more extracellular DNA, but there was no significant difference between the *nif*H abundances detected from these two filter types ($p=0.4$).

Another potential contributor of non-cyanobacteria *nif*H template could come from cyanophages. *Prochlorococcus*-specific cyanophages have been confirmed to contain identical copies of *Prochlorococcus* PSII genes (Sullivan *et al*. 2005). *Trichodesmium* may also harbour phages (Hewson *et al*. 2004), but evidence for a *Trichodesmium*-specific phage is inconclusive at current (Brown *et al*. 2013). *Trichodesmium*-associated phages appear to be phylogenetically distinct from the virioplankton community, and some even contained *Trichodesmium*–like genes (Brown *et al*. 2013). It seems likely that a *Trichodesmium*-specific phage exists, but it remains to be assessed whether DNA from said phage carrying identical *nif*H gene copies could account for some of the observed discrepancy between gene copies and cell counts. Nonetheless, we hypothesize that the entirety of the discrepancy cannot be explained by cyanophage contributions as investigations are currently being

carried on the *het*R, 16S rRNA, and *psb*A genes in *Trichodesmium* via qPCR, and premilinary results suggest that are also inflated relative to cell counts (Sargent *et al*. *In Prep*). It would be unlikely that a phage would harbour identical copies of all of these diverse genes. Additionally, if the qPCR determined ratio of *nifH* to multiple copy number genes is in close agreement with the ratio predicted from the *Trichodesmium* genome sequence (Genbank accession NC_008312) (i.e *nifH*:*hetR*:16S rRNA:*psbA* of 1:1:2:3), this would provide further evidence against phage contribution to the gene pool. Even if a *Trichodesmium*-specific phage contained each of these *Trichodesmium* genes, it is very unlikely that it would contain identical gene quantities to the host across all of these genes, especially as they are distant within the genome making horizontal acquisition extremely unlikely.

If we dismiss extracellular and viral contributions to *nif*H template and assume the discrepancy must be explained in a deficit of optical cell counts rather than enhanced gene-based abundances, then we would expect other species-specific physiological parameters to correlate with the gene-based abundances. However, if we assume each detected n*if*H gene copy attributable to *Trichodesmium* represents a single cell, the estimated chlorophyll-content per cell is a fraction of what is reported in the literature (Figure 4-5) further indicating gene-based abundances are not an accurate representation of actual cell abundance.

Further related evidence for ploidy in *Trichodesmium* is revealed when comparing the contribution that *Trichodesmium* would make to total *in situ* chlorophyll from gene-abundances reported in the literature if we assume a single gene copy represents a single cell and if a single cell contains 1.1 pg chl (La Roche and Breitbarth 2005). The lowest of the reported *Trichodesmium* chlorophyll content per cell was chosen to test whether cellular contribution to total would sill exceed 100% even if all cells contained a minimal amount of chlorophyll. As average *Trichodesmium* contribution to total *in situ* chlorophyll equals or exceeds 100% in all gene-based abundance conversions derived from the literature (Table 4-3), it is clear that *nif*H abundances cannot be considered a 1:1 proxy for cell abundance in *Trichodesmium.* The work discussed here that is derived from *Trichodesmium* abundances reported in Chapters 2 and 3 represents the only study for which we have data that assesses *in situ* optical and gene-based abundances side by side. Although *Trichodesmium*

contribution to total *in situ* chlorophyll derived from gene-based abundances does not exceed 100% on average in this study (D361), it should be noted that *Trichodesmium nif*H was dominant in the surface samples at only two stations, and at both of these stations gene-abundance derived *Trichodesmium* contribution to *in situ* chlorophyll exceeded 100% of total.

Table 4-3. Estimated *Trichodesmium* spp. contribution to total *in situ* chlorophyll based on cell counts and gene copies.

***Trichodesmium* contribution to total chlorophyll %**			
Cell counts	**Gene copies**	**n**	**Source**
0-8.02 (4.1 ± 1.74)	NA	16	This study, AMT 21
0-11.61 (4.43 ± 7.92)	NA	33	Fernández *et al*. 2010**
0.2-13.7 (7.19 ± 4.45)	NA	22	Letelier & Karl 1996**
0-175.52 (18.75 ± 30.26)	NA	336	Capone *et al*. 2004**
0-243.93 (22.93 ± 33.97)	NA	335	Borstad 1978**
0.6-276 (32.9 ± 47.89)	NA	67	This study, CH0711
0-6 (2.14 ± 2.45)	0-98.37 (10 ± 24.93)	31	This study, AMT 17
0-17.8 (4.14 ± 4.3)	0-138.7 (44.33 ± 63.88)	15	This study, D361
NA	0-1163.83 (99.58 ± 275.56)	23	Kong *et al*. 2011**
NA	0-2065.48 (120.33 ± 319.11)	125	Moisander *et al*. 2010**
NA	1-440 (136.0 ± 126.1)	13	Goebel *et al*. 2010*

*Data estimated from figures, **Data taken from Luo *et al*. 2012 dataset; AMT17 data was supplied by Dr. Mark Moore. AMT21 data was supplied by doctoral candidate Joe Snow.

Moreover, current gene-based abundances are likely underestimations of actual gene abundance due to both extraction efficiency (Foster *et al*. 2009) and undersampling of diazotroph biomass (Carpenter *et al*. 2004). This suggests that the discrepancy between gene and optical-based abundances may be even larger. Previous work has documented a 10 L sample requirement for accurate representation of *Trichodesmium* populations *in situ* when conducting optical cell counts and note that even larger volumes may be required when sampling in areas of low biomass (Carpenter *et al*. 2004). Smaller sample volumes run the risk of excluding colonies of *Trichodesmium* especially when these samples come from Niskin bottles as the buoyant nature of *Trichodesmium* could result in colonies only being accessible when the last bit of water was sampled. Gene based abundances were determined from a 2 L Niskin sample for this study (D361 cruise) as well as for one of the studies

documented in Table 4-3 (Goebel *et al*. 2010). The other aforementioned studies sampled 4-5 L (Moisander *et al*. 2010) and 0.5-1 L from Niskin bottles (Kong *et al*. 2011). Thus, all are potentially underestimations of actual gene abundance, and therefore we have potential underestimated the level of ploidy in *in situ* population of *Trichodesmium spp*.

Trichodesmium, like all living organisms, requires phosphorus for growth, and although cellular phosphorus pools in phytoplankton are often dominated by RNA (Geider and La Roche 2002), genomic P contribution to cellular P can exceed 50% in some cyanobacteria, such as *Synechococcus* and *Prochlorococcus* (Bertilsson *et al*. 2003). To assess whether the ploidy level of *Trichodesmium* determined herein is plausible, an evaluation of genomic P contribution to cellular P was carried out after converting colonial P values reported in the literature to cellular P concentrations (Figure 4-6) to insure estimations of genomic P would not exceed 100% of cellular P. A single *Trichodesmium* genome was calculated to contain 7.97×10^{-16} g of P, and the range of cellular P content for *Trichodesmium* spp. was calculated as 3.10×10^{-13} – 1.41×10^{-12} g P *in situ* (Tovar-Sanchez *et al*. 2011; Neuster *et al*. 2012; this study), and 6.19×10^{-13} - 2.17×10^{-12} g P in *Trichodesmium* IMS 101 in culture (Barcelos e Ramos *et al*. 2007). The range of ploidy in the *in situ* samples from D361 and AMT17 correspond to a maximal genomic contribution to total P of just over 25%. The same assessment for *Trichodesmium* IMS101 spans nearly the entire range from 6-95% genomic P contribution to cellular P (Figure 4-6).

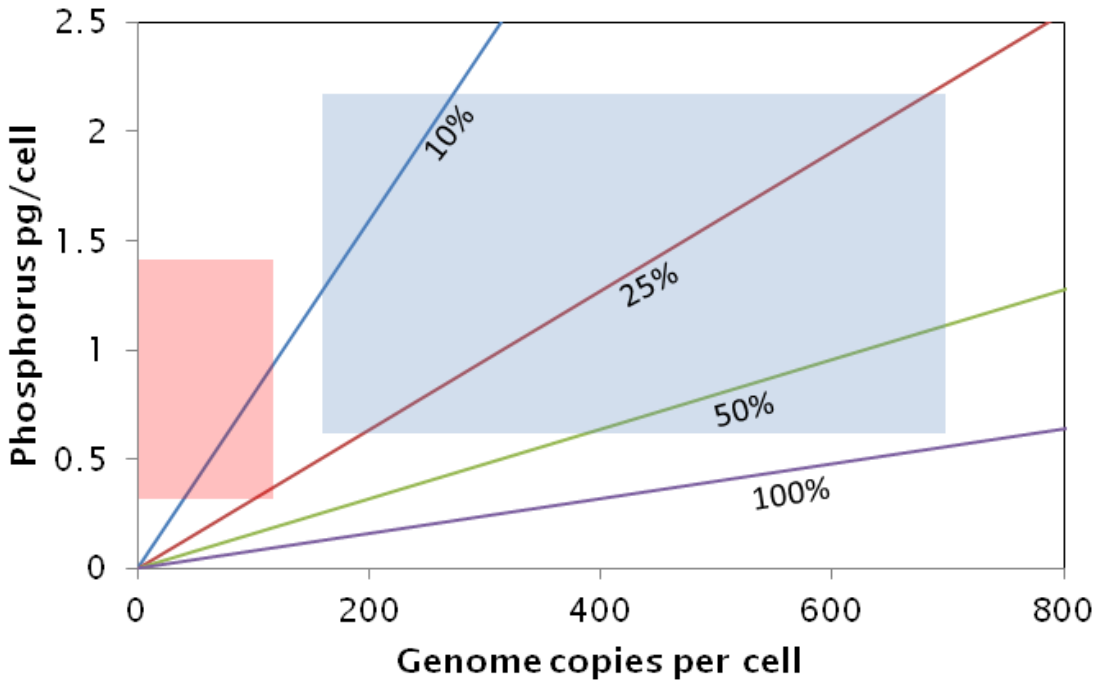

Figure 4-6. Genomic contribution to total cellular phosphorus in *Trichodesmium*. Diagonal lines indicate the ranges within which genomic P accounts for 10, 25, 50, and 100% of total cellular P. The red box incorporates the observed range of genome copies per cell in *Trichodesmium* spp. from D361 and AMT17 and the range of cellular P content for *Trichodesmium* spp. *in situ* (Tovar-Sanchez *et al*. 2011; Neuster *et al*. 2012; this study) following conversion from colonial P to cellular P assuming 200 trichomes per colony and 100 cells per trichome (Carpenter *et al*. 2004). The blue box incorporates the range of observed genome copies per cell (this study) and the range of cellular P content for *T. erythraeum* IMS101 (Barcelos e Ramos *et al*. 2007).

As the range of genome copies per cell in *Trichodesmium* is so large, it is difficult to normalise the contribution genomic P would make to cellular P based on population assessments where cells may be under different environmental stressors or in different growth phases. Potentially, the ploidy level, and thus the genomic P contribution to total cellular P, in *Trichodesmium* IMS101 is inflated relative to *in situ* populations simply because replete nutrient conditions allow for excess P uptake. Previously Bertilsson *et al*. (2003) theorised that decreased nutrient availability may lead to a marked depletion in RNA and DNA concentrations in *Prochlorococcus* and *Synechococcus*. The same may also be the case for P-stressed *Trichodesmium* spp. populations *in situ*. The remaining cellular P in these populations may come from polyphosphate, which has been previously reported to compose 8% - 25% of cellular P in nutrient deplete conditions in the Sargasso Sea (Orchard *et al*. 2010), and other P-rich cellular components, such as RNA, phospholipids,

and ATP (Geider and La Roche 2002). Further evidence for polyploidy in *Trichodesmium* relative to cellular P content stems from genomic P contribution to total cellular P if only one genome was present in the cell. In this case, genomic P would compose less than 0.5% of total cellular P, which would force P contributions from other cellular components much higher than has been previously reported (Bertilsson *et al*. 2003). Future investigation of the elemental composition and physiology of ploidy in *Trichodesmium* IMS101 and *in situ* populations is essential to better interpret these findings.

4.6 Conclusion

The discrepancy between *nif*H gene copy abundances and cell count abundances supports polyploidy in *Trichodesmium*, as gene-based abundances consistently exceed optical abundances both in field and culture samples. Along with reconfirmation of this discrepancy, the additional optical and molecular assessments strongly suggest that *Trichodesmium* is polyploid as the demonstrated method for determining ploidy in other cyanobacteria, comparison of optical and gene-based abundance reveals the potential for a high level of ploidy in *Trichodesmium*. This has serious implications for any research relying on biomass estimates derived from *Trichodesmium nif*H-based abundances as such conversions would almost surely result in largely inflated values. Additionally, as variance in growth phase results in marked differences in genome copies per cell in other cyanobacteria dependent (Griese *et al*. 2011), and since we also observed variations in genome copies in *Trichodesmium* under varying conditions, we are unable to suggest a useful conversion metric for determining accurate cell abundance from *nif*H gene copy abundances in *Trichodesmium* at present.

Apart from the previously described advantages of polyploidy, such as insurance of chromosome presence in daughter cells, it remains to be investigated whether *Trichodesmium* may benefit in other ways from being polyploid. Such investigations would be integral to increasing our understanding of the ecophysiology of this organism. Although polyploidy in

Trichodesmium is anomalous when compared to other marine cyanobacteria which are mostly monoploid (Table 4-2), *Trichodesmium* is also anomalous in its physiological capabilities. It would be interesting to assess whether the level of ploidy in *Trichodesmium* varies with growth phase as is seen in other polyploid organisms or if *Trichodesmium* may use production and storage of multiple genome copies as a mechanism for phosphorus storage.

At minimum these results do necessitate that the physiology and ploidy level of *Trichodesmium* be more thoroughly investigated before any conversion from gene copy abundances to biomass are integrated into standard practice. We suggest that special consideration be taken when only compiling *nif*H-based abundances, and that these assessments be limited to biogeography and *nif*H community structure diversity at present. This work also provides motivation for future investigations of polyploidy in other *nif*H-containing organisms, such as the heterocystous diazotroph *Richelia intracellularis*.

5. Ultrastructure of negatively buoyant *Trichodesmium* and implications for cell death pathways

5.1 Abstract

Previous observations indicate that *Trichodesmium* is important in export production through a variety of mechanisms, and that it is likely remineralised in the upper twilight zone (<500 m), thus contributing to the N* anomaly in the thermocline of the subtropical North Atlantic (Chapter 3). However, the cellular integrity and intracellular storage products in sinking *Trichodesmium* colonies have yet to be assessed. As earlier estimations of *Trichodesmium* contribution to particulate organic nitrogen (PON) standing stock hinge on assumptions of standard nitrogen content per cell, investigations of the ultrastructure of negatively buoyant *Trichodesmium* is necessary to determine whether these assumptions are accurate. Here, Transmission Electron Microscopy (TEM) was used to assess the intracellular integrity and ultrastructural storage components of negatively buoyant *Trichodesmium* colonies collected below 100 m in the Sargasso Sea. Results suggest that due to extensive vacuolisation of negatively buoyant *Trichodesmium* cells and associated loss of cellular DON, it appears sinking colonies do not contain as much PON as previously assumed in Chapter 3. However, collapsed gas vesicles were observed in these negatively buoyant cells indicating *Trichodesmium*'s inability to return to the surface layer, and other ultrastructural characteristics strongly indicate programmed cell death (PCD) is responsible for sinking in *Trichodesmium*. This well characterised cell death pathway eventually results in apoptosis, thus ensuring any *Trichodesmium* biomass that exits the mixed layer during PCD would be rapidly available for remineralisation at depth following apoptosis (cellular lysis). This study provides further insight into impending release of fixed N into the water column, which is essential to understand how much nitrogen is being exported in this organism, and highlights previously undescribed mechanisms by which *Trichodesmium* can contribute to the anomalous nutrient distributions in the North Atlantic thermocline.

5.2 Introduction

The ultrastructure and intracellular storage components of both *in situ* populations of *Trichodesmium* spp. and of the cultured *Trichodesmium* IMS 101 are thoroughly described in the literature (van Baalen and Brown 1969; Haxo *et al*. 1987; Siddiqui *et al*. 1992; Janson *et al*. 1995; Berman-Frank *et al*. 2004), but the ultrastructural details of negatively buoyant colonies are currently unknown. The fate of *Trichodesmium* blooms is still not fully defined, but lytic viral destruction of cells (Hewson *et al*. 2004) and programmed cell death (PCD) (Bar-Zeev *et al*. 2013) are assumed to be the two main pathways by which bloom demise occurs. The fate of *Trichodesmium* in non-bloom conditions is even more ambiguous, but results suggest a variety of mechanisms transport this organism out of the upper ocean where it is then remineralised (Chapter 3). As enhanced PON export has been observed following the collapse of an artificial bloom of *Trichodesmium* (Bar-Zeev *et al*. 2013) and colonies have been known lose their innate buoyancy and sink during senescence (Berman-Frank *et al*. 2004), investigations of the quality and integrity of sinking *Trichodesmium* are crucial to better understand the fate of *Trichodesmium*-derived nitrogen.

The optical observations of sinking *Trichodesmium* and subsequent estimations of *Trichodesmium*-specific contribution to PON (Chapter 3) rely on the assumption that colonies are engaging in over-ballasted vertical migration and that cells are otherwise healthy and intact when they exit the mixed layer. The link between enhanced N* distributions and *nif*H concentrations (Chapter 2) also suggest that remineralisation of nitrogen-rich diazotrophic material, including *Trichodesmium*, is occurring between 100 and 500 m. What remains to be assessed is the quality of this sinking diazotroph biomass, confirmation of the mechanism(s) causing *Trichodesmium* colonies to sink, and elucidation of the species involved.

Some ultrastructural assessments aid in taxonomic classification of *Trichodesmium* allowing for speculation on the effect species-specific physiology has on the fate of *Trichodesmium*. For example, only *T. thiebautii* is known to possess intracellular scroll-like bodies, which are

involved in anti-grazing toxin production (Siddiqui 1992; Janson *et al*. 1995). Using this and other ultrastructural markers to establish the species type of negatively buoyant *Trichodesmium* colonies is of particular interest when considering variability in gas vacuole dynamics between *Trichodesmium* species. *Trichodesmium erythraeum* is seemingly much more susceptible to gas vacuole collapse than *T. thiebautii* (Walsby 1978), which has implications for colonial ability to return to the surface layer following a nutrient mining attempt as gas vacuole collapse in these cells eliminates their innate buoyancy (Chapter 3). Determining species type ultimately aids in expanding our understanding of the fate of *Trichodesmium*-derived new nitrogen.

Transmission Electron Microscopy (TEM) can be used to assess intracellular storage components, such as cyanophycin granules. Cyanophycin granules are a known nitrogen storage structure in *Trichodesmium* (Siddiqui *et al*. 1992; Romans *et al*. 1994; Fredriksson and Bergman 1997; Finzi-Hart *et al*. 2009). These nitrogen storage vacuoles a rich in newly fixed nitrogen (Finzi-Hart *et al*. 2009). They have been observed to be produced during active nitrogen fixation in the day time and are subsequently consumed at night (Finzi-Hart 2009). Thus, the presence of cyanophycin granules within negatively buoyant *Trichodesmium* cells would indicate both recent nitrogen fixation activity, and enhanced, concentrated nitrogen stores available for remineralisation if these colonies are unable to return to the surface layer.

TEM allows visualisation of other intracellular storage structures, such as ballasting components, which can shed light on the mechanism behind sinking in these *Trichodesmium* colonies. We have yet to confirm whether over ballasted vertical migration is a plausible explanation for *Trichodesmium*'s presence below 100 m (Chapter 3). If vertical migration is taking place, ballasting components should be present in negatively buoyant *Trichodesmium* cells. Suspected ballasting components in *Trichodesmium* include poly-β-hydroxybutyric acid (PHB) granules and polyglucoside granules (Siddiqui *et al*. 1992; Romans 1994). This is important in determining the quality of sinking *Trichodesmium* as over ballasted *Trichodesmium* would theoretically transport all of its PON out of the mixed layer (Figure 5-1).

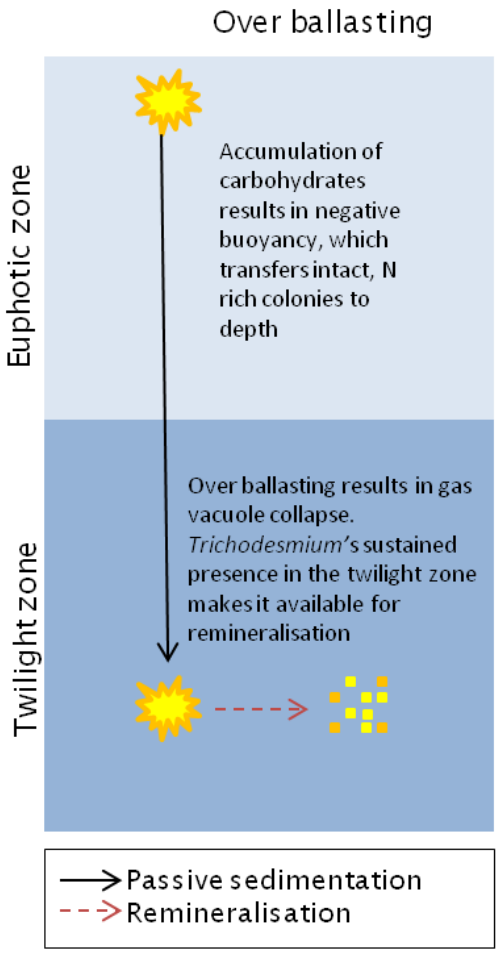

Figure 5-1. Schematic representation of over ballasting and Trichodesmium PON quality.

Another potential cause of sinking in *Trichodesmium* colonies includes cell death, and various cell death pathways can be determined via ultrastructural assessments, including cell wall integrity. Although cell wall integrity is often maintained during the early stages of programmed cell death (PCD) in *Trichodesmium (*Berman-Frank *et al*. 2004), other cell death pathways, such as necrotic cell death, result in marked degradation of cellular membranes (Jiménez *et al*. 2009). PCD is an apoptotic-like cell death pathway that is well characterised in eukaryotes (Jiménez *et al*. 2009), and has recently been described as a common cell death pathway in *Trichodesmium* (Berman-Frank *et al*. 2004; Bar-Zeev *et al*. 2013). PCD can occur in *Trichodesmium* as cells age or following exposure to various environmental stressors (Berman-Frank *et al*. 2004). PCD is characterised by unique intra and extracellular characteristics in *Trichodesmium*, such as

cellular shrinkage and cytoplasmic vacuolisation, which precedes cellular lysis (Berman-Frank *et al*. 2004). The presence of these and other characteristics could indicate PCD as the trigger for sinking of *Trichodesmium* colonies.

Results from ultrastructural assessments of *Trichodesmium erythraeum* IMS101, positively buoyant surface colonies, and negatively buoyant colonies collected between 100 and 250 m in the Western Sargasso Sea suggest that the negatively buoyant *Trichodesmium* colonies we observe herein are senescent and may be in the process of PCD. These cells were of highly vacuolated compared to surface cells, and some also contained ballasting components. As vacuolisation precedes lysis during PCD in *Trichodesmium* (Berman-Frank *et al*. 2004), the highly vacuolated negatively buoyant cells we observe imply impending release of fixed N into the water column. Thus, although these negatively buoyant cells are "element-light" compared to surface populations due to extensive vacuolisation, any nitrogen and phosphorus remaining in sinking *Trichodesmium*, such as the newly fixed nitrogen in cyanophycin granules, would be available for remineralisation at depth.

5.3 Methods

5.3.1 Colony collection and culture conditions

Positively buoyant colonies were collected via surface net tows and negatively buoyant colonies were collected using the Marine Snow Catcher between 100 and 250 m on the BATS284 research cruise in August 2012 in the Sargasso Sea. Colonies were picked using a glass Pasteur pipette and transferred into an individual well of a 24-well culture plate containing 1 mL of 0.2 µm filtered seawater. Following a sinking rate assessment to confirm positive/negative buoyancy, colonies were picked from the 24-well culture plate using an inoculation loop to minimise liquid transfer, and were placed

into 1.5 mL microcentrifuge tubes containing 1mL of 3% glutaraldehyde, 4% formaldehyde in 14% sucrose 0.1 M PIPES buffer at pH 7.2, hereafter referred to as 'main fixative'. Samples were stored at 4 ˚C until alginate embedment, postfixation and TEM processing post cruise.

Trichodesmium IMS101 cultures were maintained in YBC-II media at 27 ˚C on a 12:12 light:dark cycle on an orbital shaker prior to preservation for TEM. Cells were filtered onto 5 µm polycarbonate filters under low vacuum pressure. Filters were transferred to 10 mL centrifuge tubes containing 0.5mL of the main fixative. Cells were rinsed off the filter into the main fixative with 1 mL of the main fixative bringing the sample volume to 1.5 mL. Samples were transferred into 1.5 mL centrifuge tubes and were stored at 4 ˚C until alginate embedment, postfixation and TEM processing as described below.

5.3.2 TEM processing and imaging

The following protocol is an amendment of the official TEM preparation and processing guidelines provided by the Biomedical Imaging Unit at the University of Southampton. *Trichodesmium* samples (colonies and culture samples) in the main fixative were transferred into 1.5 mL centrifuge tubes containing 1 drop (approximately 100 µL) of 5% sodium alginate. Each suspension was then spun at 1250 *g* for 10 minutes to allow the cells to embed in the sodium alginate pellet at the bottom of the tube. The remaining main fixative was decanted and replaced with a 50:50 solution of 6% glutaraldehyde, 8% formaldehyde in 28% sucrose 0.2 M PIPES buffer to 0.1 M calcium chloride. After 10 minutes, the s*et al*ginate pellet containing the *Trichodesmium* cells was dislodged from the bottom of the microcentrifuge tube using a Pasteur pipette and was allowed to set for a further 5 minutes. The pellet and fixative/calcium chloride solution was then decanted into a TEM processing vial (0.5 mL glass vial), and loaded onto a rotator. The fixative/calcium chloride solution was aspirated and replaced with 1 ml of main fixative, and the sample was left to rotate for one hour. Once the main fixative was aspirated, the pellet was then twice rinsed in 14

% sucrose, 0.1M PIPES buffer, hereafter known as 'buffer'. The buffer was then replaced with osmium tetroxide, hereafter known as 'postfixative', and was rotated for one hour. The postfixative was aspirated and the pellet was then twice rinsed in buffer for ten minutes. The buffer was then replaced by water, and then immediately replaced by 2% aqueous uranyl acetate. Pellets were rotated in this solution for 20 minutes before beginning the dehydration series.

For dehydration, the uranyl acetate was aspirated and replaced with 30% ethanol, which was then replaced by 50% ethanol following a 10 minute rotation. This was repeated for the transfer from 50% ethanol to 70% ethanol and the transfer from 70% ethanol to 95% ethanol. The 95% ethanol was replaced by absolute ethanol and the pellet was rotated for 20 minutes before refreshing the absolute ethanol and repeating the 20 minute rotation. The absolute ethanol was then replaced with acetonitrile for a 10 minute rotation before the pellet was left to rotate in a 50:50 solution of acetonitrile:TAAB resin overnight. The aceonitrile:TAAB resin was then aspirated and the pellet was rotated in TAAB resin for 6 hours. The pellet was then embedded in fresh TAAB resin and was polymerised at 60 °C for 20-24 hours.

Polymerised resin blocks were trimmed and mounted into a Reichert Ultracut E microtome. Ribbons of ~70 nm sections were produced using glass knives (Figure 5-2), and suitable gold sections were mounted on copper grids. Grids were then lead stained. As lead stain precipitates in the presence of CO_2, drops of Reynold's lead stain were placed on dental wax inside a petri dish surrounded by pellets of NaOH to minimise CO_2 concentrations. Grids were inverted onto the lead stain drops for 5 minutes, and were then rinsed in distilled water. Grids were then blotted dry and stored until imaging. Grids were imaged on a Hitachi H7000 Transmission Electron Microscope and a FEI Technai 12 Transmission Electron Microscope at the Biomedical Imaging Unit at Southampton General Hospital. Ultrastructural characteristics were assessed according to the features described by Siddiqui *et al*. (1992) and Janson *et al*. (1995) (Table 5-2), and were identified in *Trichodesmium* IMS 101 cultures samples for reference against *in situ* samples (Figure 5-3).

Table 5-1 Species specific storage products and qualitative observations of the ultrastructure of colonies collected *in situ*.

Structure/Inclusion	Function	Literature*		This study		
		T. erythraeum	*T. thiebautii*	*Trichodesmium* IMS 101	Positively buoyant, surface colonies	Negatively buoyant colonies (100-250 m)
Vacuole-like structures (Figure 5-2A; Figure 5-5D)	Storage	Not reported	Extensive	Present	Present; extensive	Present; extensive
Gas vacuoles (Figure 5-4)	Buoyancy	Peripheral	Irregularly arranged	Intact; irregular	Intact; irregular	Intact; irregular
Polyhedral bodies (Figure 5-2A)	Storage	Central core	Scattered	Present; scattered	Not observed	Not observed
Cyanophycin granules (Figure 5-2C; Figure 5-5A)	Storage	Not reported	Present in all cells except for highly vacuolated cells	Present	Present	Present except for in highly vacuolated cells
Scroll-like bodies (Figure 5-5B)	Toxin production	Not reported	Present in all cells	Present	Not observed	Present
Cylindrical bodies (not pictured)	Storage	1-3 per cell	Occasionally present	Not observed	Not observed	Not observed
Polyphosphate bodies (not pictured)	Storage	Present	Absent	Not observed	Not observed	Not observed
PHB granules (Figure 5-5C)	Ballast	Not reported	Frequent	Present	Present	Present
Epibionts (Figure 5-7)	P uptake	N/A	N/A	Not observed	Not observed	Present

*Species specific ultrastructural characteristics derived from Siddiqui *et al*.(1992) and Janson *et al*.(1995)

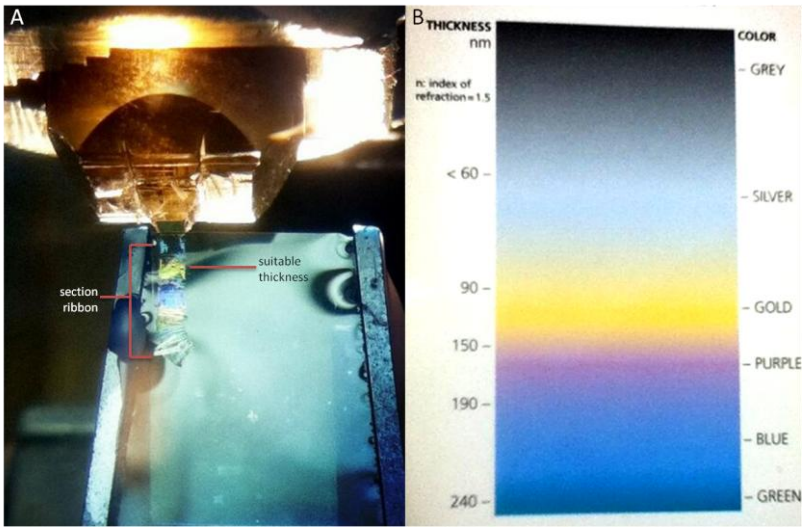

Figure 5-2. (A) Sectioning of resin block using a glass knife resulting in a ribbon of sections including gold-coloured sections which are the suitable thickness for TEM imaging. (B) Ultramicrotome section colour reference chart (Drukker international).

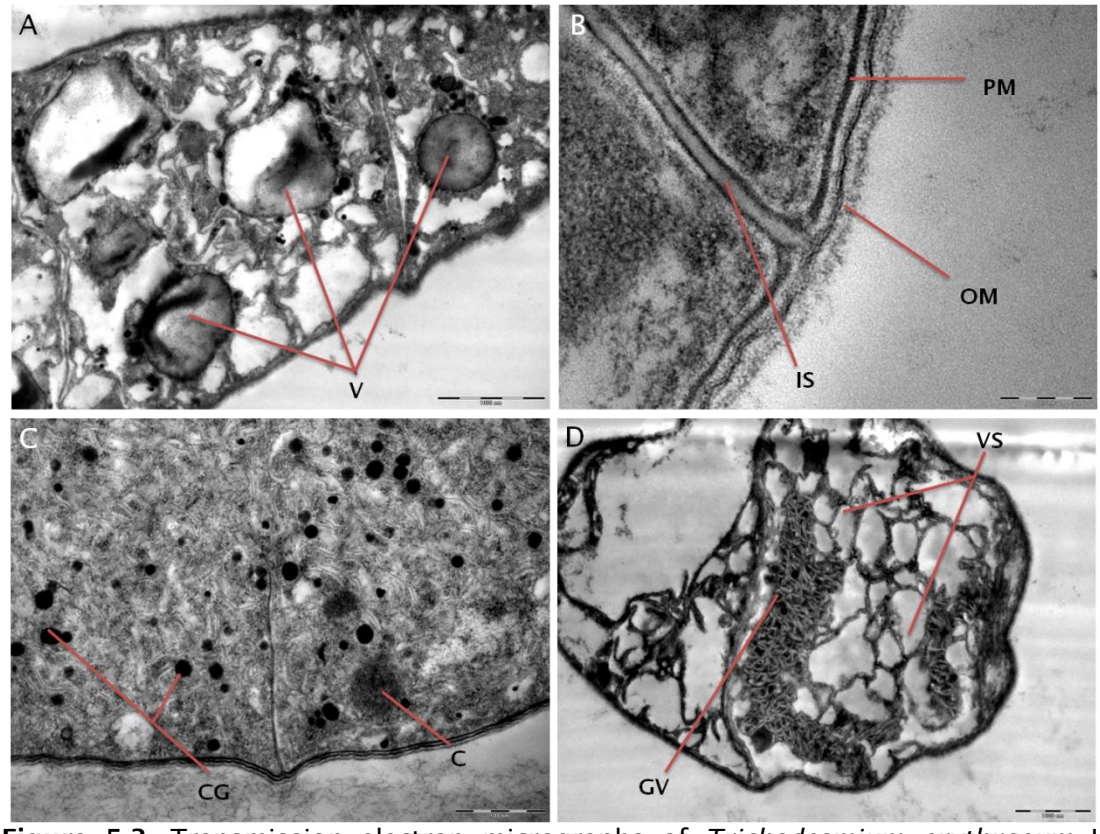

Figure 5-3. Transmission electron micrographs of *Trichodesmium erythraeum* IMS 101cells showing various ultrastructural components and variable integrity: vacuoles (V), intercellular space (IS), outer membrane (OM), plasma-membrane (PM), nitrogen storage vacuoles known as cyanophycin granules (CG), carboxysomes (C), gas vesicles (GV), and vacuolisation (VS), which were used for reference in subsequent identification of ultrastructural components of *in situ* samples. Scale bars represent 1 µm in panels A and D, 100 nm in panel B, and 500 nm in panel C.

5.4 Results

5.4.1 Gas vesicles

Gas vesicles were present in all cells viewed (n=145), and were intact in cells from the positively buoyant surface colonies (Figure 5-4A,B). However, gas vesicles were not fully intact in the cells of the negatively buoyant colonies (n=113). In negatively buoyant colonies, some cells contained both intact and degraded gas vesicles (Figure 5-4C-F).) Intact gas vesicles were indicated by regular arrangement of the electron dense fibres within the gas vacuole (Figure 5-5A) and the clear definition of the electron transparent center regions of each gas vesicle (Figure 5-4B). Partially collapsed and degrading gas vesicles were indicated by uneven distribution of electron dense fibres within the gas vacuole and reduction in marked circular vesicle walls (Figure 5-5C). Collapsed gas vesicles were indicated by a complete lack of structural regularity within the gas vacuoles, as well as a lack of electron transparent regions (Figure 5-5F). Gas vesicle distribution varied between samples. Gas vesicles were occasionally distributed around the periphery of the cell as is consistent with the *Trichodesmium* species *T. erythraeum*, but were more often irregularly arranged within the cell as is consistent with *T. thiebautii*.

5.4.2 Storage products

Trichodesmium cells contained an assortment of storage products (Figure 5-5). Positively buoyant surface cells (Figure 5-5A, B) and *Trichodesmium* IMS101 (Figure 5-3C) contained cyanophycin granules in every cell assessed, while only 27% of negatively buoyant cells assessed contained these structures, which known to be involved in nitrogen storage (Finzi-Hart *et al*. 2009) (Figure 5-5C). 0.9% of negatively buoyant cells contained multimembranous scroll-like structures known to be involved in toxin production (present in *T. thiebautii*

only) (Figure 5-5D), which were not present in positively buoyant surface cells or *Trichodesmium* IMS101. 33% of negatively buoyant cells contained poly-β-hydroxybutyric acid (PHB) granules which are a suspected ballast component (Figure 5-5E). PHB granules were also observed in positively buoyant surface cells and *Trichodesmium* IMS101 (not pictured). 5.3% of negatively buoyant cells contained vacuole-like structures suspected to be involved in the storage of photosynthetic metabolites (Figure 5-5F), which were also observed in positively buoyant surface cells (Figure 5-5B) and *Trichodesmium* IMS101 (Figure 5-3A).

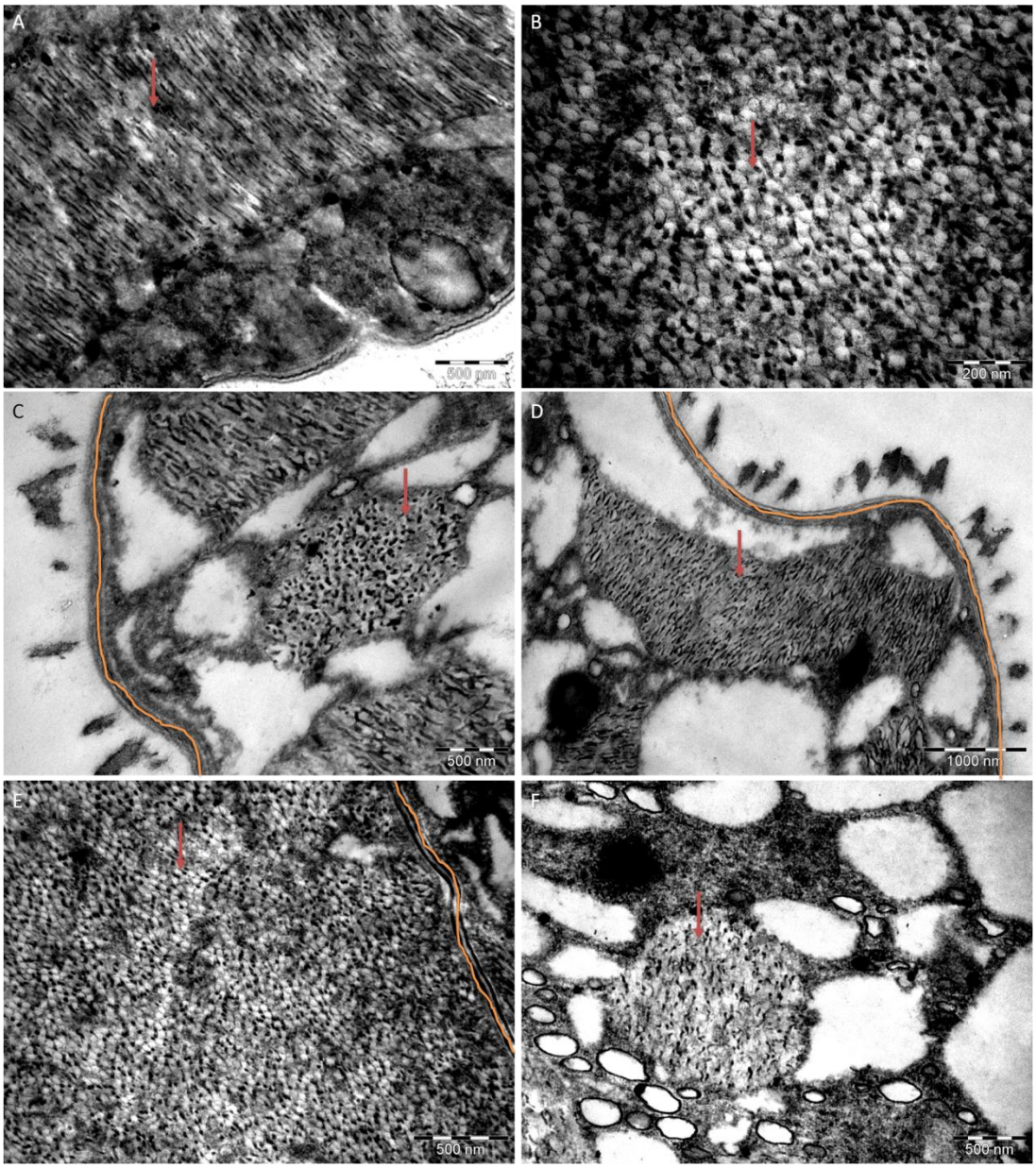

Figure 5-4. Gas vacuole integrity. Transmission electron micrographs of positively (A, B) and negatively (C-F) buoyant *Trichodesmium* colonies collected in the western Sargasso Sea showcasing varying degrees of gas vesicle integrity (red arrows). Orange lines mark cellular borders. (A) View of intact gas vesicles indicated by parallel distribution of electron dense fibres interspaced by electron transparent regions. (B) Intact gas vesicles in a cell from a positively buoyant surface colony indicated by normal, regular arrangement of the electron dense fibres within the gas vacuole and the clearly defined gas vesicle with electron transparent center regions. (C) Partially collapsed gas vesicles in a negatively buoyant colony indicated by the uneven distribution of electron dense fibres within the gas vacuole and reduction in marked circular vesicle walls. (D, E) Intact gas vesicles in a negatively buoyant colony are indicated as above. (F) Collapsed gas vesicles in a negatively buoyant colony indicated by a complete lack of structural regularity within the gas vacuoles, as well as a lack of electron transparent regions. Scale bars represent 500 nm in panels A, C, E and F, 200 nm in panel B and 1000 nm in panel D.

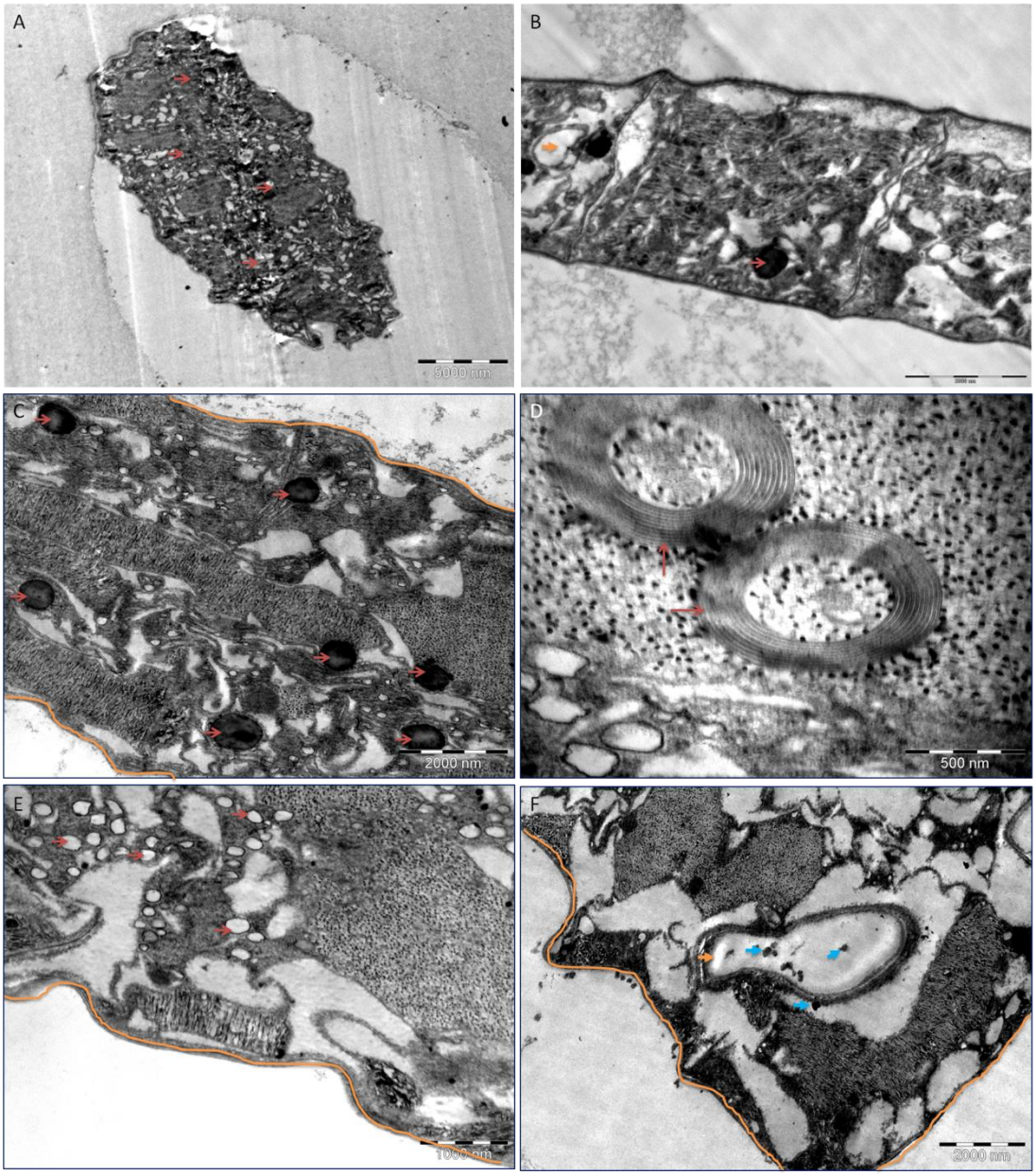

Figure 5-5. Intracellular storage components. Transmission electron micrographs of positively (A, B) and negatively (C - F) buoyant *Trichodesmium* colonies collected in the western Sargasso Sea. Orange lines mark cellular borders. Various storage components are indicated by red and orange arrows, such as (A, B, C) cyanophycin granules known to be involved in nitrogen storage, (D) scroll-like bodies associated with toxin production, (E) poly-β-hydroxybutyric acid granules theorised to be involved in carbohydrate ballasting, (B, F, orange arrow) vacuole-like structures suspected to store photosynthetic metabolites, and (F, blue arrows) medium electron dense granules assumed to serve a short-term storage role and are important in nitrogen metabolism function. Scale bars represent 5000 nm in panel A, 3000 nm in panel B, 2000 nm in panels C and F, 500 nm in panel D, and 1000 nm in panel E.

5.4.3 Cellular integrity

Trichodesmium IMS 101 samples and positively buoyant surface colonies contained a mixture of intact and vacuolated cells (Figure 5-3; Figure 5-6A, B). All negatively buoyant cells were heavily vacuolated (Figure 5-6C - F). Additionally all cells from negatively buoyant colonies suffered from minimal to extensive cellular shrinkage indicated by the irregular shape of cellular perimeters (Figure 5-6D, E). This cellular shrinkage is not an artefact of TEM preparation as osmolarity was carefully controlled during processing to ensure hypoosmotic and hyperosmotic conditions were not encountered. Reductions in intracellular density may be indicative of senescence, but some storage bodies are still present despite vacuolisation, such as PHB granules (Figure 5-6E, red arrows) and cyanophycin granules (Figure 5-6F, red arrow).

5.4.4 Epibionts

Epibionts were not observed around cells from *Trichodesmium* IMS101 cultures (Figure 5-3) or on positively buoyant surface colonies (Figure 5-4A, 5-5A, 5-6A). Epibionts extensively colonised the mucilaginous sheath of 2 negatively buoyant colonies (19% of analysed cells from negatively buoyant colonies) (Figure 5-7); all of the colonised *Trichodesmium* cells also contained the ballasting component PHB granules (Figure 5-5E), and nearly half (11% of total) contained another ballasting component, polyglucoside granules (Figure 5-8D). Epibiont distribution spanned the entire perimeter of these *Trichodesmium* cells (Figure 5-7A, B, C). Individual epibionts were tightly packed, irregularly arranged along the perimeter, and were occasionally overlapping (Figure 5-7D).

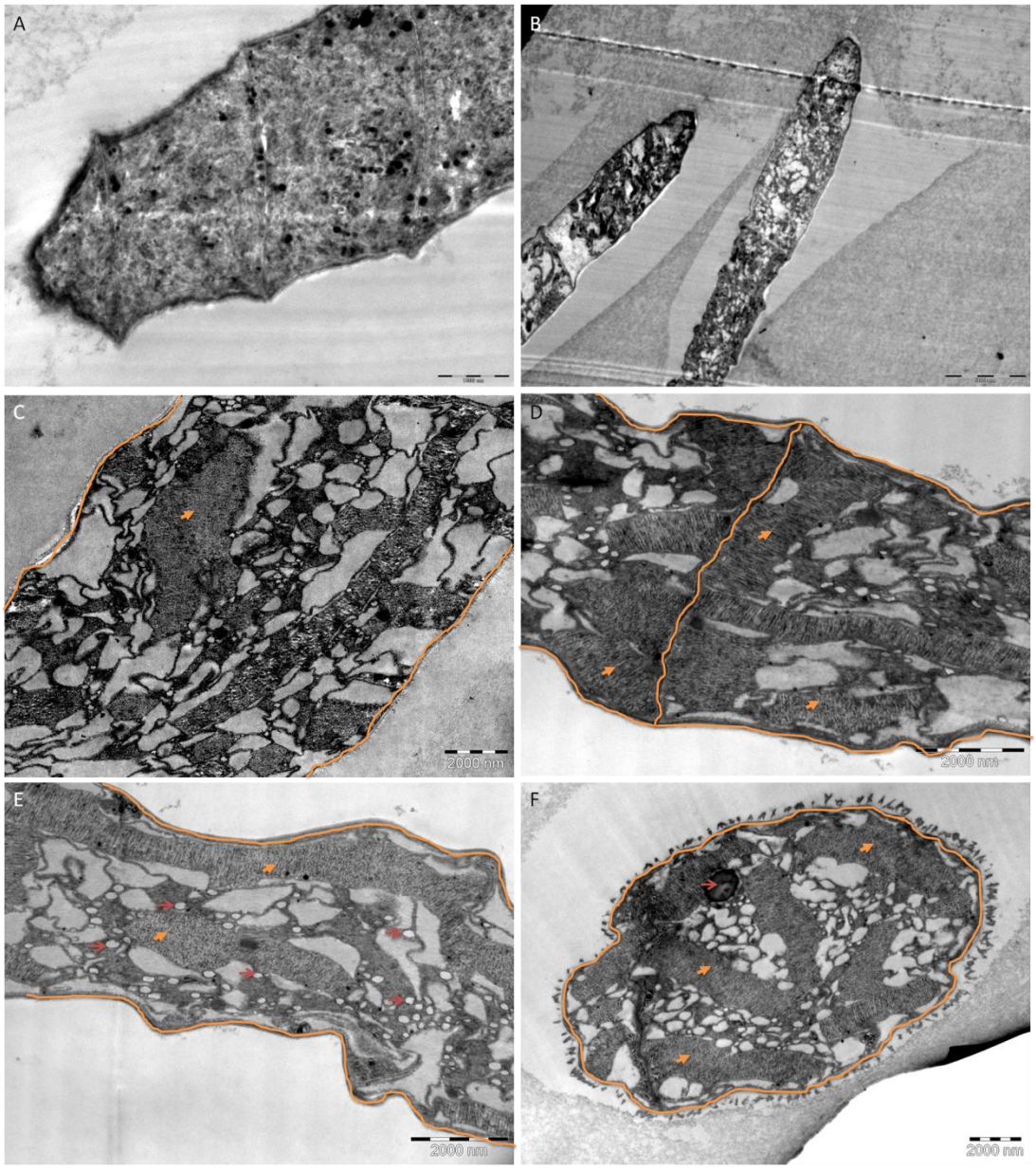

Figure 5-6. Intracellular vacuolisation. Transmission electron micrographs of Postively (A, B) and negatively (C - F) buoyant *Trichodesmium* colonies collected in the western Sargasso Sea illustrating variation in cellular density. (A) Healthy, intact cells. (B, C, D, E, F) moderate to extensive intracellular vacuolisation and cellular shrinkage compared to panel A. Orange lines mark cellular borders. Reductions in intracellular density may be indicative of senescence. The shaded, electron dense regions of the cell are gas vacuoles (C - F, orange arrows). Some storage bodies are still present despite vacuolisation, such as PHB granules (E, red arrows) and cyanophycin granules (F, red arrow). Scale bars represent 1000 nm in panel A, 5000 nm in panel B, and 2000 nm in panels C – F.

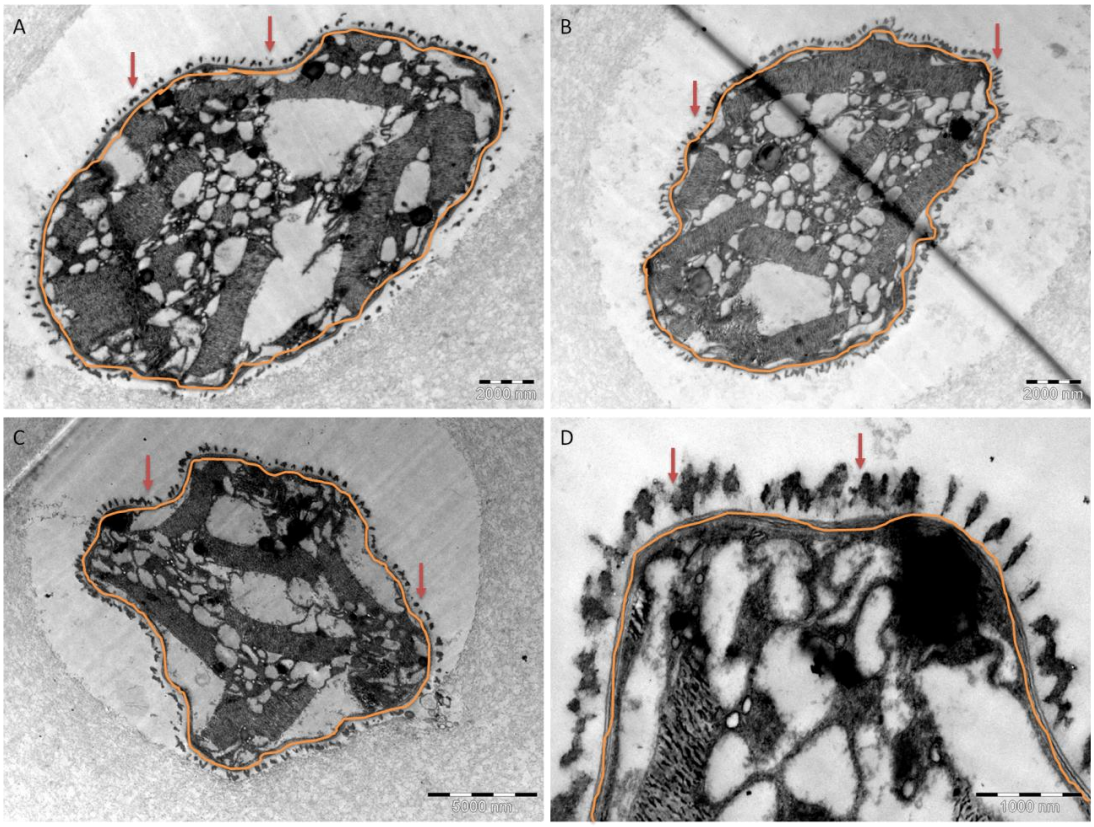

Figure 5-7. Epibionts. Transmission electron micrographs of cells from negatively buoyant *Trichodesmium* colonies collected in the western Sargasso Sea showcasing extensive colonisation of the mucilaginous sheath by epibionts indicated by red arrows. Orange lines mark cellular borders. Epibiont distribution appears to span the entire perimeter of the *Trichodesmium* cell (A, B, C). Individual epibionts are tightly packed, irregularly arranged along the perimeter, and are occasionally overlapping (D). Scale bars represent 2 µm in panels A and B, 5 µm in panel C, and 1 µm in panel C. Epibionts were not observed around cells from positively buoyant surface colonies (Figure 5-4A, 5-5A, 5-6A).

5.4.5 Other cellular inclusions

One cell in a negatively buoyant colony contained distinct thylakoid lamellae (Figure 5-8A). All of the cells containing epibionts (19%) were also surrounded by an extracellular matrix that was not detectable in any of the other negatively buoyant samples (Figure 5-8B). Polyglucoside granules, which are present only in *T. thiebautii* and are theorised to be involved in carbon storage and ballasting, were also present in 11% of negatively buoyant cells. In one negatively buoyant colony, multiple extracellular bodies were observed (Figure 5-8D).

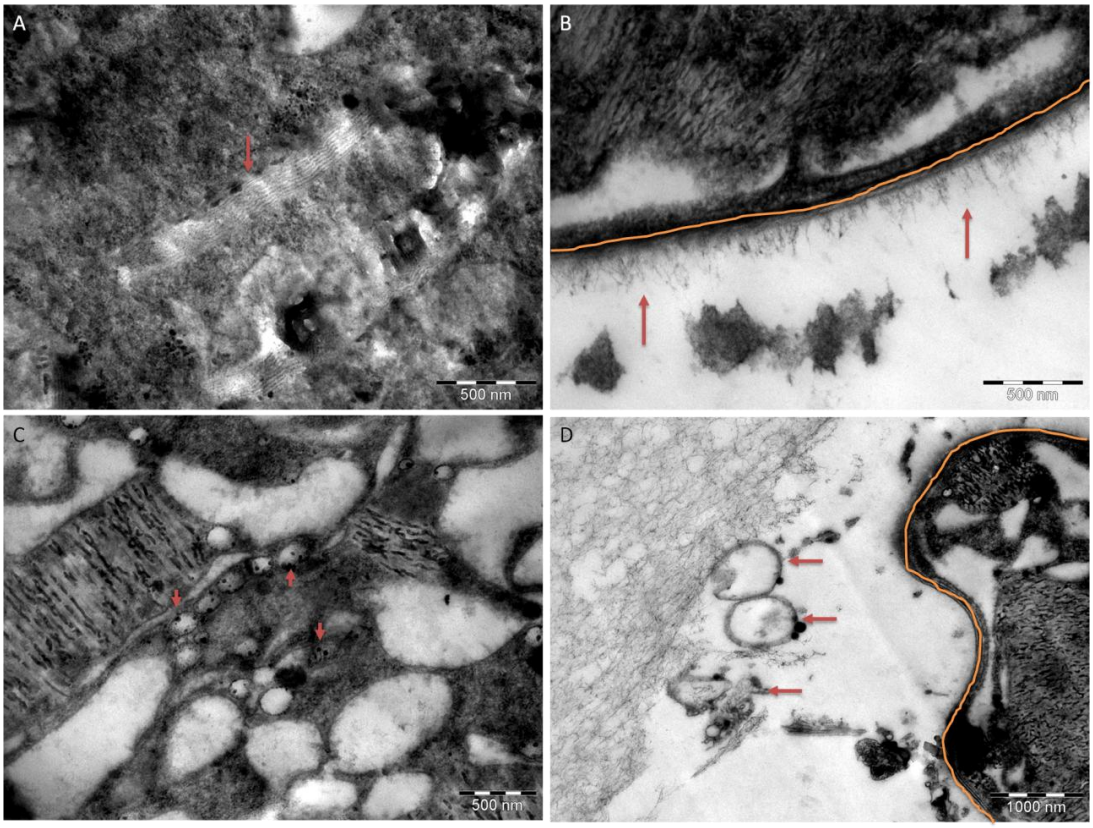

Figure 5-8. Other inclusions of note. Transmission electron micrographs of cells from negatively buoyant *Trichodesmium* colonies collected in the western Sargasso Sea. Orange lines mark cellular borders. Various other inclusions encountered in the samples are indicated by red arrows, such as (A) thylakoid lamellae, (B) the extracellular matrix, (C) polyglucoside granules, which are theorised to be involved in ballasting, and (D) extracellular bodies, which may indicate the presence of compromised cells within the colony although we cannot rule out that they may simply be from associated organisms living in/on the colony. Scale bars represent 500 nm in panels A, B, and C, and 1000 nm in panel D.

5.5 Discussion

Poly-β-hydroxybutyric acid (PHB) and polyglucoside granules may act as part of the ballast required for vertical migration in *Trichodesmium* (Romans 1994). The presence of PHB granules in 33% of cells in negatively buoyant *Trichodesmium* colonies, as well as the presence of polyglucoside granules in 11% of cells, offers some support to the over ballasting for vertical migration theory postulated in Chapter 3. However, in order to thoroughly assess whether vertical migration is a likely mechanism by which *Trichodesmium* is escaping the euphotic zone, we must also consider other conditions that could

cause *Trichodesmium* to sink, such as programmed cell death (PCD) or necrosis, which could result in passive sedimentation during senescence or following cell death (Bar-Zeev *et al*. 2013) or viral infection and eventual viral lysis, a known contributor to *Trichodesmium* bloom demise (Hewson *et al*. 2004; Brown *et al.* 2013).

PCD can occur with ageing or following prolonged exposure to high irradiance, oxidative stress, and nutrient starvation in *Trichodesmium* (Berman-Frank *et al*. 2004). Osmotic shock, UV shock, and heat shock, are also known to stimulate PCD in other organisms (Jiménez *et al*. 2009). Of these we assume *Trichodesmium* wouldn't be normally exposed to osmotic or heat shock in the environment, but could plausibly suffer from nutrient starvation and senescence in a number of situations including during blooms. Additionally *Trichodesmium* could experience prolonged exposure to high irradiance following entrapment at the surface due to uncompensatable buoyancy (Berman-Frank *et al*. 2004). This condition is often encountered in buoyancy models where the organism is unable to produce enough ballast to overcome the positive buoyancy provided by gas vacuoles (Kromkamp and Walsby 1992; White *et al*. 2006). In such situations, long-standing exposure to high irradiance may then result in prolonged photoinhibition (Lewis *et al*. 1988; Kromkamp and Walsby 1992), which could render cells unable to produce the ballast necessary to escape the surface layer, eventually resulting in sinking and cell death (Berman-Frank *et al*. 2004).

As 67% of the cells from negatively buoyant colonies lacked known ballast components, and as viruses were not observed in these samples, cell death may be the cause of sinking in these colonies. Since the colonies assessed were not associated with surface blooms, we assume high irradiance was not a trigger of PCD in these samples. Instead, we hypothesis that senescence during the stationary growth phase preceded cell death initiation in these samples. In *Trichodesmium* cell death is characterised by unique intra and extracellular characteristics, such as cellular shrinkage (Figure 5-6), cytoplasmic vacuolisation (Figure 5-6), and degradation of other intracellular components such as thylakoids (only observed in one cell from a negatively buoyant colony), carboxysomes (not observed in the negatively buoyant cells assessed), gas vesicles (Figure 5-4), and cyanophycin granules (absent in over 70% of negatively buoyant cells assessed) (Berman-Frank *et al*. 2004). We observed

extensive vacuolisation in these samples, and with the exception of one cell that contained thylakoids, all observed cells from negatively buoyant colonies lacked thylakoids and carboxysomes, and contained degraded/collapsed gas vesicles. All negatively buoyant cells assessed also displayed signs of cellular shrinkage. Taken together these characteristics offer support to cell death as an explanation for sinking in these colonies. There is also evidence that although compromised cell membrane integrity, sometimes including leakage of cellular material, occurs during PCD in other organisms (Jiménez *et al*. 2009; Zheng *et al*. 2013), PCD in *Trichodesmium* may not immediately present these characteristics as the plasmamembrane can remain intact following extensive intracellular vacuolisation (Berman-Frank *et al*. 2004).

If senescence and PCD are responsible for sinking in this study, it remains to be assessed whether senescence commenced prior to *Trichodesmium* exiting the euphotic zone. If so, *Trichodesmium* would transport much less new nitrogen to depth if biomass was lost in the upper ocean. Thus, the intracellular integrity of negatively buoyant *Trichodesmium* cells within the upper 100 m requires further investigation. In light of this, *Trichodesmium* contribution to PON standing stock may be much less than previously calculated (Chapter 3). On the other hand, as 33% of the assessed cells from negatively buoyant colonies contained ballasting materials, these colonies may have become senescent following their exit from the upper ocean. In these colonies, there remains the potential for the exudation of intracellular biomass to occur below 100 m.

The presence of cyanophycin granules in over a quarter of cells from negatively buoyant colonies (27.4%) also warrants further assessment when considering new-nitrogen fate and *Trichodesmium* taxonomy. Cyanophycin granules are a nitrogen storage structure in cyanobacteria (Siddiqui *et al*. 1992), and although the cells from negatively buoyant colonies were highly vacuolated, they were transporting concentrated new nitrogen stores to depth.

Cyanophycin granules were originally thought to be absent in *T. erythraeum* (Siddiqui *et al*. 1992) and in highly vacuolated *T. thiebautii* cells (Li and Lee 1990), but have since been described in *T. erythraeum* (Janson *et al*. 1995). Due to this duality we cannot use the presence/absence of these granules as a taxonomic marker, but the absence of cyanophycin granules in

the majority of cells coupled with cellular vacuolisation again hints at a late growth phase regardless of species type. The loss of cyanophycin granules during the stationary growth phase in other cyanobacteria has been previously observed (Allen 1984), and vacuolisation may be representative of the cell density decrease consistent with cellular senescence in other organisms (Jiménez *et al*. 2009). Thus, cellular senescence may play a more important role than over ballasting in the sinking/settling of these *Trichodesmium* colonies.

Other storage products present in the negatively buoyant colonies are able to provide some taxonomic insight. The multimembranous scroll-like structures (Figure 5-5B) are known to be involved in toxin production and are so far described only in *T. thiebautii* (Siddiqui 1992; Janson *et al*. 1995). The vacuole-like structures observed in some of the negatively buoyant colonies (Figure 5-5D) are unique to the vacuolisation process previously described and serve a suspected photosynthetic metabolites storage role. Vacuole-like structures are described as extensive in *T. thiebautii*, but are not reported for *T. erythraeum* in the literature (Siddiqui 1992). Polyphosphate bodies were not observed in any of these collections, but are only described for *T. erythraeum*. Medium electron dense granules were also not observed in the negatively buoyant *Trichodesmium* samples. They are thought to serve a nitrogen metabolism function and are described for *T. thiebautii* only (Li and Lee 1990). Taking all of these factors into consideration, we tentatively assume the majority of these colonies are *T. thiebautii* which is consistent with observations that *T. thiebautii* is the dominant *Trichodesmium* species in the Atlantic Ocean (O'Neil 1998; Carpenter *et al*. 2004; Capone *et al*. 2005). *T. thiebautii* has higher carbon content, and thus higher nitrogen content, per cell than *T. erythraeum* (120 ± 57 pgC cell^{-1} and 65 ± 32 pgC cell^{-1} respectively) (Luo *et al*. 2012), which again supports the potential for substantial *Trichodesmium*-attributable N availability at depth even in highly vacuolated cells.

5.6 Conclusion

When PCD was induced in the laboratory, cellular lysis has been shown to occur within 24 hours following the onset of decreased intracellular density (i.e. extensive vacuolisation) (Berman-Frank *et al*. 2004). Potentially then, with an average colonial sinking rates of 62.1 ± 39.7 m d^{-1} (Chapter 3), and depending on the depth of PCD onset, all negatively buoyant *Trichodesmium* observed in this study would have apoptosed within hours. During apoptosis the transfer of *Trichodesmium* biomass from the fast sinking pool of POM to the suspended pool would occur nearly instantaneously. A constant rain of senescent *Trichodesmium* colonies destined to burst in the upper twilight zone would result in the injection of *Trichodesmium*-attributable PON directly into the water column thus making it readily available for remineralisation and contribution to enhanced N*. Further assessments of the ultrastructure and/or elemental composition of negatively buoyant *Trichodesmium* colonies would aid in constraining the estimations of *Trichodesmium* contribution to PON standing stock, and would be integral in expanding the understanding of *Trichodesmium* contribution to enhanced N* in the thermocline of the sub-tropical North Atlantic gyre.

6. Conclusions and Future Directions

6.1 Summary and main findings

The role that diazotrophs play in marine nitrogen dynamics is well described in the surface ocean, but species-specific fates are still not completely defined. This work provides novel insights into the potential for these organisms to contribute to the anomalous nutrient distributions in the thermocline of the subtropical Atlantic Ocean despite previously reports that diazotrophic growth fuels export production rather than remineralisation (Michaels and Silver 1988) and that unicellular and filamentous diazotroph-derived N is likely constrained to cycling in the surface ocean (Thompson and Zehr 2013). This work has also revealed that previous assumptions on the mechanisms by which *Trichodesmium* exits the euphotic zone being limited to incorporation in faecal material (Mulholland 2007), active transport (Guidi *et al*. 2012), or sweeping mechanisms (Scharek *et al*. 1999b) also require redefinition. We can confirm that *Trichodesmium* is incorporated into faecal material and is involved in sweeping mechanisms by incorporation into aggregates (Chapter 3), but this organism also exits the euphotic zone via free sinking of potentially senescent colonies (Chapters 3 and 5). The presence of *nif*H from the unicellular and heterocystous diazotrophs below the euphotic zone (Chapter 2) also implies additional mechanisms of transport exist for these organisms, but further investigation specifically into these groups would be beneficial in better defining their fate.

This final chapter is a synthesis of Chapters 2-5 and will discuss the implications of the findings of each previous chapter in relation to the findings of the other chapters. Limitations of this study and recommendations for future work will also be discussed.

6.1.1 Implications of polyploidy in *Trichodesmium*

The assessments of the *nif*H community carried out in Chapter 2 revealed *Trichodesmium*-specific *nif*H to be dominant in many of the samples, such as at the surface between the equator and 10°N on the D361 transect. As we now know that gene copies exceed cell counts by two orders of magnitude on this cruise and that *Trichodesmium* is potentially polyploid (Chapter 4), these conclusions may not reflect the actual diazotrophic community structure in this region.

The maximal discrepancy between cell counts and gene copies on D361 resulted in a theoretical ploidy level of 120 genome copies per cell for *Trichodesmium.* If this upper threshold of ploidy is applied to the dataset, and *Trichodesmium*-specific *nif*H is reduced by a factor of 120 to bring *nif*H copies in the theoretical range of cell numbers, *Trichodesmium*-specific *nif*H would no longer be the largest component of the *nif*H community structure between the equator and 10°N. Instead, it would only composes the majority of *nif*H community structure at station 16 (8°20 N), and other phylotypes could increase in contribution, such as the heterocystous *Richelia-Hemaulus* (Figure 6-1).

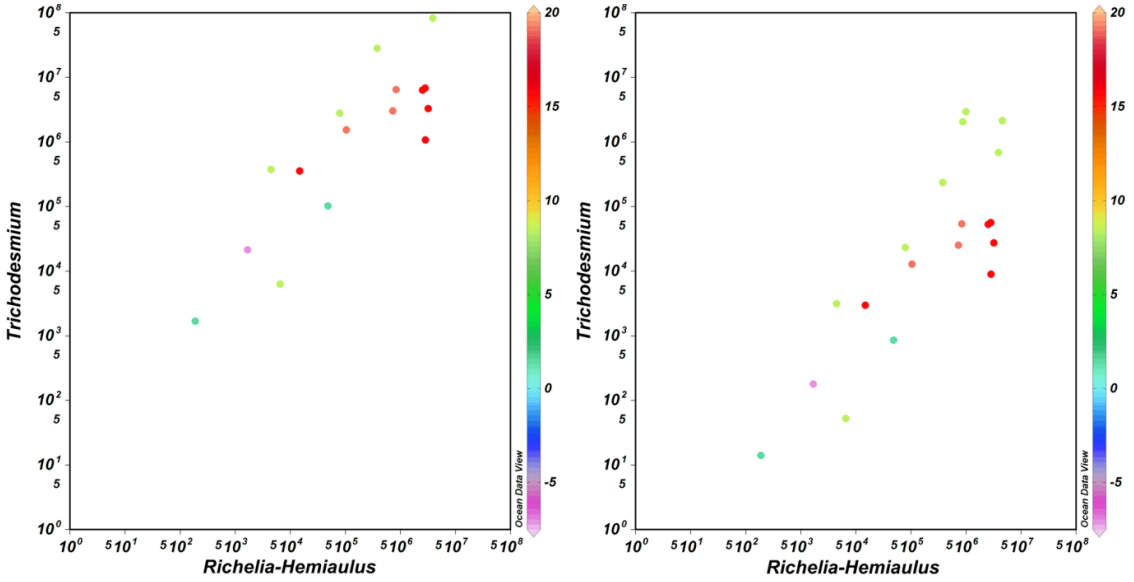

Figure 6-1. Raw (left) and amended (right) *nif*H gene abundances for *Trichodesmium* following reduction of *Trichodesmium*-specific *nif*H in accordance with the theoretical upper threshold of polyploidy observed *in situ* (120 genome copies) compared to raw *Richelia-Hemiaulus nif*H. Color bar represents section latitude.

However, as the ploidy level of the other phylotypes is unconfirmed and as the ploidy level of *Trichodesmium* is highly variable, these sorts of manipulations are premature. If the other diazotrophs are monoploid, the dominance of *Trichodesmium*-specific *nif*H may still echo the dominance of *Trichodesmium* biomass in diazotrophic communities, but if any of the other diazotrophic genera are also polyploid, such as the similarly sized *Richelia intracellularis*, more thorough physiological assessments will need to be conducted before speculation on biomass and community structure can be determined from qPCR data.

In future, it would be advantageous for cell counts to be conducted alongside *nif*H-based abundances on research cruises, especially for *Trichodesmium* and *Richelia intracellularis*. Such a dataset would be largely valuable in the development of a proxy for conversions from gene-based abundances to actual cell numbers that would be representative of true diazotroph biomass. This is especially important as oceanographic sampling techniques advance. The future of ocean sampling will surely involve increased use of gliders, floats, and other autonomous sampling platforms. Many of these sampling platforms may harbour molecular technologies, which would be

beneficial in increasing gene-based abundance datasets, but inadequate for biomass estimates if accurate conversion factors are not available.

6.1.2 Refining diazotroph contribution to N* and *Trichodesmium* contribution to PON export

When comparing diazotroph abundance and distribution with N*, there is a clear trend observed between high *nif*H abundances in the surface and enhanced N* at depth, which implies diazotrophs likely influence enhanced nitrate below the mixed layer (Figure 6-2). This is supported by the isotopic signature of the nitrate pool in the subtropical North Atlantic thermocline, which indicates that newly fixed nitrogen is likely contributing to the N* anomaly (Knapp *et al*. 2008). Maximum N* anomalies in the North Atlantic gyre are associated with a potential density interval in the σ_θ = 26.1-27.1 range (Gruber and Sarmiento 1997, Hansell *et al*. 2007), which was located between 100 and 500 m along the transect in this study. We hypothesize that sinking diazotrophs are being remineralised shortly after their exit from the mixed layer, relatively rapidly, consequently depositing their N-rich cellular contents into the water column between 100 and 500 m, which provides a mechanism for generating some of the N* anomaly observed at depth (Figure 6-2). This is consistent with the accumulation of the N* signal only occurring in regions where these isopycnals are shallower than ~400m (Hansell *et al*. 2004), where release of diazotroph-derived material between 100 and 500 m could inject into this density layer following the shoaling of the permanent thermocline at low latitudes near the equator (Sarmiento *et al*. 2004). The dominant diazotrophs north of the equator, *Trichodesmium* and unicellular Group A cyanobacteria, may be larger contributors to the N* anomaly than *R. intracellularis*, which may not contribute as readily to the N* anomaly as its host diatoms are more apt to aggregate and sink too quickly for remineralisation in the upper twilight zone (Alldredge and Gotschalk 1988, Villareal *et al*. 2011). However, the contribution individual diazotrophs make to N* remains unresolved.

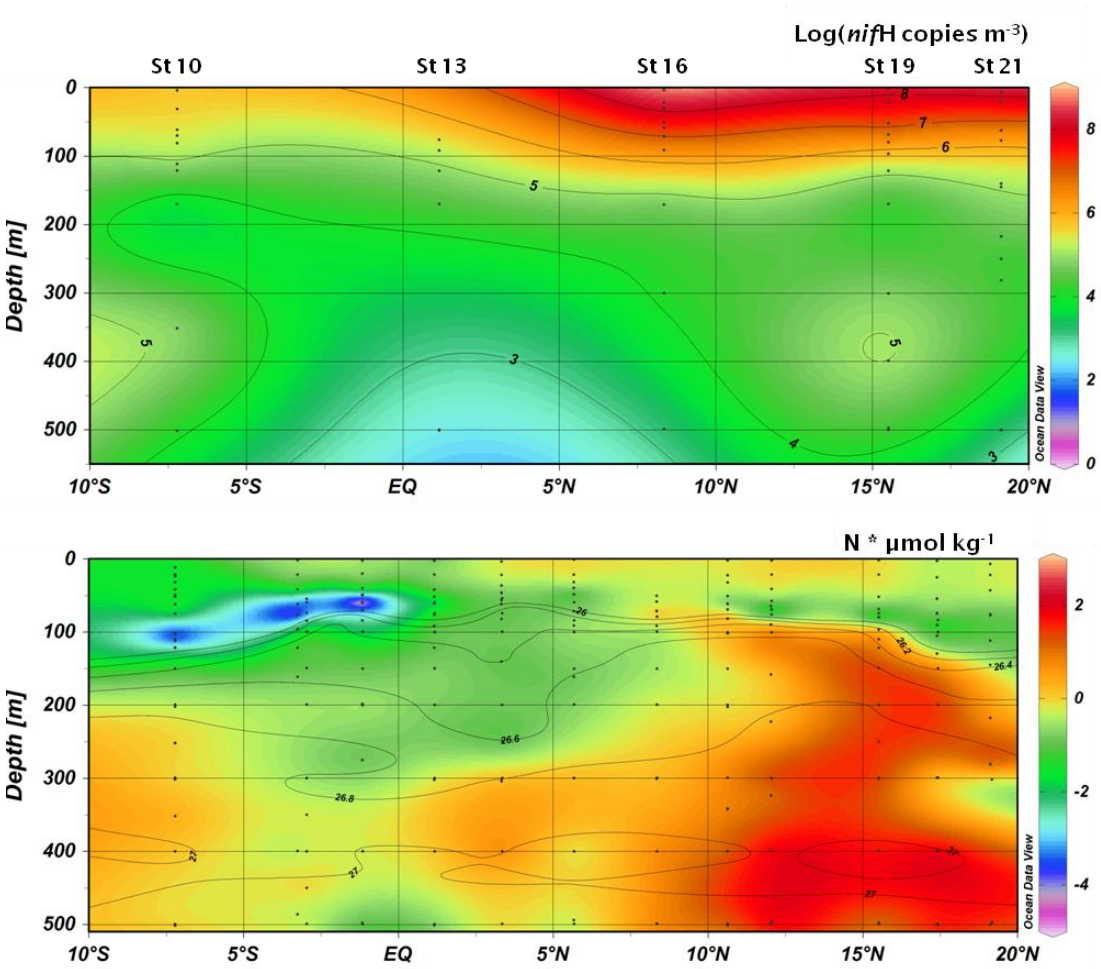

Figure 6-2. Log *nif*H abundance and N* with potential density (σ_θ) contours highlighting enhanced N* within the σ_θ=26.6-27.0 range along the transect corresponding to increased *nif*H abundance in the same depth range. Note slight difference in scale of the y axis for each panel.

Trichodesmium colonies collected on the D361 cruise were exiting the mixed layer via passive sedimentation, theorised to be due to over-ballasted vertical migration attempts. These negatively buoyant colonies were present as deep as 300 m (Chapter 3), but the cellular integrity of these colonies was unknown. Ultrastructural assessments of negatively buoyant colonies collected on the BATS284 cruise between 100 and 250 m revealed the presence of ballasting components in 33% of cells assessed, thus confirming the potential for over ballasting to transport some *Trichodesmium* colonies to depth, but the majority of negatively buoyant cells (the remaining 77%) did not contain ballasting components, and were instead highly vacuolated (100% of negatively buoyant cells assessed), which is indicative of a programmed cell death (PCD) pathway (Chapter 5). If the PCD pathway is initiated while colonies are still in

the surface layer, then the exudation of intracellular material would result in the loss of *Trichodesmium*-derived biomass to the upper ocean. Conversely, if the PCD pathway is initiated below the mixed layer, the loss of intracellular material would still be available for remineralisation and contribution to N*. This would also be the case for intact colonies exiting the mixed layer via the over ballasting mechanism. These various passive sedimentation and remineralisation pathways for *Trichodesmium* colonies are illustrated in Figure 6-3.

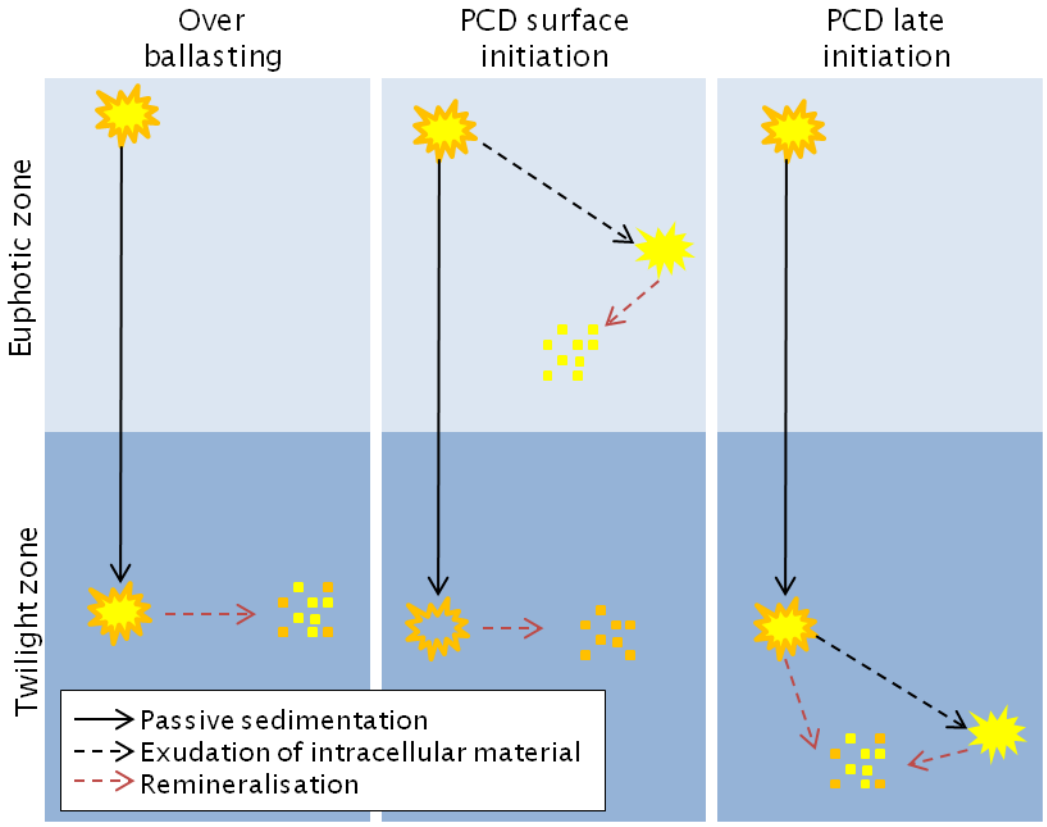

Figure 6-3. Schematic representation of potential passive sedimentation and remineralisation pathways for *Trichodesmium* colonies. The orange colony border represents intact cell membranes and yellow colony interior represents non-vacuolated cells. Exudation of intracellular material and subsequent remineralisation are represented by dashed arrows as indicated above.

Due to the potential range of fates for *Trichodesmium*-derived material, such as surface cycling of *Trichodesmium*-derived biomass or export and remineralisation of *Trichodesmium* biomass below the euphotic zone, it is difficult to quantify the contribution of *Trichodesmium* to PON export at the present stage. If surface initiated PCD is responsible for the presence of some

colonies at depth, then previous estimates of T*richodesmium* contribution to PON standing stock described in Chapter 3 would decrease due to a combination of full contribution of biomass by ballasted cells and a decreased contribution of biomass by the cells involved in the PCD pathway. This would decrease *Trichodesmium* contribution to PON standing stock at 10 m below the mixed layer, which would also decrease *Trichodesmium* derived export fluxes.

However, over a quarter of the cells assessed from negatively buoyant colonies contained multiple cyanophycin granules in each cell, which are a known nitrogen storage structure (Siddiqui *et al*. 1992). Although these cells were highly vacuolated, they contained these concentrated new nitrogen stores. Thus, the amended estimates of *Trichodesmium* contribution to PON standing stock should be considered conservative, as cellular nitrogen content was derived from a 6.3 conversion of C:N in *Trichodesmium* (Mulholland 2007) in Chapter 3, and the maintenance of nitrogen stores during cell density loss in these cells would likely skew that ratio to a higher N content. Additional assessments of cellular integrity in sinking *Trichodesmium*, such as cell death stains during cell counts or caspase activity assays, would aid in a better definition of *Trichodesmium* contribution to PON export.

Additionally, as the PCD pathway eventually results in cellular lysis (Berman-Frank *et al*. 2004), much more recently apoptosed *Trichodesmium*-derived material may be present in the water column below the mixed layer than is detectable optically. Similarly, the degradation of *Trichodesmium*-derived biomass present in aggregates and faecal material may also contribute more to *Trichodesmium*-derived PON at depth than we are able to quantify optically. This is particularly apparent after assessments of aggregates using standard light microscopy versus epifluorescent microscopy where recently degraded trichomes are only revealed when the phycoerythrin pigment is excited (Figure 6-4). Unfortunately, this assessment was not available on the D361 cruise, so estimated *Trichodesmium* contribution to PON and PON fluxes should be considered conservative as biomass may have been missed due to methodological limitations.

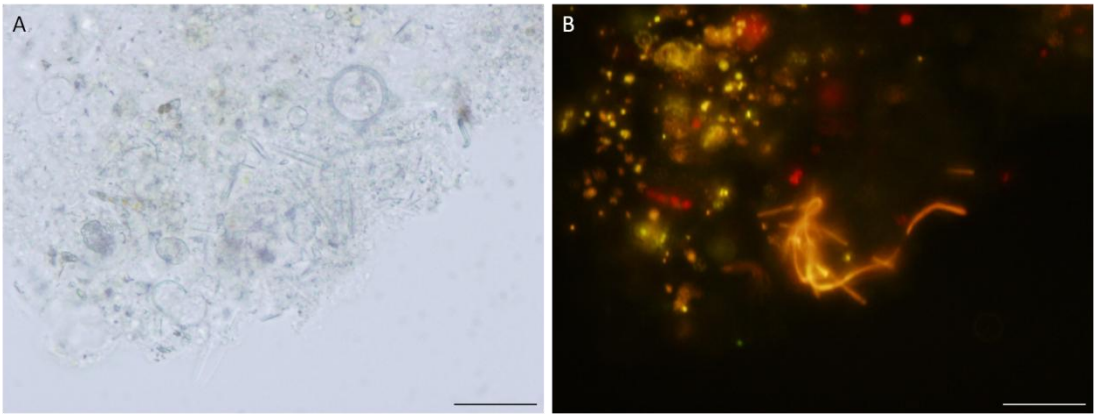

Figure 6-4. Micrographs of an aggregate using (A) standard light microscopy, and (B) excitation of the phycoerythrin pigment using epifluorescent microscopy showcasing that *Trichodesmium* presence can sometimes only be revealed via the latter technique. This aggregate was collected at 175 m in the Gulf of Mexico. Scale bars represent 50µm.

6.1.3 New mechanisms of diazotroph contribution to export

Previously, the only mechanisms assumed in the transfer of diazotrophic biomass to depth were direct export of DDAs following aggregation (Karl *et al*. 2012), direct export of *Trichodesmium* via sweeping mechanisms (Sharek *et al*. 1999b), indirect export of diazotrophic material following ingestion and repackaging into faecal pellets (Mulholland 2007), and indirect export following incorporation of diazotroph derived material into the biomass of other organisms in the surface ocean (Mulholland 2007; Loick-Wilde 2012), which themselves contribute to export both directly and indirectly (Discussed in more detail in Chapter 1.7). This study has revealed that *Trichodesmium* is also capable of contributing to export via passive sedimentation (Chapter 3). The presence of *nif*H specific to the unicellular and heterocystous diazotrophs in sinking material as deep as 500 m (Chapter 2) highlights the need for more thorough assessments of diazotroph presence in sinking material to confirm the mechanisms of export in these organisms.

There is also the potential for variation of diazotroph-derived nitrogen within each group of diazotrophs depending on the mechanism of transport between the surface layer and depth, or depending on individual physiologies and cell death. All but a single cell assessed from negatively buoyant

Trichodesmium colonies seemingly suffering from PCD in this study lacked thylakoids (Chapter 5), whereas chlorophyll and other pigments were maintained in sinking *Trichodesmium* which was incorporated in aggregates and faecal pellets (Chapter 3; Figure 6-4). Thus, there may also be variation in the elemental composition of *Trichodesmium* cells depending on the mechanism of export. The potential for plasticity in *Trichodesmium*-derived POC and PON under these different conditions increases the difficulty of quantifying their contribution to export fluxes.

6.2 Applications of this work

It was previously assumed that nitrogen fixation was contributing to enhanced N* in the thermocline of the subtropical North Atlantic Ocean (Hansell *et al*. 2004, 2007), but mechanisms to describe the transfer of newly fixed nitrogen to depth were lacking. This work reveals those mechanisms and allows for redefinition of the fate of diazotrophic organisms for incorporation into future biogeochemical models and estimations of their importance and function in the marine nitrogen cycle. This work additionally provides motivation for further investigation of the fate of diazotrophs in other ocean regions.

This work also highlights a physiological trait previously undescribed in *Trichodesmium*, polyploidy. This work warrants redefinition of the applications of the qPCR method for assessing diazotrophic abundance. This method still proves valuable in assessments of biogeography and *nif*H community structure, but the potential for polyploidy in *Trichodesmium* and other diazotrophs introduces difficulties in the extension of this method to use in biomass estimates. These findings also provide a stimulus for ploidy assessments in the other diazotrophic cyanobacterial groups as well as continued assessments of the conditions under which the ploidy level of *Trichodesmium* varies.

6.3 Revisiting Hypotheses

6.3.1 Hypotheses

H_1: *Trichodesmium* is not a likely constituent of export

i. Conclusions: H_1 partially rejected. Previous assessments of *Trichodesmium* have overlooked this organism's potential to sink out of the mixed layer, but it's contribution to PON flux appears to be minimal.

H_2 Remineralisation of *Trichodesmium* between the mixed layer and 500 m, north of the equator in the Atlantic, is contributing to the N* anomaly seen in the thermocline of the northern subtropical gyre, while DDA export likely results in sequestration of carbon and nitrogen rather than remineralisation.

i. Conclusions: H_2 partially accepted. While significant loss of *Trichodesmium* biomass between the mixed layer and 500 m suggests the organism is being remineralised within this depth range, and thus is contributing to N*, we have yet to quantify this contribution. Our assessments of DDA fate are inconclusive as we encountered them far less often than anticipated.

H_3: There are multiple mechanisms by which diazotroph export occurs

i. Conclusions: H_3 accepted. It appears a variety of mechanism transport diazotrophs to depth including sweeping, grazing, free sinking, and active transport.

H_4: Over ballasting of *Trichodesmium* in the surface layer is causing it to sink past phosphocline and terminating the ability for the colony to return to the surface.

i. Conclusions: H_4 inconclusive: although there was evidence of ballasting components in negatively buoyant *Trichodesmium* colonies, it appears PCD may play a larger role in facilitating the transfer of *Trichodesmium* biomass to depth

H_5: If over ballasting is the mechanism by which *Trichodesmium* is exported, the intracellular POC/PON is high quality.

i. Conclusions: H_5 rejected: negatively buoyant *Trichodesmium* colonies contained highly vacuolated cells, and thus a smaller, more degraded quantity of POC/PON than would be present in a cell that was sinking solely due to ballasting.

H_6: Gas vacuole collapse in colonies collected between 100 and 300 m guarantees sinking *Trichodesmium* at these depths lacks the ability to return to the surface.

i. Conclusions: H_6 partially accepted. Although gas vacuoles were degraded and collapsed in negatively buoyant colonies, we cannot be sure whether this is due to pressure or PCD associated breakdown. Regardless, negative buoyancy would be irreversible in either case.

H_7: Quantification of the *nif*H gene via qPCR can be directly related to cell number.

i. Conclusions: *H7* rejected. There is a large discrepancy between cell counts and gene copy numbers in *Trichodesmium.* This discrepancy has yet to be confirmed with other phylotypes.

6.4 Final remarks

Contrary to previous expectations molecular assessments revealing the presence of all three groups of diazotrophs below the euphotic zone (Chapter 2) and optical confirmation of the conspicuous diazotrophs present in these depth ranges (Chapter 3) reveal that previous assessments of the fate of diazotrophs have underestimated their ability to exit the euphotic zone.

Marine diazotrophs play an important role in marine biogeochemical cycles by fixing N_2 into bioavailable forms. Elucidation of the extent to which these diazotrophs are contributing to the biogeochemistry of deeper waters provides novel insight into the cycling of fixed nitrogen in the oligotrophic ocean thus highlighting the importance of these organisms in both the supply of nutrients to the thermocline and in the sustenance of ocean productivity on longer time scales.

Appendices

Appendix 1

Table A1. SAPS deployment details

Station	Lat	Lon	Depth (m)	Size fraction (µm)	Deployment time (minutes)	Total volume filtered (L)
10	07°13 S	25°00 W	70	53	137	2066
10	07°13 S	25°00 W	70	1	137	2066
10	07°13 S	25°00 W	170	53	140	2343
10	07°13 S	25°00 W	170	1	140	2343
10	07°13 S	25°00 W	500	53	137	2174
13	07°13 S	25°00 W	70	53	138	1915
13	01°09 N	26°02 W	70	1	138	1915
13	01°09 N	26°02 W	170	53	138	2041
13	01°09 N	26°02 W	170	1	138	2041
13	01°09 N	26°02 W	500	53	133	3419
16	08°20 N	28°20 W	70	53	138	2024
16	08°20 N	28°20 W	70	1	138	2024
16	08°20 N	28°20 W	170	53	138	2053
16	08°20 N	28°20 W	170	1	138	2053
16	08°20 N	28°20 W	500	53	142	2148
19	15°30 N	28°23 W	85	53	138	2025
19	15°30 N	28°23 W	85	1	138	2025
19	15°30 N	28°23 W	170	53	138	2342
19	15°30 N	28°23 W	170	1	138	2342
19	15°30 N	28°23 W	500	53	138	2117
21	19°10 N	28°07 W	140	53	138	2012
21	19°10 N	28°07 W	140	1	138	2012
21	19°10 N	28°07 W	250	53	138	2368
21	19°10 N	28°07 W	250	1	138	2368
21	19°10 N	28°07 W	500	53	138	2146

List of References

Agawin, N. S. R., A. Tovar-Sánchez, et al. (2013). "Variability in the abundance of Trichodesmium and nitrogen fixation activities in the subtropical NE Atlantic." Journal of Plankton Research.

Alldredge, A. L. and C. C. Gotschalk (1988). "Direct observations of the mass flocculation of diatom blooms: characteristics, settling velocities and formation of diatom aggregates." Deep-Sea Research **36**(2): 159-171.

Alldredge, A. L. and M. W. Silver (1988). "Characteristics, Dynamics and Significance of Marine Snow." Progress in Oceanography **20**: 41-82.

Allen, M. M. (1984). "Cyanobacterial Cell Inclusions." Annual Review of Microbiology **38**(1): 1-25.

Anderson, L. A. and J. L. Sarmiento (1994). "Redfield ratios of remineralization determined by nutrient data analysis." Global Biogeochemical Cycles **8**(1): 65-80.

Armbrust, E. V., J. D. Bowen, et al. (1989). "Effect of light on the cell cycle of a marine *Synechococcus* strain." Applied and Environmental Microbiology **55**: 425-432.

Armstrong, R. A., C. Lee, et al. (2002). "A new, mechanistic model for organic carbon fluxes in the ocean based on the quantitative association of POC with ballast minerals." Deep Sea Research Part II: Topical Studies in Oceanography **49**(1–3): 219-236.

Baker, A. R., K. Weston, et al. (2007). "Dry and wet deposition of nutrients from the tropical Atlantic atmosphere: Links to primary productivity and nitrogen fixation." Deep Sea Research Part I: Oceanographic Research Papers **54**(10): 1704-1720.

Bar-Zeev, E., I. Avishay, et al. (2013). "Programmed cell death in the marine cyanobacterium Trichodesmium mediates carbon and nitrogen export." ISME J.

Bar-Zeev, E., T. Yogev, et al. (2008). "Seasonal dynamics of the endosymbiotic, nitrogen-fixing cyanobacterium *Richelia intracellularis* in the eastern Mediterranean Sea." The ISME Journal **2**: 911-923.

Bergman, B., G. Sandh, et al. (2013). "Trichodesmium – a widespread marine cyanobacterium with unusual nitrogen fixation properties." FEMS Microbiology Reviews **37**(3): 286-302.

Berman-Frank, I., K. D. Bidle, et al. (2004). "The Demise of the Marine Cyanobacterium, Trichodesmium SPP., via an Autocatalyzed Cell Death Pathway." Limnology and Oceanography **49**(4): 997-1005.

Berman-Frank, I., P. Lundgren, et al. (2001). "Segregation of Nitrogen Fixation and Oxygenic Photosynthesis in the Marine Cyanobacterium Trichodesmium." Science **294**(5546): 1534-1537.

Bertilsson, S., O. Berglund, et al. (2003). "Elemental composition of marine *Prochlorococcus* and *Synechococcus*: Implications for the ecological stoichiometry of the sea." Limnology and Oceanography **48**(5): 1721-1731.

Binder, B. J. and S. W. Chisholm (1990). "Relationship between DNA cycle and growth rate in *Synechococcus* sp. strain PCC 6301." Journal of Bacteriology **172**(2312-2319).

Binder, B. J. and S. W. Chisholm (1995). "Cell cycle regulation in marine *Synechococcus* sp. strains." Applied and Environmental Microbiology **61**: 708-717.

Blais, M., J.-É. Tremblay, et al. (2012). "Nitrogen fixation and identification of potential diazotrophs in the Canadian Arctic." Global Biogeochemical Cycles **26**(3): GB3022.

Borstad, G. A. (1978). Some aspects of the occurrence and biology of *Trichodesmium* (Cyanophyta) in the western tropical Atlantic near Barbados, West Indies. Marine Sciences Centre. Montreal, Quebec, Canada, McGill University. **PhD:** 234.

Boyd, P. W. and S. C. Doney (2002). "Modelling regional responses by marine pelagic ecosystems to global climate change." Geophysical Research Letters **29**(16): 53-51-53-54.

Boyd, P. W. and W. E. Newton (1995). "Evidence of the potential influence of planktonic community structure on the interannual variability of particulate carbon flux." Deep-Sea Research I **42**: 619-639.

Boyd, P. W. and W. E. Newton (1999). "Does planktonic community structure determine downward particulate organic carbon flux in different oceanic provinces." Deep-Sea Research I **46**: 61-91.

Brandes, J. A. and A. H. Devol (2002). "A global marine-fixed nitrogen isotopic budget: Implications for Holocene nitrogen cycling." Global Biogeochemical Cycles **16**(4).

Braun, S. T., L. M. Proctor, et al. (1999). "Molecular evidence for zooplankton-associated nitrogen-fixing anaerobes based on amplification of the nifH gene." FEMS Microbiology Ecology **28**(3): 273-279.

Breitbarth, E., A. Oschlies, et al. (2007). "Physiological constraints on the global distribution of Trichodesmium – effect of temperature on diazotrophy." Biogeosciences **4**(1): 53-61.

Broecker, W. S. and G. M. Henderson (1998). "The sequence of events surrounding Termination II and their implications for the cause of the glacial-interglacial CO_2 changes." Paleooceanography **13**: 352-364.

Brown, J. M., B. A. LaBarre, et al. (2013). "Characterization of Trichodesmium-associated viral communities in the eastern Gulf of Mexico." FEMS Microbiology Ecology **84**(3): 603-613.

Buesseler, K. O. (1998). "The decoupling of production and particulate export in the surface ocean." Global Biogeochemical Cycles **12**: 297-310.

Capone, D. G., J. A. Burns, et al. (2005). "Nitrogen fixation by *Trichodesmium spp.*: An important source of new nitrogen to the tropical and subtropical North Atlantic Ocean." Global Biogeochemical Cycles **19**.

Capone, D. G., M. D. Ferrier, et al. (1994). "Amino Acid Cycling in Colonies of the Planktonic Marine Cyanobacterium Trichodesmium thiebautii." Applied and Environmental Microbiology **60**(11): 3989-3995.

Capone, D. G., A. Subramaniam, et al. (1998). "An extensive bloom of the N_2-fixing cyanobacterium *Trichodesmium erythraeum* in the central Arabian Sea." Marine Ecology Progess Series **172**: 281-292.

Capone, D. G., J. P. Zehr, et al. (1997). "*Trichodesmium*, a globally significant marine cyanobacterium." Science **276**: 1221-1229.

Caron, D. A., E. L. Lim, et al. (1991). "Grazing and utilization of chroococcoid cyanobacteria and heterotrohpic bacteria by protozoa in laboratory cultures and a coastal plankton community." Marine Ecology Progess Series **76**: 205-217.

Carpenter, E. and C. Price (1976). "Marine oscillatoria (Trichodesmium): explanation for aerobic nitrogen fixation without heterocysts." Science **191**(4233): 1278-1280.

Carpenter, E. J. (1983). "Physiology and ecology of marine planktonic *Oscillatoria (Trichodesmium)*." Marine Biology Letter **4**: 69-85.

Carpenter, E. J. and D. G. Capone (2008). Nitrogen in the marine environment. Nitrogen in the Marine Environment. D. G. Capone, D. A. Bronk, M. R. Mulholland and E. J. Carpenter. San Diego, Academic Press**:** 141-198.

Carpenter, E. J., R. G. Harbison, et al. (1977). "Rhizosolenia Mats." Limnology and Oceanography **22**(4): 739-741.

Carpenter, E. J. and S. Janson (2000). "Intracellular cyanobacterial symbionts in the marine diatom *Climacodium frauenfeldianum* (Bacillariophyceae)." Journal of Phycology **36**: 540-544.

Carpenter, E. J., J. P. Montoya, et al. (1999). "Extensive bloom of a N_2-fixing diatom/cyanobacterial association in the tropical Atlantic Ocean." Marine Ecology Progess Series **185**: 273-283.

Carpenter, E. J. and C. C. I. Price (1977). "Nitrogen fixation, distribution, and production of *Oscillatoria* (*Trichodesmium*) spp. in the western Sargasso and Caribbean Seas." Limnology and Oceanography **22**(1): 60-72.

Carpenter, E. J., A. Subramaniam, et al. (2004). "Biomass and primary productivity of the cyanobacterium *Trichodesmium* spp. in the tropical N Atlantic ocean." Deep Sea Research Part I: Oceanographic Research Papers **51**: 173-203.

Checkley Jr, D. M. and C. A. Miller (1989). "Nitrogen isotope fractionation by oceanic zooplankton." Deep Sea Research Part A. Oceanographic Research Papers **36**(10): 1449-1456.

Chen, Y.-l. L., H.-Y. Chen, et al. (2003). "Distribution and downward flux of *Trichodesmium* in the South China Sea as influenced by the transport from the Kuroshio Current." Marine Ecology Progess Series **259**: 47-57.

Choo, Q.-C., M.-R. Samian, et al. (2003). "Phylogeny and Characterization of Three nifH-Homologous Genes from Paenibacillus azotofixans." Applied and Environmental Microbiology **69**(6): 3658-3662.

Christian, J. R., M. R. Lewis, et al. (1997). "Vertical fluxes of carbon, nitrogen, and phosphorus in the North Pacific Subtropical Gyre near Hawaii." Journal of Geophysical Research: Oceans **102**(C7): 15667-15677.

Church, M. J., B. D. Jenkins, et al. (2005). "Vertical distributions of nitrogen-fixing phylotypes at Stn ALOHA in the oligotrophic North Pacific Ocean." Aquatic Microbial Ecology **38**: 3-14.

Church, M. J., C. M. Short, et al. (2005). "Temporal Patterns of Nitrogenase Gene (nifH) Expression in the Oligotrophic North Pacific Ocean." Applied and Environmental Microbiology **71**(9): 5362-5370.

Corinaldesi, C., M. Barucca, et al. (2011). "Preservation, origin and genetic imprint of extracellular DNA in permanently anoxic deep-sea sediments." Molecular Ecology **20**(3): 642-654.

Davis, C. S. and D. J. McGillicuddy Jr. (2006). "Transatlantic abundance of the N_2-fixing colonial cyanobacterium *Trichodesmium*." Science **312**(9): 1517-1520.

Dugdale, R. C. and J. J. Goering (1967). "Uptake of new and regenerated forms of nitrogen in primary productivity." Limnology and Oceanography **12**: 196-207.

Dyhrman, S. T., E. A. Webb, et al. (2006). "Cell-specific detection of phosphorus stress in *Trichodesmium* from the western north Atlantic." Limnology and Oceanography **47**(6): 1832-1836.

Eckford, R., F. D. Cook, et al. (2002). "Free-Living Heterotrophic Nitrogen-Fixing Bacteria Isolated from Fuel-Contaminated Antarctic Soils." Applied and Environmental Microbiology **68**(10): 5181-5185.

Eppley, R. W. and B. J. Peterson (1979). "Particulate organic matter flux and planktonic new production in the deep ocean." Nature **282**: 677-680.

Falkowski, P. G. (1997). "Evolution of the nitrogen cycle and its influence on the biological sequestration of CO2 in the ocean." Nature **387**(6630): 272-275.

Falkowski, P. G., R. T. Barber, et al. (1998). "Biogeochemical Controls and Feedbacks on Ocean Primary Production." Science **281**(5374): 200-206.

Farnelid, H., A. F. Andersson, et al. (2011). "Nitrogenase Gene Amplicons from Global Marine Surface Waters Are Dominated by Genes of Non-Cyanobacteria." PLoS ONE **6**(4): e19223.

Fay, P. (1992). "Oxygen relations of nitrogen fixation in cyanobacteria." Microbiology **56**: 340-373.

Fernández, A., B. Mouriño-Carballido, et al. (2010). "Latitudinal distribution of *Trichodesmium* spp. and N_2 fixation in the Atlantic Ocean." Biogeosciences Discussions **7**: 2195-2225.

Finzi-Hart, J. A., J. Pett-Ridge, et al. (2009). "Fixation and fate of C and N in the cyanobacterium *Trichodesmium* using nanometer-scale secondary ion mass spectrometry." Proceedings of the National Academy of Sciences **106**(15): 6345-6350.

Foster, R. A., M. M. M. Kuypers, et al. (2011). "Nitrogen fixation and transfer in open ocean diatom–cyanobacterial symbioses." The ISME Journal.

Foster, R. A., A. Subramaniam, et al. (2007). "Influence of the Amazon River plume on distributions of free-living and symbiotic cyanobacteria in the western tropical north Atlantic Ocean." Limnology and Oceanography **52**(2): 517-532.

Foster, R. A., A. Subramaniam, et al. (2009). "Distribution and activity of diazotrophs in the Eastern Equatorial Atlantic." Environmental Microbiology **11**(4): 741-750.

Foster, R. A., S. Sztejrenszus, et al. (2013). "Measuring carbon and N2 fixation in field populations of colonial and free-living unicellular cyanobacteria using nanometer-scale secondary ion mass spectrometry1." Journal of Phycology **49**(3): 502-516.

Foster, R. A. and J. P. Zehr (2006). "Characterization of diatom–cyanobacteria symbioses on the basis of nifH, hetR and 16S rRNA sequences." Environmental Microbiology **8**(11): 1913-1925.

Fredriksson, C. and B. Bergman (1997). "Ultrastructural characterisation of cells specialised for nitrogen fixation in a non-heterocystous cyanobacterium,Trichodesmium spp." Protoplasma **197**(1-2): 76-85.

Garcia, H. E. and L. I. Gordon (1992). Oxygen solubility in seawater : better fitting equations. Waco, TX, ETATS-UNIS, American Society of Limnology and Oceanography.

Geider, R. and J. La Roche (2002). "Redfield revisited: variability of C:N:P in marine microalgae and its biochemical basis." European Journal of Phycology **37**(1): 1-17.

Glibert, P. M. and D. A. Bronk (1994). "Release of Dissolved Organic Nitrogen by Marine Diazotrophic Cyanobacteria, Trichodesmium spp." Applied and Environmental Microbiology **60**(11): 3996-4000.

Glibert, P. M. and D. A. Bronk (1994). "Release of dissolved organic nitrogen by marine diazotrophic cyanobacteria, *Trichodesmium* spp." Applied and Environmental Microbiology: 3996-4000.

Goebel, N. L., K. A. Turk, et al. (2010). "Abundance and distribution of major groups of diazotrophic cyanobacteria and their potential contribution to N_2 fixation in the tropical Atlantic Ocean." Environmental Microbiology.

Golden, J. W. and H. S. Yoon (2003). "Heterocyst development in *Anabaena*." Current Opinion in Microbiology **6**: 557-563.

Goldman, J. C. (1993). "Potential role of large oceanic diatoms in new primary production." Deep Sea Research Part I: Oceanographic Research Papers **40**(1): 159-168.

Goméz, F., K. Furuya, et al. (2005). "Distribution of the cyanobacterium *Richelia intracellularis* as an epiphyte of the diatom *Chaetoceros compressus* in the western Pacific Ocean." Journal of Plankton Research **27**(4): 323-330.

Griese, M., C. Lange, et al. (2011). "Ploidy in cyanobacteria." FEMS Microbiology Letters **323**: 124-131.

Großkopf, T., W. Mohr, et al. (2012). "Doubling of marine dinitrogen-fixation rates based on direct measurements." Nature **488**(7411): 361-364.

Gruber, N. (2008). The marine nitrogen cycle: overview and challenges. Nitrogen in the Marine Environment. E. J. Carpenter and D. G. Capone. Burlington, MA, Elsevier Inc.**:** 1-50.

Gruber, N. and J. N. Galloway (2008). "An Earth-system perspective of the global nitrogen cycle." Nature **451**(7176): 293-296.

Gruber, N. and J. L. Sarmiento (1997). "Global patterns of marine nitrogen fixation and denitrification." Global Biogeochemical Cycles **11**(2): 235-266.

Guidi, L., P. H. R. Calil, et al. (2012). "Does eddy-eddy interaction control surface phytoplankton distribution and carbon export in the North Pacific Subtropical Gyre?" Journal of Geophysical Research: Biogeosciences **117**(G2): G02024.

Halm, H., P. Lam, et al. (2012). "Heterotrophic organisms dominate nitrogen fixation in the South Pacific Gyre." ISME J **6**(6): 1238-1249.

Hamersley, M. R., K. A. Turk, et al. (2011). "Nitrogen fixation within the water column associated with two hypoxic basins within the Southern California Bight." Aquatic Microbial Ecology.

Hansell, D. A., N. R. Bates, et al. (2004). "Excess nitrate and nitrogen fixation in the North Atlantic Ocean." Marine Chemistry **84**: 243-265.

Hansell, D. A., D. B. Olson, et al. (2007). "Assessment of excess nitrate development in the subtropical North Atlantic." Marine Chemistry **106**: 562-579.

Haxo, F. T., R. A. Lewin, et al. (1987). "Fine structure and pigments of Oscillatoria (Trichodesmium) aff. thiebautii (Cyanophyta) in culture." Phycologia **26**(4): 443-456.

Heerkloss, R., H. Arndt, et al. (1984). "Consumption and assimilation by zooplankton related to primary production in the batlic coastal water inlet Barther Bodden." Limnologica **15**(2): 387-394.

Heinbokel, J. F. (1986). "Occurrence of *Richelia intracellularis* (Cyanophyta) within the diatoms *Hemiaulus Haukii* and *H. membranaceus* off Hawaii." Journal of Phycology **22**(3): 399-399.

Hewson, I., S. R. Govil, et al. (2004). "Evidence of *Trichodesmium* viral lysis and protential significance for biogeochemical cycling in the oligotrophic ocean." Aquatic Microbial Ecology **36**: 1-8.

Hewson, I., P. H. Moisander, et al. (2007). "Diazotrophic bacterioplankton in a coral reef lagoon: phylogeny, diel nitrogenase expression and response to phosphate enrichment." The ISME Journal **1**(1): 78-91.

Hoering, T. C. and H. T. Ford (1960). "The isotope effect in the fixation of nitrogen by *Azotobacter*." Journal of the American Chemical Society **82**: 376-378.

Holl, C., A. Waite, et al. (2007). "Unicellular diazotrophy as a source of nitrogen to Leeuwin Current coastal eddies." Deep Sea Research Part II: Topical Studies in Oceanography **54**(8-10): 1045-1054.

Howarth, R. W., T. Butler, et al. (1993). "Turbulence and planktonic nitrogen fixation: a mesocosm experiment." Limnology and Oceanography **38**(8): 1696-1711.

Hu, B., G. Yang, et al. (2007). "MreB is important for cell shape but not for chromosome segregation of the filamentous cyanobacterium *Anabaena* sp. PCC 7120." Molecular Microbiology **63**: 1640-1652.

Hutchins, D. A., F.-X. Fu, et al. (2007). "CO_2 controls of *Trichodesmium* N_2 fixation, photosynthesis, growth rates, and elemental ratios: Implications for past, present, and future ocean biogeochemistry." Limnology and Oceanography **52**(4): 1293-1304.

Hynes, A., E. A. Webb, et al. (2012). "Comparison of cultured *Trichodesmium* (Cyanophyceae) with species characterized from the field." Journal of Phycology **48**: 196-210.

Janson, S., A. N. Rai, et al. (1995). "Intracellular cyanobiont *Richelia intracellularis*: ultrastructure and immno-localisation of phycoerythrin, nitrogenase, Rubisco, and glutamine synthase." Marine Biology **124**.

Janson, S., J. Woulters, et al. (1999). "Host specificity in the *Richelia*-diatom symbiosis revealed by *het*R gene sequence analysis." Environmental Microbiology **1**(5): 431-438.

Jiménez, C., J. M. Capasso, et al. (2009). "Different ways to die: cell death modes of the unicellular chlorophyte Dunaliella viridis exposed to various environmental stresses are mediated by the caspase-like activity DEVDase." Journal of Experimental Botany **60**(3): 815-828.

Karl, D., A. Michaels, et al. (2002). "Dinitrogen fixation in the world's oceans." Biogeochemistry **57/58**: 47-98.

Karl, D. M. (2002). "Nutrient dynamics in the deep blue sea." Trends in Microbiology **10**(9): 410-418.

Karl, D. M. and M. D. Bailiff (1989). "The Measurement and Distribution of Dissolved Nucleic Acids in Aquatic Environments." Limnology and Oceanography **34**(3): 543-558.

Karl, D. M., M. J. Church, et al. (2012). "Predictable and efficient carbon sequestration in the North Pacific Ocean supported by symbiotic nitrogen fixation." Proceedings of the National Academy of Sciences **109**(6): 1842-1849.

Kelly, D. C., R. D. Norris, et al. (2003). "Deciphering the paleoceanographic significance of Early Oligocene Braarudosphaera chalks in the South Atlantic." Marine Micropaleontology **49**(1–2): 49-63.

Kemp, A. E. S., J. Pike, et al. (2000). "The "Fall dump" - a new perspective on the role of a "shade flora" in the annual cycle of diatom production and export flux." Deep Sea Research Part II: Topical Studies in Oceanography **47**: 2129-2154.

Kemp, A. E. S. and T. A. Villareal (2013). "High diatom production and export in stratified waters – A potential negative feedback to global warming." Progress in Oceanography(0).

Kerbrat, A.-S., H. T. Darius, et al. (2010). "Detection of ciguatoxin-like and paralysing toxins in Trichodesmium spp. from New Caledonia lagoon." Marine Pollution Bulletin **61**(7–12): 360-366.

Key, R. M., A. Kozyr, et al. (2004). "A global ocean carbon climatology: Results from Global Data Analysis Project (GLODAP)." Global Biogeochemical Cycles **18**(4): n/a-n/a.

Kimor, B., N. Gordon, et al. (1992). "Symbiotic associations among the microplankton in oligotrophic marine environments, with specials reference to the Gulf of Aqaba, Red Sea." Journal of Plankton Research **14**(9): 1217-1231.

Kirchman, A. L. and R. S. Alberte (1985). "Phycoerythrin as a nitrogen storage pool in Synechococcus." EOS, Transactions, American Geophysical Union **66**: 1302.

Knapp, A. N., P. J. DiFiore, et al. (2008). "Nitrate isotopic composition between Bermuda and Puerto Rico: Implications for N2 fixation in the Atlantic Ocean." Global Biogeochemical Cycles **22**(3): n/a-n/a.

Kong, L., H. Jing, et al. (2011). "Phylogenetic diversity and spatio-temporal distribution of nitrogenase genes (nifH) in the northern South China Sea." Aquatic Microbial Ecology **65**(1): 15-27.

Kovala, P. E. and J. D. Larrence (1966). "Computation of phytoplankton number, cell volume, cell surface and plasma volume per litre from microscope counts." Office of Naval Research, Seattle, Washington.

Kromkamp, J. and A. E. Walsby (1992). Buoyancy regulation and vertical migration of *Trichodesmium*: a computer model prediction. . Marine Pelagic Cyanobacteria: *Trichodesmium* and other Diazotrophs. E. J. Carpenter, D. G. Capone and J. G. Reuter. Boston, Kluwer Academic Publishers**:** 239-248.

Kumar, K., R. A. Mella-Herrera, et al. (2010). "Cyanobacterial heterocysts." Cold Spring Harbor Perspectives in Biology **2**: a000315.

Kurmayer, K. and T. Kutzenberger (2003). "Application of real time PCR for quantification of microcystin genotypes in a population of the toxic cyanobacterium *Microcystis* sp." Applied and Environmental Microbiology **69**: 6723-6730.

Kustka, A., S. Sañudo-Wilhelmy, et al. (2003). "A revised estimate of the iron use efficiency of nitrogen fixation, with special reference to the marine cyanobacterium *Trichodesmium spp.* (Cyanophyta)." Journal of Phycology **39**(1): 12-25.

La Roche, J. and E. Breitbarth (2005). "Importance of the diazotrophs as a source of new nitrogen in the ocean." Journal of Sea Research **53**(1-2): 67-91.

Labarre, J., F. Chauvat, et al. (1989). "Insertional mutagenesis by random cloning of antibiotic resistance genes into the genome of the cyanobacterium *Synechocystis* strain PCC 6803." Journal of Bacteriology **171**: 3449-3457.

Lampitt, R. S., K. F. Wishner, et al. (1993). "Marine snow studies in the Northeast Atlantic Ocean: distribution, composition and role as a food source for migrating plankton." Marine Biology **116**: 689-702.

Langlois, R. J., D. Hummer, et al. (2008). "Abundances and distributions of the dominant *nif*H phylotypes in the northern Atlantic Ocean." Applied and Environmental Microbiology **74**(6): 1922-1931.

Langlois, R. J., J. LaRoche, et al. (2005). "Diazotrophic diversity and distribution in the tropical and substropical Atlantic Ocean." Applied and Environmental Microbiology **71**(12): 7910-7919.

Lemmerman, E. (1905). "Die algenflora der Sandwich-Islen. Ergebnisse einer Reise nach dem Pacific. H. Schauinsland 1896/97." Botanische Jahrbu¨cher fu¨r Systematik, Pflanzengeschichte und Pflanzengeographie **34**: 607-663.

Letelier, R. M. and D. M. Karl (1996). "Role of Trichodesmium spp. in the productivity of the subtropical North Pacific Ocean." Marine Ecology Progress Series **133**: 263-273.

Lewis, R., O. ULLOA, et al. (1988). Photosynthetic action, absorption, and quantum yield spectra for a natural population of Oscillatoria in the North Atlantic.

Li, C. and M. Lee (1990). "Cellular differentiation in the trichome of *Trichodesmium thiebautii* (Cyanophyta)." Botanica Marina **33**(4): 347-353.

Loick-Wilde, N., J. Dutz, et al. (2012). "Icorporation of nitrogen from N_2 fixation into amino acids of zooplankton." Limnology and Oceanography **57**(1): 199-210.

Lorenz, M. G. and W. Wackernagel (1987). "Adsorption of DNA to sand and variable degradation rates of adsorbed DNA." Applied and Environmental Microbiology **53**(12): 2948-2952.

Lundgren, P., S. Janson, et al. (2005). "Unveiling of Novel Radiations within Trichodesmium Cluster by hetR Gene Sequence Analysis." Applied and Environmental Microbiology **71**(1): 190-196.

Lundgren, P., E. Söderbäck, et al. (2001). "*Katagymene*: characterization of a novel marine diazotroph." Journal of Phycology **37**(6): 1052-1062.

Luo, Y.-W., S. C. Doney, et al. (2012). "Database of diazotrophs in global ocean: abundances, biomass and nitrogen fixation rates." Earth Systems Science Data Discussions **5**: 47-106.

Mahaffey, C., A. F. Michaels, et al. (2005). "The conundrum of marine N_2 fixation." American Journal of Science **305**: 546-595.

Mahaffey, C., R. Williams, et al. (2003). "Biogeochemical signature of nitrogen fixation in the eastern North Atlantic." Geophyscial Reserach Letters **30**(6): 1300-1303.

Mariotti, A. (1983). "Atmospheric nitrogen is a reliable standard for natural ^{15}N abundance measurements." Nature **303**.

Martin, P., J. T. Allen, et al. (2010). "Sedimentation of acantharian cysts in the Iceland Basin: Strontium as a ballast for deep ocean particle flux, and implications for acantharian reproductive strategies." Limnology and Oceanography **55**(2): 604-614.

Mehta, M. P., D. A. Butterfield, et al. (2003). "Phylogenetic Diversity of Nitrogenase (nifH) Genes in Deep-Sea and Hydrothermal Vent Environments of the Juan de Fuca Ridge." Applied and Environmental Microbiology **69**(2): 960-970.

Michaels, A. F., D. Olson, et al. (1996). "Inputs, losses and transformations of nitrogen and phosphorus in the pelagic North Atlantic Ocean." Biogeochemistry **35**(1): 181-226.

Michaels, A. F. and M. W. Silver (1988). "Primary production, sinking fluxes and the microbial food web." Deep-Sea Research **35**(4): 473-490.

Mills, M. M., C. Ridame, et al. (2004). "Iron and phosphorus co-limit nitrogen fixation in the eastern tropical North Atlantic." Nature **429**: 292-294.

Moisander, P. H., R. A. Beinart, et al. (2010). "Unicellular Cyanobacterial Distributions Broaden the Oceanic N2 Fixation Domain." Science **327**(5972): 1512-1514.

Montoya, J. P., E. J. Carpenter, et al. (2002). "Nitrogen fixation and nitrogen isotope abundances in zooplankton of the oligotrophic North Atlantic." Limnology and Oceanography **47**(6): 1617-1628.

Montoya, J. P., M. Voss, et al. (1996). "A simple, high-precision, high-sensitiviy tracer assay for N_2 fixation." Applied and Environmental Microbiology **62**(3): 986-993.

Moore, C. M., M. M. Mills, et al. (2009). "Large-scale distribution of Atlantic nitrogen fixation controlled by iron availability." Nature Geoscience **2**: 867-871.

Moore, C. M., M. M. Mills, et al. (2013). "Processes and patterns of oceanic nutrient limitation." Nature Geosci **advance online publication**.

Moore, K. J., S. C. Doney, et al. (2002). "Iron cycling and nutrient-limitation patterns in surface waters of the world ocean." Deep Sea Research Part II **49**(1-3): 463-507.

Mori, T., B. Binder, et al. (1996). "Circadian gating of cell division in cyanobacteria growing with average doubling times of less than 24 hours." Proceedings of the National Academy of Sciences **93**: 10183-10188.

Mourino-Carballido, B., R. Grana, et al. (2011). "Importance of N2 fixation vs. nitrate eddy diffusion along a latitudinal transect in the Atlantic Ocean." Limnology and Oceanography **56**(3): 999-1007.

Mulholland, M. R. (2007). "The fate of nitrogen fixed by diazotrophs in the ocean." Biogeosciences **4**: 37-51.

Mulholland, M. R. and D. A. Bronk (2004). "Dinitrogen fixation and release of ammonium and dissolved organic nitrogen by Trichodesmium IMS101." Aquatic Microbial Ecology **37**(1): 85-94.

Mulholland, M. R. and D. G. Capone (2000). "The nitrogen physiology of the marine N2-fixing cyanobacteria Trichodesmium spp." Trends in Plant Science **5**(4): 148-153.

Mulholland, M. R., S. Floge, et al. (2002). "Phosphorus dynamics in cultures and natural populations of Trichodesmium spp." Marine Ecology Progress Series **239**: 45-55.

Mullineaux, C. W., V. Mariscal, et al. (2008). "Mechanism of intercellular molecular exchange in heterocyst-forming cyanobacteria." The EMBO Journal **27**.

Needoba, J. A., R. A. Foster, et al. (2007). "Nitrogen fixation by unicelluar diazotrophic cyanobacteria in the temperate oligotrophic North Pacific Ocean." Limnology and Oceanography **52**(4): 1317-1327.

Newton, W. E. (2007). Physiology, biochemistry and molecular biology of nitrogen fixation. Biology of the nitrogen cycle. H. Bothe, S. J. Ferguson and W. E. Newton. Amsterdam, Netherlands, Elsevier.

Nuester, J., S. Vogt, et al. (2012). "The unique biogeochemical signature of the marine diazotrophic *Trichodesmium*." Frontiers in Microbiology **3**: 1-15.

O'Neil, J. M. (1998). "The colonial cyanobacterium *Trichodesmium* as a physical and nutritional substrate for the harpacticoid copepod *Macrostella gracilis*." Journal of Plankton Research **20**(1): 43-59.

O'Neil, J. M. (1999). "Grazer interactions with nitrogen-fixing marine Cyanobacteria: adaptation for N-acquisition?" Bull. Inst. Oceanogr. Monaco **19**: 293-317.

O'Neil, J. M., P. Metzler, et al. (1996). "Ingestion of $^{15}N_2$-labelled *Trichodesmium*, and ammonium regeneration by the pelagic harpacticoid copepod *Marcosetella gracilis*." Marine Biology **125**: 89-96.

O'Neil, J. M. and M. R. Roman (1994). "Ingestion of the cyanobacterium *Trichodesmium* spp. by the pelagic harpacticoid copepods *Macrosetella*, *Miracia*, and *Oculosetella*." Hydrobiologia **292-293**: 235-240.

Ohlendieck, U., A. Stuhr, et al. (2000). "Nitrogen fixation by diazotrophic cyanobacteria in the Baltic Sea and transfer of the newly fixed nitrogen to picoplankton organisms." Journal of Marine Systems **25**(3–4): 213-219.

Orchard, E. D., C. R. Benitez-Nelson, et al. (2010). "Polyphosphate in *Trichodesmium* from the low-phosphorus Sargasso Sea." Limnology and Oceanography **55**(5): 2161-2169.

Orcutt, K. M., U. Rasmussen, et al. (2002). "Characterization of Trichodesmium spp. by Genetic Techniques." Applied and Environmental Microbiology **68**(5): 2236-2245.

Ostenfeld, C. H. and J. Schmidt (1901). "Plankton fra det Rde hav og Adenbugten." Copenhagen: Vidensk Meddel Naturh Forening i Kbhvn: 141-182.

Padmakumar, K. B., N. R. Menon, et al. (2010). "Occurrence of endosymbiont *Richelia intracellularis* (Cyanophyta) within the diatom *Rhizosolenia hebetata* in Northern Arabian Sea." International Journal of Biodiversity and Conservation **2**(4): 70-74.

Paerl, H. W., J. C. Priscu, et al. (1989). "Immunochemical localization of nitrogenase in marine *Trichodesmium* aggregates: relationship to N_2 fixation potential." Applied and Environmental Microbiology **55**(11): 2965-2975.

Paerl, H. W., L. E. Prufert-Bebout, et al. (1994). "Iron-Stimulated N2 Fixation and Growth in Natural and Cultured Populations of the Planktonic Marine Cyanobacteria Trichodesmium spp." Applied and Environmental Microbiology **60**(3): 1044-1047.

Pecoraro, V., K. Zerulla, et al. (2011). "Quantification of Ploidy in Proteobacteria Revealed the Existence of Monoploid, (Mero-)Oligoploid and Polyploid Species." PLoS ONE **6**(1): e16392.

Peters, J. W., K. Fisher, et al. (1995). "Nitrogenase structure and funtion: A biochemical-genetic perspective." Annual Review of Microbiology **49**: 335-366.

Pike, S. M., K. O. Buesseler, et al. (2005). "Quantification of 234Th recovery in small volume sea water samples by inductively coupled plasma-mass spectrometry." Journal of Radioanalytical and Nuclear Chemistry **263**(2): 355-360.

Riemann, L., H. Farnelid, et al. (2010). "Nitrogenase genes in non-cyanobacterial plankton: prevalence, diversity and regulation in marine waters." Aquatic Microbial Ecology **61**(3): 235-247.

Romans, K. M., E. J. Carpenter, et al. (1994). "Buoyancy regulation in the colonial diazotrophic cyanobacterium *Trichodesmium tenue*: ultrastructure and storage of carbohydrate, polyphosphate, and nitrogen." Journal of Phycology **30**: 935-942.

Rueter, J. G. (1988). "Iron stimulation of photosynthesis and nitrogen fixation in *Anabaena* 7120 and *Trichodesmium* (Cyanophyceae)." Journal of Phycology **24**: 249-254.

Sabine, C. L., R. A. Feely, et al. (2004). "The Oceanic Sink for Anthropogenic CO_2." Science **305**(5682): 367-371.

Saino, T. and A. Hattori (1980). "^{15}N natural abundance in oceanic suspended particulate matter." Nature **283**.

Sanders, R., P. J. Morris, et al. (2010). "Does a ballast effect occur in the surface ocean?" Geophysical Research Letters **37**(8): L08602.

Sandh, G., L. Xu, et al. (2012). "Diazocyte developement in the marine diazotropic cyanobacterium *Trichodesmium*." Microbiology.

Sañudo-Wilhelmy, S. A., A. Kustka, et al. (2001). "Phosphorus limitation of nitrogen fixation by *Trichodesmium* in the central Atlantic Ocean." Nature **411**.

Sarmiento, J. L. and N. Gruber (2006). Air-Sea Interface. Ocean Biogeochemical Dynamics. Princeton, Princeton University Press**:** 73-101.

Sarmiento, J. L., N. Gruber, et al. (2004). "High-latitude controls of thermocline nutrients and low latitude biological productivity." Nature **427**: 56-60.

Scharek, R., M. Latasa, et al. (1999). "Temporal variations in diatom abundance and downward verticle flux in the oligotrophic North Pacific gyre." Deep Sea Research Part I: Oceanographic Research Papers **46**: 1051-1075.

Scharek, R., L. M. Tupas, et al. (1999). "Diatom fluxes to the deep sea in the oligotrophic North Pacific gyre at Station ALOHA." Marine Ecology Progress Series **182**: 55-67.

Schneider, B. and R. Schlitzer (2003). "Depth-dependent elemental compositions of particulate organic matter (POM) in the ocean." Global Biogeochem. Cycles **17**(2).

Schneider, D., E. Fuhrmann, et al. (2007). "Fluorescence staining of live cyanobacterial cells suggest non-stringent chromosome segregation and absence of a connection between cytoplasmic and thylakoid membranes." BioMed Central Cell Biology **8**: 39.

Sellner, K. G. (1992). Trophodynamics of marine cyanobacteria blooms. Marine Pelagic Cyanobacteria: *Trichodesmium* and other Diazotrophs. E. J. Carpenter, D. G. Capone and J. G. Reuter. Boston, Kluwer Academic Publishers**:** 75-94.

Sellner, K. G. (1997). "Physiology, ecology, and toxic properties of marine cyanobacteria blooms." Limnology and Oceanography **42**(5): 1089-1104.

Shaffer, G., J. Bendtsen, et al. (1999). "Fractionation during remineralization of organic matter in the ocean." Deep Sea Research Part I: Oceanographic Research Papers **46**(2): 185-204.

Siddiqui, P. J. A., E. J. Carpenter, et al. (1992). *Trichodesmium*: ultrastructure and protein localization. Marine Pelagic Cyanobacteria: *Trichodesmium* and other Diazotrophs. E. J. Carpenter, D. G. Capone and J. G. Reuter. Dordrecht, The Netherlands, Kluwer Academic Publishers**:** 9-28.

Sigee, D. C., A. Selwyn, et al. (2007). "Patterns of cell death in freshwater colonial cyanobacteria during the late summer bloom." Phycologia **46**(3): 284-292.

Silver, M. W. and K. W. Bruland (1981). "Differential feeding and fecal pellet composition of salps and pteropods, and the possible origin of the deep-water flora and olive-green "cells"." Marine Biology **62**(263-273).

Simon, R. (1977). "Macromolecular composition of spores from the filamentous cyanobacterium *Anabaena cylindrica*." Journal of Bacteriology **129**: 1154-1155.

Simon, R. (1980). "DNA content of heterocysts and spores of the filamentous cyanobacterium *Anabaena variabilis*." FEMS Microbiology Letters **8**: 241-245.

Sohm, J. A., A. Subramaniam, et al. (2011). "Nitrogen fixation by *Trichodesmium* spp. and unicellular diazotrophs in the North Pacific Subtropical Gyre." Journal of Geophysical Research **116**.

Sohm, J. A., E. A. Webb, et al. (2011). "Emerging patterns of marine nitrogen fixation." Nat Rev Micro **9**(7): 499-508.

Staal, M., F. J. R. Meysman, et al. (2003). "Temperature excludes N2-fixing heterocystous cyanobacteria in the tropical oceans." Nature **425**(6957): 504-507.

Steppe, T. F. and H. W. Paerl (2002). "Potential N_2 fixation by sulfate-reducing bacteria in a marine intertidal microbial mat." Aquatic Microbial Ecology **28**: 1-12.

Straub, M., D. M. Sigman, et al. (2013). "Changes in North Atlantic nitrogen fixation controlled by ocean circulation." Nature **501**(7466): 200-203.

Subramaniam, A., P. L. Yager, et al. (2008). "Amazon River enhances diazotrophy and carbon sequestration in the tropical North Atlantic Ocean." Proceedings of the National Academy of Sciences **105**(30).

Sullivan, M. B., M. L. Coleman, et al. (2005). "Three *Prochlorococcus* Cyanophage Genomes: Signature Features and Ecological Interpretations." PLoS Biol **3**(5): e144.

Sweeney, E. N., D. J. McGillicuddy, et al. (2003). "Biogeochemical impacts due to mesoscale eddy activity in the Sargasso Sea as measured at the Bermuda Atlantic Time Series (BATS) site." Deep Sea Research II **50**: 3017-3039.

Taniuchi, Y., Y.-l. L. Chen, et al. (2012). "Isolation and characterization of the unicellular diazotrophic cyanobacterium Group C TW3 from the tropical western Pacific Ocean." Environmental Microbiology **14**(3): 641-654.

Thompson, A. W., R. A. Foster, et al. (2012). "Unicellular Cyanobacterium Symbiotic with a Single-Celled Eukaryotic Alga." Science **337**(6101): 1546-1550.

Thompson, A. W. and J. P. Zehr (2013). "Cellular interactions - lessons from the nitrogen-fixing cyanobacteria." Journal of Phycology: n/a-n/a.

Throndsen, J. (1978). Preservation and storage. Phytoplankton manual. A. Sournia: 69-74.

Toepel, J., E. Welsh, et al. (2008). "Differential transcriptional analysis of the cyanobacterium *Cyanothece* sp. strain ATCC 51142 during light-dark and continuous-light growth." Journal of Bacteriology **190**(11): 3904-3913.

Tovar-Sanchez, A. and S. A. Sañudo-Wilhelmy (2011). "Influence of the Amazon River on dissolved and intra-cellular metal concentrations in Trichodesmium colonies along the western boundary of the sub-tropical North Atlantic Ocean." Biogeosciences **8**(1): 217-225.

Tripp, H. J., S. R. Bench, et al. (2010). "Metabolic streamlining in an open-ocean nitrogen-fixing cyanobacterium." Nature **464**: 90-94.

Turner, J. T. (2002). "Zooplankton fecal pellets, marine snow and sinking phytoplankton blooms." Aquatic Microbial Ecology **27**(1): 57-102.

Tyrrell, T., E. Marañón, et al. (2003). "Large-scale latitudinal distribution of Trichodesmium spp. in the Atlantic Ocean." Journal of Plankton Research **25**(4): 405-416.

van Baalen, C. and R. M. Brown, Jr. (1969). "The ultrastructure of the marine blue green alga, Trichodesmium erythraeum, with special reference to the cell wall, gas vacuoles, and cylindrical bodies." Archiv für Mikrobiologie **69**(1): 79-91.

Van Mooy, B. A. S., L. R. Hmelo, et al. (2012). "Quorum sensing control of phosphorus acquisition in Trichodesmium consortia." ISME J **6**(2): 422-429.

Vaulot, D., D. Marie, et al. (1995). "Growth of *Prochlorococcus*, a photosynthetic prokaryote, in the equitorial Pacific Ocean." Science **268**: 1480-1482.

Venrick, E. L. (1974). "The distribution and significance of *Richelia intracellularis* Schmidt in the North Pacific Central Gyre." Limnology and Oceanography **19**(3).

Verity, P. G., C. Y. Robertson, et al. (1992). "Relationships between cell volume and the carbon and nitrogen content of marine photosynthetic nanoplankton." Limnology and Oceanography **37**(7): 1434-1446.

Villareal, T. A. (1990). "Laboratory culture and preliminary characterization of the nitrogen-fixing *Rhizosolenia-Richelia* symbiosis." Marine Ecology **11**(2).

Villareal, T. A. (1991). "Nitrogen-fixation by the cyanobacterial symbiont of the diatom genus *Hemiaulus*." Marine Ecology Progess Series **76**: 201-204.

Villareal, T. A. (1992). Marine nitrogen-fixing diatom-cyanobacteria symbioses. . Marine Pelagic Cyancobacteria: *Trichodesmium* and other Diazotrophs.

E. J. Carpenter, D. G. Capone and J. G. Reuter. Kluwer, Dordecht, Netherlands, Springer: 163-175.

Villareal, T. A. (1994). "Widespread occurrence of the *Hemiaulus*-Cyanobacterial symbiosis in the southwest North Atlantic Ocean." Bulletin of Marine Science **54**(1): 1-7.

Villareal, T. A., L. Adornato, et al. (2011). "Summer blooms of diatom-diazotroph assemblages (DDA's) and surface chlorophyll in the N. Pacific gyre - a disconnect." Journal of Geophysical Research **116**.

Villareal, T. A. and E. J. Carpenter (2003). "Buoyancy regulation and the potential for vertical migration in the oceanic *Trichodesmium*." Microbial Ecology **45**: 1-10.

Vincent, W. (2002). Cyanobacterial Dominance in the Polar Regions. The Ecology of Cyanobacteria. B. Whitton and M. Potts, Springer Netherlands: 321-340.

Volk, T. and M. I. Hoffert (1985). Ocean carbon pumps: Analysis of relative strengths and efficiencies in ocean-driven atmospheric CO₂ changes. The Carbon Cycle and Atmospheric CO₂: Natural Variations Archean to Present. Washington, DC, AGU. **32:** 99-110.

Wada, E., T. Kadonaga, et al. (1975). "^{15}N abundance in nitrogen of naturally occuring substances and global assesment of denitrification from isotopic viewpoint." Geochemical Journal **9**: 139-148.

Waite, A., V. Rossi, et al. (2013). "Formation and maintenance of high-nitrate, low pH layers in the Eastern Indian Ocean and the role of nitrogen fixation." Biogeosciences Discussions **10**: 3951-3976.

Waksman, S. A., M. Hotchkiss, et al. (1933). "Marine bacteria and their role in the cycle of life in the sea." The Biological Bulletin **65**(2): 137-167.

Walsby, A. E. (1978). "The properties and buoyancy-providing role of gas vacuoles in *Trichodesmium* Ehrenberg." European Journal of Phycology **13**(2): 103-116.

Ward, B. a., S. Dutkiewicz, et al. (2013). "Iron, phosphorus, and nitrogen supply ratios define the biogeography of nitrogen fixation." Limnology and Oceanography **58**(6): 2059-2075.

Weare, N. M., F. Azam, et al. (1974). "Microautoradiographic studies of the marine phycobionts *Rhizosolenia* and *Richelia*." Journal of Phycology **10**(3): 369-371.

White, A. E., F. G. Prahl, et al. (2007). "Summer surface waters in the Gulf of California: Prime habitat for biological N_2 fixation." Global Biogeochemical Cycles **21**.

White, A. E., Y. H. Spitz, et al. (2006). "Modeling carbohydrate ballasting by *Trichodesmium* spp." Marine Ecology Progress Series **323**: 35-45.

Wilson, S. T., D. Böttjer, et al. (2012). "Comparitive assesment of nitrogen fixation methodologies conducted in the oligotrophic North Pacific Ocean." Applied and Environmental Microbiology **78**(18): 6516-6523.

Wu, J., W. Sunda, et al. (2000). "Phosphate Depletion in the Western North Atlantic Ocean." Science **289**(5480): 759-762.

Yeatman, S. G., L. J. Spokes, et al. (2001). "Comparisons of aerosl nitrogen isotpic composition at two polluted coastal sites." Atmospheric Environment **35**: 1307-1320.

Yoon, W., S. Kim, et al. (2001). "Morphology and sinking velocities of fecal pellets of copepod, molluscan, euphausiid, and salp taxa in the northeastern tropical Atlantic." Marine Biology **139**(5): 923-928.

Yoshikawa, C., V. J. Coles, et al. (2013). "Modeling how surface nitrgoen fixation influences subsurface nutrient patterns in the North Atlantic." Journal of Geophysical Research **1118**: 2520-2534.

Young, J. P. W. (1992). Phylogenetic classification of nitrogen-fixing organisms. Biological Nitrogen Fixation. G. Stacey, H. J. Evans and R. H. Burris. New York, N.Y., Chapman and Hall**:** 42-86.

Zehr, J. P. (2011). "Nitrogen fixation by marine cyanobacteria." Trends in Microbiology **19**(4): 162-173.

Zehr, J. P., B. D. Jenkins, et al. (2003). "Nitrogenase gene diversity and microbial community structure: a cross-system comparison." Environmental Microbiology **5**(7): 539-554.

Zehr, J. P. and R. M. Kudela (2011). "Nitrogen Cycle of the Open Ocean: From Genes to Ecosystems." Annual Review of Marine Science **3**: 197-225.

Zehr, J. P., M. Mellon, et al. (1995). "Diversity of heterotrophic nitrogen fixation genes in a marine cyanobacterial mat." Applied and Environmental Microbiology **61**(7): 2527-2532.

Zehr, J. P., M. T. Mellon, et al. (1997). "Phylogeny of cyanobacterial *nif*H genes: evolutionary implications and potential applications to natural assemblages." Microbiology **143**: 1443-1450.

Zehr, J. P., M. T. Mellon, et al. (1998). "New nitrogen fixing microorganims detected in oligotrophic oceans by the amplification of nitrogenase (*nif*H) genes." Applied and Environmental Microbiology **64**(9): 3444-3450.

Zehr, J. P., J. B. Waterbury, et al. (2001). "Unicellular cyanobacteria fix N_2 in the subtropical North Pacific Ocean." Nature **412**: 635-638.

Zheng, W., U. Rasmussen, et al. (2013). "Multiple Modes of Cell Death Discovered in a Prokaryotic (Cyanobacterial) Endosymbiont." PLoS ONE **8**(6): e66147.